JOHANNES KEPLER UNIVERSITÄT LINZ | JKU

Technisch-Naturwissenschaftliche Fakultät

Fast Solvers and Adaptive High-Order FEM in Elastoplasticity

DISSERTATION

zur Erlangung des akademischen Grades

Doktor

im Doktoratsstudium der

Technischen Wissenschaften

Eingereicht von:

Dipl.-Ing. Peter G. Gruber

Angefertigt am:

Institut für Numerische Mathematik

Beurteilung:

O.Univ.Prof. Dipl.Ing. Dr. Ulrich Langer (Betreuung)

Prof. Dr.-Ing. habil. Alexander Düster

Linz, Jänner, 2011

For my mother Bernadette

Contents

Abstract This work is concerned with the numerical solution to elastoplastic problems. Since the whole class of all possible elastoplastic problems is far too large for a common treatment, we restrict ourselves to the investigation of problems which are geometrically linear (strain and displacements are related linearly) and which are quasistatic. Further, the isotropic and homogeneous material should obey the Prandtl-Reuß flow, and a linear isotropic hardening principle.

In the first part of this work the pseudo time variable is discretized and a minimization problem in the so called primal formulation is derived. After elimination of the stresses, the only unknown variables are the displacements, plastic strain, and hardening parameters.

Both the plastic strain and hardening parameters may be determined exactly and pointwise in dependence on the displacement field. These dependencies, as well as the minimization functional itself, are not differentiable. Surprisingly, after substitution of the exact minimizers (with respect to the plastic strain and the hardening parameters), a new minimization functional, depending now smoothly on the displacement, is obtained. The first derivative of the (strictly convex) functional is known explicitly, thus the solution to the problem is given by the root of this first derivative.

This can be achieved by a Newton or Newton-like method. It turns out, that the second derivative of the minimization functional does not exist. However, the recently developed concept of slant differentiability serves as a remedy, and the local super-linear convergence rate of the slant Newton method can be rigorously shown under certain assumptions. These assumptions are not needed in the spatially discrete case. In other words, the spatially discrete version of the slant Newton iterates converges locally super-linear without any extra assumptions.

The second part of this work is devoted to specially adapted choices of the spatial discretization, which is accomplished by the widely known Finite Element Method (FEM) of low and high order (*hp*-FEM). While low order FEM is used in regions where the solution has low regularity, the use of high order FEM speeds up the convergence in regions where the solution has high regularity. Several strategies for determining the corresponding regions (for using low or high order FEM) are discussed. Particularly a very new strategy, the boundary concentrated FEM (BC-FEM), or more precisely, a zone concentrated FEM (ZC-FEM), is applied to elastoplastic problems.

The elastoplastic solver, in combination with several adaptive *hp*-FEM strategies, has been developed within the software framework NETGEN/NGSolve. Numerous experiments affirm the theoretical results of this work, and provide an extent overview regarding the several techniques for spatial discretization.

Zusammenfassung Diese Arbeit beschäftigt sich mit der numerischen Lösung von elastoplastischen Problemen. Da die gesamte Klasse aller möglichen elastoplastischer Probleme viel zu groß für eine einheitliche Untersuchung ist, beschränken wir uns auf die Betrachtung von quasistatischen Problemen. Die Verzerrung soll ferner linear von der Verschiebung abhängen (man spricht hierbei von geometrisch linearen Problemen), und das isotrope und homogene Material soll die Prandtl-Reuß Fließregel, sowie eine lineare isotrope Verfestigung aufweisen.
Im ersten Teil dieser Arbeit wird bezüglich der Pseudozeit diskretisiert und ein Minimierungsproblem in sogenannter primaler Formulierung modelliert. Hier treten nach Eliminierung der Spannungen nur mehr Verschiebung, plastische Verzerrung und Verfestigungsparameter als gesuchte Größen auf.
Sowohl die plastische Verzerrung als auch der Verfestigungsparameter können abhängig von den Verschiebungen exakt und punktweise minimiert werden. Diese Abhängigkeiten, sowie das Minimierungsfunktional sind nicht differenzierbar. Umso überraschender ist, dass nach Substitution der exakten Minimierer (bezüglich plastischer Verzerrung und Verfestigungsparameter) ein Funktional zu minimieren bleibt, welches allein von den Verschiebungen abhängt und differenzierbar ist. Die erste Ableitung des (strikt konvexen) Funktionals ist explizit bekannt, wodurch die Lösung des Problems durch das Finden der Nullstelle derselben gegeben ist.
Dazu eignet sich ein Newton, oder Newton-ähnliches Verfahren. Es zeigt sich, dass die zweite Ableitung des Minimierungsfunktionals nicht existiert. Allerdings kann hier das erst kürzlich entwickelte Konzept von sogenannten schiefen Ableitungen zur Anwendung kommen, und die lokale superlineare Konvergenz des "schiefen" Newtonverfahrens unter bestimmten Voraussetzungen bewiesen werden. Diese Voraussetzungen sind aber nur im räumlich kontinuierlichen Minimierungsproblem, nicht aber im Fall einer fixen räumlichen Diskretisierung erforderlich.
Der zweite Teil dieser Arbeit beschäftigt sich mit der speziellen Wahl der räumlichen Diskretisierungen. Dies geschieht mittels Finiter Elemente Methode (FEM) niedriger oder hoher Ordnung (*hp*-FEM). In Bereichen wo die Regularität der Lösung niedrig ist, diskretisiert man mittels FEM niedriger Ordnung. Ist die Regularität der Lösung aber hoch, so kann durch Anwendung einer FEM höherer Ordnung eine schnelle Konvergenz erzielt werden. Es werden mehrere adaptive Strategien einander gegenüber gestellt. Im speziellen wird eine erst kürzlich entwickelte Strategie, die Randkonzentrierte FEM (engl. Boundary Concentrated FEM, BC-FEM), oder präziser, eine Zonenkonzentrierte FEM (ZC-FEM), auf elastoplastische Probleme angewandt.
Der elastoplastische Löser wurde in Kombination mit einigen adaptiven FEM-Strategien im Software-Framework NETGEN/NGSolve entwickelt. Durch zahlreiche numerische Experimente werden schließlich die theoretischen Resultate dieser Arbeit belegt und ein Überblick zu den verschiedenen Methoden der räumlichen Diskretisierung gegeben.

Chapter 1

Introduction

History and Basics of Elastoplasticity: Elastoplasticity is a branch of solid and structural mechanics, where the deformation of solid bodies under load is studied. In difference to the well known theory of elasticity, it is assumed in elastoplasticity, that the body may stay in a deformed state when the load is released. In other words, a permanent (and also irreversible) deformation of the body is allowed. In order to be able to store the information of such a permanent deformation, H. E. Tresca [105] suggested to additively split the strain into two additive and symmetric parts. One part should correspond to the elastic amount of deformation. This part is called the elastic strain, which enters the constitutive equations of the theory of elasticity, e.g., Hooke's law. The other part is called the plastic strain, an internal variable, in which the permanent deformation of the material can be stored (at each time step). However, since by this splitting of the strain the number of unknowns is increased, some more mathematical relations are needed in order to keep the problem uniquely solvable.

One relation is obtained by the observation, that a permanent deformation occurs wherever the stresses are (in some sense) too high during the load history. Mathematically, this issue is formulated in the so called *yield criterion*, which was originally stated by H. E. Tresca, and later modified by R. v. Mises [74]. It says, that only those stresses are admissible, which are contained in a certain convex set around zero. The size of this set is governed by a material depending constant called the yield stress.

Another relation addresses the time increment of the plastic strain. L. Prandtl [85, 86] formulated this relation for the 2D-case, by which the principal axes of the plastic strain increment are forced to coincide with the principal axes of the stress tensor. This relation was extended to the 3D-case by A. Reuß [88], and later generalized to fit into the scope of non-smooth yield surfaces by W. T. Koiter [66]. His formulation is today known as the *Prandtl-Reuß normality law* or the *Prandtl-Reuß flow law*.

The combination of the yield criterion, together with the Prandtl-Reuß normality law, and the classical formulation of elasticity for the elastic strain, form the system of equations, which is today known as the classical formulation of *perfect plasticity*. Additionally, many materials show another property, which is called *hardening*. The meaning of hardening is as follows: A material shows hardening effects, if its hardness increases at points, where plastic deformation has occurred. Vice versa (and this holds for every material) the harder a material is, the less likely it deforms plastically. This is due to the fact, that the hardness of a material is proportional to the yield stress. Since steel, and many other materials in industry show hardening behavior, this effect cannot be neglected. L. Prandtl [86] was the first one to consider hardening effects among elastoplastic problems.

Other variations of elastoplasticity, such as for example the counterpart of hardening, which is called *softening*, or the *multiplicative* splitting of the strain into elastic and plastic parts, or the concepts of Drucker-Prager plasticity [84, 34], or the Cosserat model (see, e. g., [79]), are not considered in this thesis. Anyway, the interested reader is referred to the monograph [110] for a more complete overview on the history of elastoplasticity.

State of the Art: By combining the equilibrium of forces with the Prandtl-Reuß flow law [85, 86, 88], a time-dependent variational inequality can be formulated. The existence of a unique solution to such problems has been proved by C. Johnson in [59, 58, 60], utilizing general results by G. Duvaut and J. L. Lions for variational inequalities [37]. Let us mention, that similar results were obtained by J. J. Moreau [76], but from a more geometric point of view.

The traditional numerical methods for solving the time dependent variational inequality are based on a backward Euler time-discretization. In doing so, one mixed variational problem is obtained per time step, where the so called generalized stress serves as the primal variable. In this case the application of implicit return mapping algorithms, developed by J. C. Simo et al. [99, 97, 98, 95, 94, 96], turned out to be fruitful for calculations. Alternatively, by the application of a duality argument from convex analysis, one variational problem of the second kind is obtained per time step. Here, the primal variables are the displacement u and the plastic strain p. Surprisingly, the original variational formulation is today called the *dual formulation*, whereas the dual one is called the *primal formulation*.

Finite Element approximations and analysis for the dual formulation have been investigated in many works of the 80s. Here, we only refer to I. Hlaváček [53], and the monographs V. Korneev and U. Langer [67], and I. Hlaváček, J. Haslinger, J. Nečas, and J. Livíšek [54].

Until the mid 90s, there were no numerical solvers based on the primal formulation, which is considered in this thesis. Various schemes of Finite Element approximation for the primal formulation were first discussed by W. Han and D. Reddy [49, 50]. They provide an extended discussion of both, the primal and the dual, formulations, based on convex analysis. Since then, many authors, particularly C. Carstensen, have paid attention to the primal formulation [20, 21, 5, 6].

Motivated by the regularity properties of the solution - which is, roughly speaking, analytical in elastic zones, and twice weakly differentiable in plastic zones of the computational domain - the spatial discretization by an adaptive combination the low order Finite Element Method (h-FEM) and the high order Finite Element Method (p-FEM) is a natural choice.

In h-FEM [28, 101, 27], the accuracy of the approximate solution is increased by decreasing the mesh size h, while the polynomial degree p of the shape functions is kept constant. Conversely, in the p-FEM [10], the mesh size is kept constant, and the polynomial degree p of the shape functions is increased in order to obtain a better approximation. The p-method yields a fast convergence, assumed that the solution has a high regularity. The combination of both methods for different regions of the domain is called hp-FEM.

Another way of adaptive refinement, the so called rp-FEM strategies, are not considered in this thesis The key of these methods is to adaptively move mesh nodes in such a way, that a high resolution is obtained in zones, where the solution has low regularity. In other zones (as in hp-FEM) the polynomial degree of the shape functions is increased. As A. Düster, V. Nübel and E. Rank demonstrate in [81, 80], such strategies may even result in an exponential convergence rate of the FE-approximation in case of the deformation theory of plasticity. The main drawback of the rp-FEM is, that it is hard to be realized in a standard Finite Element software, where mesh-operations are mostly limited to just the adaptive marking and refinement.

Let us turn back to the construction of adaptive strategies for hp-FEM, which generally involves three main instances: The first instance is the development of a sharp (reliable and efficient) a-posteriori error estimator. It is used as a stopping criterion to terminate the adaptive algorithm, if a desired level of accuracy has been reached. The second instance is the definition of an appropriate refinement indicator. It is responsible for marking elements, whether the degree of freedoms should be enriched in h- or p-FEM manner. Let be mentioned, that often a localized a-posteriori error estimator is used as such refinement indicator. The third instance is then to apply a certain prescription of how to apply mesh-refinement, or how much the polynomial degree should be increased.

For certain linear problems (apart from elastoplasticity), a proper adaptive strategy in hp-FEM may lead even to an exponential convergence rate [7] of the Finite Element approximation to the solution. Let be mentioned, that both h- and p-FEM asymptotically yield a polynomial convergence rate. Such exponential convergence, however, is only guaranteed for problems, where the solution is analytic almost everywhere. To be precise, the set, where the solution is not analytic, has to be of measure zero with respect to the domain's boundary dimension [93, 102]. This property cannot be guaranteed for elastoplastic problems with hardening in general. Nevertheless, a fast polynomial convergence rate, faster than the convergence of uniform h- or p-FEM can be expected, due to regularity properties of the solution.

Since the elastic and plastic zones are not known in advance, the use of clever hp-adaptive strategies in elastoplasticity is particularly important. Here, we shall remark one problem concerning error estimators in elastoplasticity: On the one hand, there exist a-posteriori error estimators for elastoplasticity with hardening which are efficient and reliable. Particularly popular are averaging error estimators like the well known ZZ error estimator, see [29]. However, for all those error estimators there holds, that either the efficiency or the reliability constant are crucially depending on the modulus of hardening, as C. Carstensen clearly pointed out in [23]. Up to the authors best knowledge, there is no efficient and reliable error estimator known up to now, which could be seriously used for "small" hardening, i. e., in the vicinity of perfect plasticity.

As mentioned before, the first two instances of a classical hp-adaptive algorithm involve the knowledge of a sharp error estimator. First (globally) to terminate the adaptive algorithm, and second (locally) to decide whether an element has to be refined or if the polynomial degree of the shape functions should be enriched. Apart from materials which significantly show hardening effects, the choice of an appropriate refinement indicator is crucial.

There is a technique, which represents more than just a remedy for the gap between reliability and efficiency of error estimators in elastoplasticity (which is the case for small hardening). It was invented by C. Mavriplis [71] for the spectral element method, and later proposed for the *hp*-Finite Element Method by P. Houston, B. Senior, and E. Süli [56, 57]. This technique is to estimate the regularity of the solution on the element by measuring the slope of the coefficients with respect to an L_2-orthogonal expansion of the finite element approximation (with Legendre polynomials). If the slope of these coefficients is falling fast enough (on a logarithmic scale) then the solution is assumed to be analytic on the element. T. Eibner and M. Melenk [38] extended this method for meshes consisting of triangles (in 2D) or tetrahedrons (in 3D), whereas the theory of Houston, Senior, and Süli was developed for elements with tensor product structure only.

Another approach for adaptive refinement is the so called Zone Concentrated FEM (ZC-FEM), which is based on the Boundary Concentrated FEM, introduced by B. N. Khoromskij and J. M. Melenk [62]. The BC-FEM is an optimal strategy of adaptive refinement for problems, where the solution is known to be smooth in the interior of the computational domain, and rough in a neighborhood of the boundary. This strategy is defined by using a geometric mesh and a polynomial degree vector. These are combined in a way, that, in the 2D-case, the convergence of the FE-approximation to the solution is inverse proportional to the degrees of freedom, whereas a uniform h-refined approximation converges inverse proportional to the square root of the degrees of freedom. In this sense, the BC-FEM shows a convergence rate which can be compared to the Boundary Element Method (BEM), and has the advantage, that mass and stiffness matrices are still sparse. ZC-FEM represents the adaption of BC-FEM to problems, where the solution is rough at the boundary *and* on (small but positive-measured) subsets of the domain, and smooth in the rest of the domain. The part of the domain, where the solution is known to be rough, is uniformly h-refined, and BC-FEM is applied for the rest of the domain. Although the superb asymptotical convergence rate of the BC-FEM cannot be preserved in this way, the ZC-FEM is nevertheless worth to be applied to elastoplastic problems, where the solution is known to be rough in plastic zones (and on the boundary), whereas, under appropriate assumptions on the data, it is known to be analytic in the interior of elastic zones.

On this Work: This PhD-Thesis is devoted to the numerical solution of special elastoplastic problems. We consider a quasi-static initial-boundary value problem for elastoplasticity with hardening. Throughout the work, only the geometrically linearized theory, i. e., a linearized strain, as well as a linear and isotropic hardening law are considered. The extension of this work's theoretical approach to geometrical nonlinearity, structural mechanics [41] and nonlinear hardening is promising. However, an extension to the linear kinematic hardening laws is straightforward, whereas softening laws definitely require different analysis tools. Several computation techniques for solving the elastoplastic problem with various kinds of hardening can be found, e. g., in [67, 19, 16, 96, 5, 36, 64, 63, 25]. However, the analysis in this work is inherently bound to the fact that the material shows hardening effects along with its plastification. This is not only due to the more realistic modeling concerning many materials in industry, but also because of the more stable numerical treatment: The weak formulation in Sobolev spaces results in positive definite tangential stiffness matrices if hardening effects are considered, whereas the tangential stiffness matrices would be semi-definite in case of perfect plasticity. Let us mention, that in perfect plasticity spaces of bounded deformation $BD(\Omega)$ are used instead of Sobolev spaces, see [104]. For the efficient solution of problems without hardening, i. e., perfect Prandtl-Reuß plasticity, we refer to [103, 108, 109]. Also, we consider the case, that the material plastifies according to just one yield criterion. The case of multi-yield elastoplasticity has been studied, e. g., in [107, 17, 18, 45].

In this work, as mentioned above, we concentrate on the primal variational formulation, which, after backward Euler time discretization, results in a variational inequality of the second kind [49]. At each time step, the variational inequality is equivalent [42] to a minimization problem with a convex but non-smooth energy functional,

$$\bar{J}(u,p) \to \min \, .$$

However, a multiplicative additive Schwartz method [21] and a (damped) Newton-like scheme [5] converge globally and linearly. A super-linear convergence was observed, but not proved in the latter article ([5, Remark 7.5]).

The main theoretical contribution of this work is collected in Chapter 4 and published in [47, 48]. Here we use two tools: the Theorem of Moreau and the concept of slant differentiability. It is possible to prove the observed local super-linear convergence in the following way: The minimization with respect to the plastic strain can be calculated locally by using an explicitly known dependence [5] of the plastic strain on the total strain, i. e., $p = \tilde{p}(\varepsilon(u))$. Thus, the equivalent energy minimization problem for the displacement u only,

$$J(u) := \bar{J}(u, \tilde{p}(\varepsilon(u)) \to \min \, ,$$

can be defined. Since the dependencies of the energy functional on the second argument, and of the minimizer $\tilde{p}$ on the total strain $\varepsilon(u)$ are not smooth, the Fréchet derivative $DJ(u)$ seems, at the first glance, not to exist. Nevertheless, we can show that the structure of the energy functional $J(u)$ satisfies the assumptions of Moreau's theorem, known from convex analysis, and therefore, the energy functional $J(u)$ is Fréchet differentiable with the explicitly computable Fréchet derivative $DJ(u)$. However, the second derivative of the energy functional, $D^2J(u)$, does not exist because of the non-differentiability of the plastic strain minimizer $\tilde{p}$ on the elastoplastic interface, which separates the deformed continuum in elastically and plastically deformed parts. By the concept of slant differentiability, introduced by X. Chen, Z. Nashed and L. Qi in [26], we define a Newton-like method using slanting functions instead of the usual derivative. We call such method a slant Newton method for short. One of the main results in [26] is, that a slant Newton method converges locally super-linear under the same assumptions as the classical Newton method. The main task is to find a slanting function for the mapping $\max\{0,\cdot\}$, which occurs within the formula of the plastic minimizer $\tilde{p}$ and causes its non-differentiability. Such slanting functions are easy to find in the spatially discrete case, e. g., after the FEM discretization. In this case, Proposition 4.2 provides the explanation to the mentioned open question formulated in [5, Remark 7.5] concerning the super-linear convergence.

The spatially continuous case is more complicated and requires some extra integrability assumptions for the trial stress in each slant Newton step. To the best knowledge of the author, there are no theoretical results yet known, which would guarantee the required integrability properties. Already existing results, such as in [40, 12], concern the integrability of the stress and displacement fields which solve the elastoplastic one-time-step problem, but not of the trial stresses during a slant Newton iteration.

Let us mention that iteration techniques were successfully used to prove regularity results for some smoothed initial boundary value problems of the plastic flow theory by V. Korneev and U. Langer in [68] (see also [67]). Also a very recent work by R. Griesse and C. Meyer [43] looks promising to help with solving the open integrability problem.

However, under weak assumptions on the given data, there are pleasing results concerning the regularity of the solution: The displacement u (in the spatially continuous case) is once weakly differentiable with respect to the time variable, and, away from the boundary, locally twice weakly differentiable with respect to the space variable [46]. This very recent result for Prandtl-Reuß plasticity with hardening was already obtained for Cosserat plasticity by D. Knees and P. Neff [65], who used regularity results on general rate-independent systems by A. Mielke [73]. Moreover, the solution is known to be analytic in open balls of the domain, where the plastic strain vanishes almost everywhere (so called elastic zones), if the volume forces and surface tractions are sufficiently smooth. This is a well known result, and can be found in the monographs A. Bensoussan and J. Frehse [12], M. Fuchs and G. Seregin [40].

This motivates the use of *hp*-FEM [7, 93] for elastoplastic problems with linear hardening. As already mentioned, the term *hp*-FEM stands for the mixed use of low order Finite Element Methods (*h*-FEM) and high order Finite Element Methods (*p*-FEM). High order Finite Elements are preferred in regions, where the solution is very smooth, i. e., in elastic zones, whereas in plastic zones low order Finite Elements are used. Although the necessary regularity assumptions for exponential convergence are not fulfilled in elastoplasticity, a much better convergence as in pure *h*-FEM or *p*-FEM can be expected.

Therefore, we investigate four strategies: The first one is a special way to estimate the local Sobolev-regularity of the solution [38] as described above. This strategy works fine asymptotically, but needs a lot of calculation time for coarse meshes. This is due to the fact, that this method only works optimal, if the initial polynomial degree is high enough (greater than 4) on each element. Therefore we proposed a second strategy, which in addition to the regularity-estimation also marks an element for *h*-refinement, if the Frobenius norm of the plastic strain is positive, i. e., if the element is deformed plastically. In this way we avoid, that in plastic zones, where by the time most of the new elements are created, the polynomial degree is too high. The third strategy, which we discuss in this PhD-Thesis is the Zone Concentrated FEM, based on the Boundary Concentrated FEM by J. M. Melenk and B. N. Khoromskij [62]. Their strategy was designed for problems, where one knows in advance, that the solution is analytic in the interior of the domain and has low regularity at the boundary. The fourth strategy is an approach where solely the ZZ error estimator [29] is used as a refinement indicator. Although this error estimator is known (see [23]) to be efficient and reliable for elastoplastic problems with hardening (for fixed positive hardening module, i. e., not for perfect plasticity), this strategy shows a comparably slow convergence of the Finite Element approximation towards the solution of the one-time step problem.

Numerical experiments in Chapter 6 conclude the paper. A lot of effort has been put into the development of computer software to support the theoretical results of this thesis by computational tests. Implementations have been performed in the frameworks of MATLAB and NETGEN/NGSOLVE, which is highlighted in the first part of this chapter. The second part is devoted to the illustration of the super-linear convergence of the slant Newton method at each time step when using uniform h-refinement. In the third part of this chapter we study the convergence of the Finite Element solution for each of the presented adaptive hp-FEM strategies.

Those numerical experiments, as well as the theoretical contribution of this thesis, are finally discussed in Chapter 7.

This PhD-Thesis is organized as follows: In Chapter 2 we fix the notation, and recall a few well known results from convex analysis. With the help of these, we can model the classical and variational formulations of the elastoplastic problems in Chapter 3. The new analytical framework for solving these problems is contained in Chapter 4. Chapter 5 addresses the temporal and spatial discretization schemes. Numerical tests are documented in Chapter 6, and the discussion of the theoretical and numerical results in Chapter 7 concludes this thesis.

Chapter 2

Preliminaries

2.1 Notation

Let $\mathbb{R}$ be the set of real numbers, $\overline{\mathbb{R}} = \mathbb{R} \cup \{-\infty, +\infty\}$ the set of extended real numbers, $\mathbb{R}^+ = \{x \in \mathbb{R} \mid x > 0\}$ the set of positive real numbers, and $\mathbb{R}_0^+ = \{x \in \mathbb{R} \mid x \geq 0\}$ the set of nonnegative real numbers. Throughout this work we deal with quantities which depend on a space variable $x = (x_1, x_2, x_3)$ in the Euclidean vector space $\mathbb{R}^3$ and on a time variable t in $\mathbb{R}_0^+$. Partial derivatives of such a quantity, say $f(x,t)$, are denoted by

$$\frac{\partial f}{\partial x_i}(x,t) \text{ or } \frac{\partial f}{\partial t}(x,t)$$

for $i \in \{1, 2, 3\}$. The temporal derivatives are often abbreviated by a dot, e. g.,

$$\dot{f}(x,t) = \frac{\partial f}{\partial t}(x,t)\,.$$

The *gradient* of f, on the other hand, collects the spatial derivatives, and is denoted by

$$\nabla f(x,t) = \left[\frac{\partial f}{\partial x_1}(x,t), \frac{\partial f}{\partial x_2}(x,t), \frac{\partial f}{\partial x_3}(x,t)\right]^T\,.$$

The gradient of a vector valued function, e. g., $f(x,t) = [f_1(x,t), f_2(x,t), f_3(x,t)]$ is matrix valued and defined by

$$\nabla f(x,t) = \begin{pmatrix} \frac{\partial f_1}{\partial x_1}(x,t) & \frac{\partial f_1}{\partial x_2}(x,t) & \frac{\partial f_1}{\partial x_3}(x,t) \\ \frac{\partial f_2}{\partial x_1}(x,t) & \frac{\partial f_2}{\partial x_2}(x,t) & \frac{\partial f_2}{\partial x_3}(x,t) \\ \frac{\partial f_3}{\partial x_1}(x,t) & \frac{\partial f_3}{\partial x_2}(x,t) & \frac{\partial f_3}{\partial x_3}(x,t) \end{pmatrix}\,.$$

The divergence of a vector valued function is defined

$$\operatorname{div} f(x,t) = \frac{\partial f_1}{\partial x_1}(x,t) + \frac{\partial f_2}{\partial x_2}(x,t) + \frac{\partial f_3}{\partial x_3}(x,t)\,,$$

and the divergence of a matrix valued function

$$f(x,t) = \begin{pmatrix} f_{11}(x,t) & f_{12}(x,t) & f_{13}(x,t) \\ f_{21}(x,t) & f_{22}(x,t) & f_{23}(x,t) \\ f_{31}(x,t) & f_{32}(x,t) & f_{33}(x,t) \end{pmatrix}$$

in the space $\mathbb{R}^{3\times 3}$ is defined by

$$\operatorname{div} f(x,t) = \begin{pmatrix} \frac{\partial f_{11}}{\partial x_1}(x,t) + \frac{\partial f_{12}}{\partial x_2}(x,t) + \frac{\partial f_{13}}{\partial x_3}(x,t) \\ \frac{\partial f_{21}}{\partial x_1}(x,t) + \frac{\partial f_{22}}{\partial x_2}(x,t) + \frac{\partial f_{23}}{\partial x_3}(x,t) \\ \frac{\partial f_{31}}{\partial x_1}(x,t) + \frac{\partial f_{32}}{\partial x_2}(x,t) + \frac{\partial f_{33}}{\partial x_3}(x,t) \end{pmatrix}.$$

Throughout this thesis, stress and strain tensors are identified by symmetrical square matrices. One frequently used operation in this regard is the so called *Frobenius norm*

$$\|A\|_F = \langle A\,,\, A\rangle_F^{1/2}\,,$$

which is defined via the scalar product

$$\langle A\,,\, B\rangle_F = \sum_{i=1}^{m}\sum_{j=1}^{n} a_{ij}\, b_{ij}$$

for the matrices $A = (a_{ij}) \in \mathbb{R}^{m\times n}$ and $B = (b_{ij}) \in \mathbb{R}^{m\times n}$, where m and n are from the set of natural numbers $\mathbb{N}$. Notice, that the *Euclidean norm* and the related scalar product – often referred to as the l_2-*scalar product* – for vectors of the vector space $\mathbb{R}^3$ can be seen as a special case ($m = 3$ and $n = 1$) of the more general Frobenius norm and scalar product. Hence, we shall denote the Euclidean norm and l_2-scalar product for vectors of the Euclidean space by the same symbols $\|\cdot\|_F$ and $\langle\cdot\,,\,\cdot\rangle_F$.

Moreover the following matrix operations are often used in this thesis: The *deviator* is defined for a square matrix $A \in \mathbb{R}^{n\times n}$, with $n \in \mathbb{N}$, by

$$\operatorname{dev} A = A - \frac{\operatorname{tr} A}{\operatorname{tr} I}\, I\,,$$

where the *trace* of a square matrix is defined by

$$\operatorname{tr} A = \langle A\,,\, I\rangle_F$$

with I denoting the identity in $\mathbb{R}^{n\times n}$.

2.2 Some Well Known Results from Convex Analysis

In this subsection, we summarize a few results from convex and functional analysis. Let X be a Banach space and X^* its dual space with the duality product $\langle x^*\,,\, x\rangle$ for $x^* \in X^*$ and $x \in X$, and the norm

$$\|x^*\|_{X^*} = \sup_{x\in X} \frac{\langle x^*\,,\, x\rangle}{\|x\|}\,.$$

Definition 2.1 (convex set)**.** A set $K \subset X$ is said to be *convex* if, for every x and y in K, we have

$$\lambda\, x + (1-\lambda)\, y \in K \qquad \forall\, \lambda \in [0,1]\ .$$

Definition 2.2 (convex function)**.** Let F be a mapping of X into $\overline{\mathbb{R}}$. F is said to be *convex* if, for every x and y in X, we have

$$F(\lambda\, x + (1-\lambda)\, y) \le \lambda\, F(x) + (1-\lambda)\, F(y) \qquad \forall\, \lambda \in [0,1]\ , \tag{2.1}$$

whenever the right hand side is defined.

Definition 2.3 (strictly convex function)**.** Let F be a mapping of X into $\mathbb{R}$. F is said to be *strictly convex* if it is convex and the strict inequality holds in (2.1) for all $x, y \in X$ with $x \neq y$ and for all $\lambda \in \,]0,1[$.

The connection between convex sets and convex functions is given by the epigraph of a function:

Definition 2.4. The *epigraph* of a function $F : X \to \overline{\mathbb{R}}$ is the set

$$\operatorname{epi} F = \{(x,c) \in X \times \mathbb{R} \mid F(x) \le c\}\,.$$

Theorem 2.1. *A function $F : X \to \overline{\mathbb{R}}$ is convex if and only if its epigraph is convex.*

Proof. See [39, Proposition 2.1]. ☐

Conversely, with the indicator function it is possible to treat convex sets in the framework of convex functions:

Definition 2.5. Let K be a set in X. The function $\mathcal{X}_K : X \to \overline{\mathbb{R}}$, defined by

$$\mathcal{X}_K(x) = \begin{cases} 0 & \text{if } x \in K\,, \\ +\infty & \text{else}\,, \end{cases} \tag{2.2}$$

is said to be the *indicator functional* of K.

Lemma 2.1. *A set $K \subset X$ is convex if and only if its indicator functional $\mathcal{X}_K$ is convex.*

Proof. If the indicator function $\mathcal{X}_K$ is convex, then

$$\mathcal{X}_K(\lambda\, x + (1-\lambda)\, y) \le \lambda\, \mathcal{X}_K(x) + (1-\lambda)\, \mathcal{X}_K(y) \quad \forall x, y \in X\ \forall \lambda \in [0,1]\ , \tag{2.3}$$

which yields

$$\mathcal{X}_K(\lambda\, x + (1-\lambda)\, y) \le 0 = \lambda\, \mathcal{X}_K(x) + (1-\lambda)\, \mathcal{X}_K(y) \quad \forall x, y \in K\ \forall \lambda \in [0,1]\ . \tag{2.4}$$

Due to the definition of the indicator function $\mathcal{X}_K$ there holds

$$\lambda\, x + (1-\lambda)\, y \in K \quad \forall x, y \in K\ \forall \lambda \in [0,1]\ . \tag{2.5}$$

Hence, K is convex. Conversely, let the set K be convex, that is, there holds (2.5), implying (2.4). If x or y are in $X \setminus K$, then due to the definition of the indicator function $\mathcal{X}_K$, the right hand side in (2.4) is no more finite. Hence, there holds (2.3). ☐

Definition 2.6 (proper function, effective domain)**.** Let F be a mapping of X into $\overline{\mathbb{R}}$. F is said to be *proper* if there exists $x \in X$ such that $F(x) < +\infty$ and if $F(y) > -\infty$ for all $y \in X$. The set

$$\operatorname{dom} F = \{x \in X \mid F(x) < +\infty\}$$

is said to be the *effective domain* of F.

Notice, that for a nonempty set $K \in X$ the indicator functional $\mathcal{X}_K$ is proper, and there holds $\operatorname{dom} \mathcal{X}_K = K$.

Definition 2.7. For every functional F of X into $\overline{\mathbb{R}}$ the *conjugate functional* of F is defined by

$$F^* : X^* \to \overline{\mathbb{R}}\,,\ x^* \mapsto \sup_{x \in X} \left(\langle x^*\,,\, x\rangle - F(x) \right). \tag{2.6}$$

Definition 2.8 (subdifferential)**.** Let F be a mapping of X into $\overline{\mathbb{R}}$. F is said to be *subdifferentiable* at the point $x \in X$ if $F(x)$ is finite, and there exists $x^* \in X^*$ such that

$$F(y) \geq F(x) + \langle x^*\,,\, y - x\rangle \tag{2.7}$$

holds for all $y \in X$. We then call x^* a *subgradient*, and the set of all subgradients in x is said to be the *subdifferential* of F in x and denoted by $\partial F(x) = \{x^* \mid (2.7)\}$.

Notice, that subgradients only exist at points, where a function is finite.

Definition 2.9 (normal cone)**.** Let K be a nonempty subset of X. The set $\mathcal{N}_K(x) \subset X^*$ is said to be the *normal cone* of K at $x \in K$, and defined by

$$\mathcal{N}_K(x) = \{x^* \in X^* \mid \langle x^*\,,\, y - x\rangle \leq 0 \text{ for all } y \in K\}\,.$$

The normal cone is illustrated in Figure 2.1 for the case $X = X^* = \mathbb{R}^2$. Notice, the normal cone $\mathcal{N}_K$ is only defined for $x \in K$. Moreover, there are two special cases:

- If x is on a smooth part of the boundary, then the normal cone is a one-dimensional manifold spanned by the exterior unit normal.
- If x is in the interior of K (which is identical to K if K is open) or on a concave part of the boundary (if K is not convex), then the normal cone consists of zero only.

The following Theorems 2.2 and 2.3 are of crucial importance in the modeling of elastoplasticity. These results are responsible for the connection of the so called *primal* and *dual* formulations of an elastoplastic problem. Theorem 2.3 makes use of the notion, that X is a reflexive Banach space, which is the case, if there exists an isometric isomorphism between the double dual space X^{**} and X, i. e., there exists a bijective mapping

$$I : X^{**} \to X\,,\ x^{**} \mapsto x\,, \tag{2.8}$$

with $\|x^{**}\|_{X^{**}} = \|x\|_X$, such that

$$\langle x^{**}\,,\, x^*\rangle_{X^{**}\times X^*} = \langle x^*\,,\, x\rangle_{X^*\times X} \quad \forall x^* \in X^*\,.$$

Both theorems are well known in the scope of convex analysis. Although their proofs can be found in literature (e. g. in [39]), we add them for the completeness of the presentation.

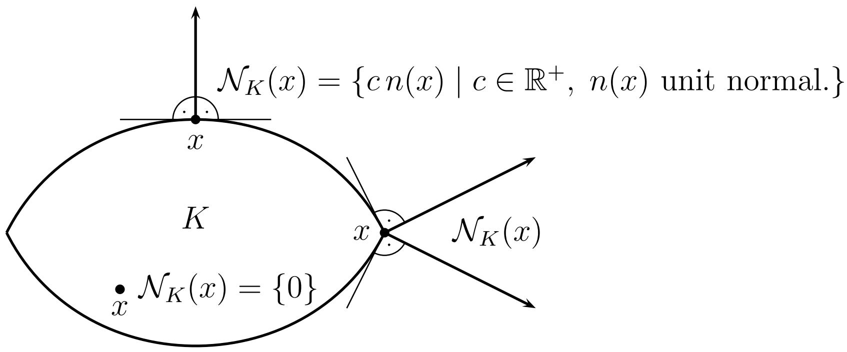

Figure 2.1: The normal cone $\mathcal{N}_K(x)$ at various points x in a closed convex set K.

Theorem 2.2. *Let K be a nonempty subset of X. Then there holds*

$$[x \in K \ \wedge \ x^* \in \mathcal{N}_K(x)] \ \Leftrightarrow \ x^* \in \partial \mathcal{X}_K(x)\,. \tag{2.9}$$

Proof. Let $x \in K$ and $x^* \in \mathcal{N}_K(x)$, that is

$$\langle x^*\,,\, y - x\rangle \leq 0 \quad \forall y \in K\,. \tag{2.10}$$

Since $\mathcal{X}_K(x) = 0$ and $\mathcal{X}_K(y) = 0$ for $y \in K$, there holds

$$\mathcal{X}_K(y) \geq \mathcal{X}_K(x) + \langle x^*\,,\, y - x\rangle \quad \forall y \in K\,, \tag{2.11}$$

and thus,

$$\mathcal{X}_K(y) \geq \mathcal{X}_K(x) + \langle x^*\,,\, y - x\rangle \quad \forall y \in X\,. \tag{2.12}$$

Conversely, let $x^* \in \partial \mathcal{X}_K(x)$, that is, $x \in K$ and there holds (2.12). Particularly for $y \in K \subset X$ we obtain (2.11), and since $\mathcal{X}_K(x) = 0$ and $\mathcal{X}_K(y) = 0$, the result is (2.10). This finishes the proof, since $x \in K$ and $x^* \in \mathcal{N}_K(x)$. □

Theorem 2.3. *Let X be a reflexive Banach space, F be a function of X into $\overline{\mathbb{R}}$, and F^* its conjugate function. Then there holds*

$$x^* \in \partial F(x) \Leftrightarrow x \in \partial F^*(x^*)\,. \tag{2.13}$$

Proof. We assume $x^* \in \partial F(x)$. Due to Definition 2.8 this is equivalent to

$$F(x) \leq \inf_{\bar{x} \in X} \left(F(\bar{x}) - \langle x^*\,,\, \bar{x}\rangle\right) + \langle x^*\,,\, x\rangle\,.$$

Swapping the sign and adding the term $\langle y^*\,,\, x\rangle$ for arbitrary $y^* \in X^*$ yield

$$\langle y^*\,,\, x\rangle - F(x) \geq \sup_{\bar{x} \in X} \left(\langle x^*\,,\, \bar{x}\rangle - F(\bar{x})\right) + \langle y^*\,,\, x\rangle - \langle x^*\,,\, x\rangle \quad \forall y^* \in X^*\,,$$

which, due to the isomorphic property $\langle x^*\,,\,x\rangle_{X^*\times X} = \langle x^{**}\,,\,x^*\rangle_{X^{**}\times X^*}$, is equivalent to

$$\langle y^*\,,\,x\rangle - F(x) \geq \sup_{\bar{x}\in X}\left(\langle x^*\,,\,\bar{x}\rangle - F(\bar{x})\right) + \langle x^{**}\,,\,y^* - x^*\rangle \quad \forall y^* \in X^*\,.$$

Hence,

$$\sup_{\bar{y}\in X}\left(\langle y^*\,,\,y\rangle - F(y)\right) \geq \sup_{\bar{x}\in X}\left(\langle x^*\,,\,\bar{x}\rangle - F(\bar{x})\right) + \langle x^{**}\,,\,y^* - x^*\rangle \quad \forall y^* \in X^*\,,$$

which precisely says, that x is in $\partial F^*(x^*)$. The opposite direction $x \in \partial F^*(x^*) \Rightarrow x^* \in \partial F(x)$ can be shown analogously. □

The following Theorem 2.4 summarizes three well known results from convex analysis which will be frequently used in the following chapters.

Theorem 2.4. *Let $F : X \to \mathbb{R}$ be a convex function. Then the following two properties hold:*

a) F is continuous on X if and only if there exists a non-empty open subset $U \subset X$ on which F is bounded from above by a constant $C \in \mathbb{R}$.

b) If F is continuous on X, then F is subdifferentiable on X.

c) If F is continuous and has a unique subgradient at $y \in X$, then F is Fréchet differentiable at y and its derivative is identical to the subgradient.

Proof. See [39, Proposition 2.5, Proposition 5.2, and Proposition 5.3 of Chapter I]. □

Definition 2.10 (coercivity)**.** Let F be a mapping of X into $\overline{\mathbb{R}}$. F is said to be *coercive*, if for all $c_1 \in \mathbb{R}$ there exists $c_2 \in \mathbb{R}$ such that for all $x \in X$ there holds

$$F(x) \leq c_1 \Rightarrow \|x\| \leq c_2\,.$$

Definition 2.11 (lower semicontinuity)**.** Let F be a mapping of X into $\overline{\mathbb{R}}$. F is said to be *lower semi continuous (l.s.c. for short)* at $x \in X$ if

$$\lim_{y\to x} F(y) \geq F(x)\,.$$

F is said to be *l.s.c. in* X if F is l.s.c. at all $x \in X$.

Theorem 2.5. *Let $F : X \to \overline{\mathbb{R}}$ be l.s.c., proper, convex and coercive. Then there exists $\hat{x} \in X$ such that $F(\hat{x}) = \inf_{x\in X} F(x)$. If F is strictly convex, then $\hat{x}$ is unique.*

Proof. See [39, Proposition 1.2 of Chapter II]. □

Chapter 3

Mathematical Modeling of Elastoplasticity

3.1 The Classical Formulation

3.1.1 Perfect Plasticity

The theory of elastoplasticity is an extension of the theory of elasticity: The equilibrium of forces as well as geometric considerations, such as the relation between the strain tensor and the displacement, have to hold for both theories in the same way. The only difference concerns the type constitutive equations. In elastoplasticity, the time increment of the so-called plastic strain plays an important role in those constitutive relations. This is why, even if we assume the acceleration to be small ($\ddot{u} \approx 0$) in the equilibrium of forces, a pseudo time variable remains in the formulation of the problem, which, due to this fact, is called a quasistatic problem.

Let $\Theta :=]0, T[\subset \mathbb{R}$ (for some given $T \in \mathbb{R}^+$) be the pseudo temporal interval, and let Ω be a bounded Lipschitz domain in the Euclidean space $\mathbb{R}^3$. The equilibrium of forces in the quasi-static case reads as follows:

$$-\operatorname{div}(\sigma(x,t)) = f(x,t) \quad \text{for } (x,t) \in \Omega \times \Theta\,, \tag{3.1}$$

where

$$\sigma(x,t) = \begin{pmatrix} \sigma_{11}(x,t) & \sigma_{12}(x,t) & \sigma_{13}(x,t) \\ \sigma_{12}(x,t) & \sigma_{22}(x,t) & \sigma_{23}(x,t) \\ \sigma_{13}(x,t) & \sigma_{23}(x,t) & \sigma_{33}(x,t) \end{pmatrix} \in \mathbb{R}^{3\times 3}_{\text{sym}}$$

is the symmetric *Cauchy's stress tensor* and $f(x,t) = [f_1(x,t), f_2(x,t), f_3(x,t)]^T \in \mathbb{R}^3$ is the *volume force density* acting at the material point $x \in \Omega$ and the time $t \in \Theta$. Let $u(x,t) = [u_1(x,t), u_2(x,t), u_3(x,t)]^T \in \mathbb{R}^3$ be the *displacement* of the body, and let

$$\varepsilon(u)(x,t) := \frac{1}{2}\left(\nabla u(x,t) + (\nabla u)^T(x,t)\right) \tag{3.2}$$

denote the linearized *Green-St. Venant strain tensor*, or just *the strain*, for short. We consider the (symmetric) strain ε to be additively split into two symmetric parts, an elastic part $e \in \mathbb{R}^{3\times 3}_{\mathrm{sym}}$ and a plastic part $p \in \mathbb{R}^{3\times 3}_{\mathrm{sym}}$, that is, at each material point $x \in \Omega$ and time $t \in \Theta$, we have

$$\varepsilon(x,t) = e(x,t) + p(x,t)\,. \tag{3.3}$$

The relation between stress σ and the elastic part of the strain e is given by Hook's law

$$\sigma = \mathbb{C}e, \tag{3.4}$$

where, under the assumption that the material is homogeneous and isotropic, the fourth-order *stiffness tensor* $\mathbb{C} = [\mathbb{C}_{ijkl}] \in \mathbb{R}^{3\times 3\times 3\times 3}$ is defined by

$$\mathbb{C}_{ijkl} := \lambda\,\delta_{ij}\,\delta_{kl} + \mu\,(\delta_{ik}\,\delta_{jl} + \delta_{il}\,\delta_{jk})\,.$$

Here, $\lambda > 0$ and $\mu > 0$ denote the *Lamé constants*, and δ_{ij} is the *Kronecker-symbol.* In case of an inhomogeneous material, the Lamé constants would depend on the space variable $x \in \Omega$.

Let the boundary of the domain $\Gamma := \partial\Omega$ be split into a *Dirichlet-part* Γ_D and a *Neumann-part* Γ_N. We assume the Dirichlet (displacement) boundary condition

$$u = u_D \quad \text{on } \Gamma_D\,, \tag{3.5}$$

and the Neumann (traction) boundary condition

$$\sigma\,n = g \quad \text{on } \Gamma_N\,, \tag{3.6}$$

where $n(x,t)$ is the exterior unit normal, $u_D(x,t) \in \mathbb{R}^3$ denotes a prescribed displacement, and $g(x,t) \in \mathbb{R}^3$ is a prescribed surface traction. By neglecting the plastic term in (3.3), i. e. $p = 0$, the system (3.1) - (3.6) describes the purely elastic behavior of the continuum Ω.

The additive splitting (3.3) into two symmetric additive parts goes back to H. E. Tresca [105]. We need two further relations, such that the unknown plastic strain p can be determined.

The first additional relation in elastoplasticity is the so-called *yield criterion*, which was originally stated by Tresca, and later modified by R. von Mises [74]. It reads as follows:

$$\sigma \in K\,, \quad K := \{\tau \in \mathbb{R}^{3\times 3}_{\mathrm{sym}} \mid \phi(\tau) \le 0\}\,, \tag{3.7}$$

where the *set of admissible stresses* K and the *yield functional* ϕ are convex. Moreover, the set K is closed. According to R. von Mises, the yield functional ϕ is defined by

$$\phi(\sigma) = \|\mathrm{dev}\,\sigma\|_F - \sigma_y\,. \tag{3.8}$$

The *yield stress* σ_y is a positive real number and material dependent. Again, we consider the material to be homogeneous with respect to the yield stress throughout this work. Notice, that due to the algebraic relations (3.4), (3.2), and (3.3), there follows

$$\sigma = \mathbb{C}(\varepsilon(u) - p)\,. \tag{3.9}$$

Hence, a condition for the stress σ can be equivalently seen as a condition for the plastic strain p. This fact will lead to two equivalent classical formulations for elasticity, and it is responsible for the use of two dual variational formulations in literature (see [50]).

The second additional relation in elastoplasticity addresses the time derivative $\dot{p}$ of the plastic strain. Originally, St. Venant [89] and M. Lévy [70] suggested, that the principal axes of the plastic strain increment should coincide with the principal axes of the stress. This suggestion was adapted by L. Prandtl [85, 86] (in 2D) and A. Reuß [88] (in 3D) and later generalized to the case of nonsmooth yield surfaces by Koiter [66]. Nowadays, this relation is known as the *Prandtl-Reuß Normality Law*

$$\dot{p} \in \mathcal{N}_K(\sigma)\,, \text{ with } \mathcal{N}_K(\sigma) := \{q \in \mathbb{R}^{3\times 3}_{\text{sym}} \mid \langle q\,,\, \tau - \sigma\rangle_F \leq 0 \text{ for all } \tau \in K\}\,. \tag{3.10}$$

Here, the set $\mathcal{N}_K(\sigma)$ is the normal cone of the convex set K at the point $\sigma \in K$ (see Definition 2.9 and Figure 2.1). Together with the initial condition

$$p(x,0) = p_0(x) \quad \forall x \in \overline{\Omega}\,, \tag{3.11}$$

with given initial plastic strain p_0, we finally arrive at the first classical formulation of the perfect elastoplastic problem.

Classical Formulation I of Perfect Plasticity

Let f, g, u_D, and p_0 be given. Find u, p, and σ, which satisfy

$$\begin{array}{rcll}
-\operatorname{div}\sigma(x,t) & = & f(x,t) & (x,t) \in \Omega\times\Theta\,, \\
\sigma & = & \mathbb{C}\,(\varepsilon(u) - p)\;, & \\
\varepsilon(u) & = & \frac{1}{2}\left(\nabla u + \nabla u^T\right)\;, & \\
\sigma(x,t) & \in & K & (x,t) \in \Omega\times\Theta\,, \\
\dot{p}(x,t) & \in & \mathcal{N}_K(\sigma) & (x,t) \in \Omega\times\Theta\,, \\
u(x,t) & = & u_D(x,t) & (x,t) \in \Gamma_D\times\overline{\Theta}\,, \\
\sigma(x,t)\,n(x,t) & = & g(x,t) & (x,t) \in \Gamma_N\times\overline{\Theta}\,, \\
p(x,0) & = & p_0(x) & x \in \overline{\Omega}\,.
\end{array} \tag{3.12}$$

Here, the sets K and $\mathcal{N}_K(\sigma)$ are defined in (3.7), (3.8), and (3.10).

The declaration of proper function spaces are omitted. This issue will later be discussed for the variational formulation of (3.12) in Section 3.2.

3.1.2 The Duality Argument

The convex analysis results presented in Section 2.2 allow us to express the classical formulation of (3.12) in an equivalent dual way. Let us mention, that throughout this subsection we shall use the abbreviations

$$p = p(x,t) \in \mathbb{R}^{3\times 3}_{\text{sym}}\,, \qquad \dot{p} = \dot{p}(x,t) \in \mathbb{R}^{3\times 3}_{\text{sym}}\,, \qquad \sigma = \sigma(x,t) \in \mathbb{R}^{3\times 3}_{\text{sym}}\,, \tag{3.13}$$

for some arbitrarily fixed $x \in \overline{\Omega}$ and $t \in \overline{\Theta}$.

Let $\mathcal{X}_K$ denote the indicator functional of the convex set K in (3.7), see Definition 2.5, let $\mathcal{X}_K{}^*$ denote its conjugate functional, see Definition 2.7, and let $\partial\mathcal{X}_K$ and $\partial\mathcal{X}_K{}^*$ denote their subgradients, see Definition 2.8.

Then, due to Theorem 2.2 and Theorem 2.3 there holds

$$[\sigma \in K \;\wedge\; \dot{p} \in \mathcal{N}_K(\sigma)] \;\Leftrightarrow\; \sigma \in \partial\mathcal{X}_K{}^*(\dot{p})\,. \tag{3.14}$$

The set $\partial\mathcal{X}_K{}^*(\dot{p})$ reads in expanded form

$$\partial\mathcal{X}_K{}^*(\dot{p}) = \{\tau \in \mathbb{R}^{3\times 3}_{\text{sym}} \mid \mathcal{X}_K{}^*(q) \geq \mathcal{X}_K{}^*(\dot{p}) + \langle \tau\,,\, q - \dot{p}\rangle_F \quad \forall q \in \mathbb{R}^{3\times 3}_{\text{sym}}\}\,, \tag{3.15}$$

where still the explicit form of the so called *dissipation functional* $\mathcal{X}_K{}^*$ has to be determined. We will return to this point later. Notice, that in the inequality (3.15) the test variable q lives in the whole space, whereas in the normality law (3.10) the test variable τ had to be an element in the convex set K. This difference is essential with regard to the variational formulation of elastoplastic problems, see Section 3.2. Consequently, another classical formulation is obtained, which is equivalent to the formulation in (3.12):

Classical Formulation II of Perfect Plasticity

Let f, g, u_D, and p_0 be given. Find u, p, and σ, which satisfy

$$\begin{aligned}
-\operatorname{div}\sigma(x,t) &= f(x,t) && (x,t) \in \Omega \times \Theta\,,\\
\sigma &= \mathbb{C}\left(\varepsilon(u) - p\right)\,, &&\\
\varepsilon(u) &= \tfrac{1}{2}\left(\nabla u + \nabla u^T\right)\,, &&\\
\sigma(x,t) &\in \partial\mathcal{X}_K{}^*(\dot{p}(x,t)) && (x,t) \in \Omega \times \Theta\,,\\
u(x,t) &= u_D(x,t) && (x,t) \in \Gamma_D \times \overline{\Theta}\,,\\
\sigma(x,t)\,n(x,t) &= g(x,t) && (x,t) \in \Gamma_N \times \overline{\Theta}\,,\\
p(x,0) &= p_0(x) && x \in \overline{\Omega}\,.
\end{aligned} \tag{3.16}$$

Here, the set $\partial\mathcal{X}_K{}^*(\dot{p})$ is defined in (3.15).

It remains to calculate the explicit form of functional $\mathcal{X}_K{}^*$:

Lemma 3.1. *Let the functional $\mathcal{X}_K{}^* : \mathbb{R}^{3\times 3}_{sym} \to \overline{\mathbb{R}}$ be defined according to Definition 2.5, Definition 2.7, and let the convex set K be defined as in* (3.7) *by the yield functional ϕ in* (3.8) *for a certain choice of $\sigma_y \in \mathbb{R}^+$.*

Then, the conjugate functional ${\mathcal{X}_K}^*$ *is given by the formula*

$$
{\mathcal{X}_K}^*(\dot{p}) = \begin{cases} \sigma_y \, \|\dot{p}\|_F \,, & \textit{if } \operatorname{tr} \dot{p} = 0 \,, \\ +\infty \,, & \textit{else} \,. \end{cases} \tag{3.17}
$$

Proof. The proof can be found in literature [50]. Nevertheless, we present the proof in detail. It may be helpful in order to obtain a conjugate functional for other specific hardening laws. The definition of the conjugate functional in Definition 2.7 yields

$$
{\mathcal{X}_K}^*(\dot{p}) = \sup_{\sigma \in \mathbb{R}^{3\times 3}_{\mathrm{sym}}} \left(\langle \dot{p} \,,\, \sigma \rangle_F - \mathcal{X}_K(\sigma) \right) \,,
$$

which, due to the definition of the indicator functional $\mathcal{X}_K$ in Definition 2.5 is equivalent to

$$
{\mathcal{X}_K}^*(\dot{p}) = \sup_{\sigma \in K} \langle \dot{p} \,,\, \sigma \rangle_F \,.
$$

In the first instance we will show

$$
{\mathcal{X}_K}^*(\dot{p}) \geq \begin{cases} \sigma_y \, \|\dot{p}\|_F \,, & \text{if } \operatorname{tr} \dot{p} = 0 \,, \\ +\infty \,, & \text{else} \,, \end{cases} \tag{3.18}
$$

and then finally,

$$
[\operatorname{tr} \dot{p} = 0] \;\Rightarrow\; [{\mathcal{X}_K}^*(\dot{p}) \leq \sigma_y \, \|\dot{p}\|_F] \,. \tag{3.19}
$$

Since $\sigma = c\, I$, with $c \in \mathbb{R}$ and I denoting the identity, is in K, there holds

$$
{\mathcal{X}_K}^*(\dot{p}) = \sup_{\sigma \in K} \langle \dot{p} \,,\, \sigma \rangle_F \geq \sup_{c \in \mathbb{R}} \langle c\, \dot{p} \,,\, I \rangle_F = \sup_{c \in \mathbb{R}} \, (c \, \operatorname{tr} \dot{p}) = \begin{cases} 0 \,, & \text{if } \operatorname{tr} \dot{p} = 0 \,, \\ +\infty \,, & \text{else} \,. \end{cases}
$$

Let $\operatorname{tr} \dot{p} = 0$, which implies $\operatorname{dev} \dot{p} = \dot{p}$. The choice $\sigma = \sigma_y \, \dot{p} \, \|\dot{p}\|_F^{-1}$ is in K due to

$$
\|\operatorname{dev} \left(\sigma_y \, \dot{p} \, \|\dot{p}\|_F^{-1} \right) \|_F = \sigma_y \, \|\operatorname{dev} \dot{p}\|_F \|\dot{p}\|_F^{-1} = \sigma_y \,.
$$

This choice of σ yields

$$
{\mathcal{X}_K}^*(\dot{p}) = \sup_{\sigma \in K} \langle \dot{p} \,,\, \sigma \rangle_F \geq \sigma_y \, \|\dot{p}\|_F \,.
$$

Hence there holds (3.18). It remains to show (3.19). Let $\operatorname{tr} \dot{p} = 0$, implying

$$
\langle \dot{p} \,,\, \sigma \rangle_F = \langle \operatorname{dev} \dot{p} \,,\, \sigma \rangle_F = \langle \dot{p} \,,\, \operatorname{dev} \sigma \rangle_F
$$

for all $\sigma \in \mathbb{R}^{3\times 3}_{\mathrm{sym}}$. Thus, there holds

$$
{\mathcal{X}_K}^*(\dot{p}) = \sup_{\sigma \in K} \langle \dot{p} \,,\, \sigma \rangle_F \leq \sup_{\sigma \in K} \left(\|\dot{p}\|_F \|\operatorname{dev} \sigma\|_F \right) = \sigma_y \|\dot{p}\|_F \,,
$$

which completes the proof. $\square$

3.1.3 Plasticity with Hardening

The elastoplastic problems in (3.12) and (3.16) were called problems of *perfect plasticity*. Although, these problems already serve as a complete description of elastoplasticity, one important property is not covered by those: the hardening of the material due to plastic deformation.

Hardening is a process where the hardness of a material increases. The hardness of a material at a point x is related to the yield stress $\sigma_y(x)$. A harder material will have a higher resistance to plastic deformation than a less hard metal, see the definition of the yield criterion in (3.7) and the definition of the yield functional in (3.8). Vice versa, the metal is hardening at locations where plastic deformation occurs, i. e., where the yield criterion is active.

There are two good reasons for considering the effect of hardening within the scope of elastoplastic problems: First, to increase the quality of the physical model regarding the mathematical description of empirical observations. Second, to benefit from the fact, that the global energy functional (see Chapter 4) will be strictly convex resulting in a positive definite FEM stiffness matrix (see Chapter 5), whereas in case of perfect plasticity, i. e., when we do not consider hardening effects, the global energy functional is just convex, resulting in a semi-definite stiffness matrix.

Already in 1828 R. v. Mises [75] took this effect into account. As can be observed from experiments, the hardening procedure is different from material to material. Thus, a lot of different models for hardening have been derived since that time. For a good overview on this topic, see [78, 50].

Before we start to model the classical formulation of plasticity with hardening, let us mention, that there is a contrary effect to hardening, which is called softening. This material property occurs for large plastic deformations, which we do not consider in the scope of this thesis. We concentrate on the so called *linear isotropic* hardening law. Extending the analytical and conceptual results to other kinds of *linear hardening* is straight forward, whereas the application of *nonlinear hardening* and *softening* laws requires a different treatment. Also the case of multi-yield [107, 55] is not considered in this thesis.

In addition to the stress σ, we need another quantity, the so-called *internal force*, which stores the information about the hardness of the material at the location $x \in \Omega$ and time $t \in \Theta$. In case of isotropic hardening, it is sufficient to store this information in a scalar variable $\alpha(x,t) \in \mathbb{R}$. Dual to the internal force α, there is another quantity $\gamma(x,t) \in \mathbb{R}$, a so called *internal variable*.

The algebraic relation between the internal variable γ and the internal force α is simple:

$$\alpha(x,t) = -\gamma(x,t) \quad (x,t) \in \Omega \times \Theta \,, \tag{3.20}$$

a consequence of the second law of thermodynamics, which says that

$$\sigma = \frac{\partial \psi}{\partial e} \,, \text{ and } \alpha = -\frac{\partial \psi}{\partial \gamma} \,,$$

where e denotes the elastic strain of (3.3) and ψ denotes the *free energy functional*

$$\psi(e,\gamma) = \frac{1}{2}\left(\langle \mathbb{C}e\,,\, e\rangle_F + \gamma^2\right)\,.$$

For more details on this topic, the interested reader is referred to the monographs [50, 2].

Henceforth, the tuples

$$\Sigma = (\sigma,\alpha) \in \mathbb{R}^{3\times 3}_{\mathrm{sym}} \times \mathbb{R}\,,\ \text{ and } P = (p,\gamma) \in \mathbb{R}^{3\times 3}_{\mathrm{sym}} \times \mathbb{R} \tag{3.21}$$

are called the *generalized stress* and the *generalized plastic strain*, respectively. Both material laws (3.7) and (3.10) or the dual law (3.15) may be formulated also in the context of generalized stresses and plastic strains.

Let $x \in \Omega$ and $t \in \Theta$ be fixed arbitrarily. Again, let us use abbreviations as in (3.13). Only generalized stresses Σ are admissible, which satisfy

$$\Sigma \in K = \{\mathcal{T} = (\tau,\beta) \in \mathbb{R}^{3\times 3}_{\mathrm{sym}} \times \mathbb{R} \mid \phi(\mathcal{T}) \le 0\}\,, \tag{3.22}$$

where the yield functional ϕ is defined (for $\Sigma = (\sigma,\alpha)$) by

$$\phi(\Sigma) = \|\mathrm{dev}\,\sigma\|_F - \sigma_y(1 + H\,\alpha) + \mathcal{X}_{\mathbb{R}^+_0}(\alpha) \tag{3.23}$$

with the *yield stress* $\sigma_y \in \mathbb{R}^+$, and the *modulus of hardening* $H \in \mathbb{R}^+$, both depending on the material. Notice, the last term $\mathcal{X}_{\mathbb{R}^+_0}(\alpha)$, which indicates that a generalized stress Σ is admissible, only if α is nonnegative. Negative α would induce isotropic softening, which we neglect due to the reasons discussed above. Just as in the case of perfect plasticity (see Section 3.1.1), the set of admissible stresses K and the yield functional ϕ are convex.

The generalized strain P, such as in the case of perfect plasticity, has to satisfy the Prandtl-Reuß Normality Law

$$\dot{P} \in \mathcal{N}_K(\Sigma) = \{Q = (q,\eta) \in \mathbb{R}^{3\times 3}_{\mathrm{sym}} \times \mathbb{R} \mid \langle Q\,,\, \mathcal{T} - \Sigma\rangle \le 0 \text{ for all } \mathcal{T} \in K\}\,. \tag{3.24}$$

Here, the scalar product is defined (for $\dot{P} = (\dot{p},\dot{\gamma})$ and $\Sigma = (\sigma,\alpha)$) by

$$\langle \dot{P}\,,\, \Sigma\rangle = \langle \dot{p}\,,\, \sigma\rangle_F + \dot{\gamma}\,\alpha\,,$$

which, in the scope of elastoplasticity, is called the *rate of dissipation*. Again, the set $\mathcal{N}_K(\Sigma)$ is the normal cone of the convex set K at the point $\Sigma \in K$ (see Definition 2.9 and Figure 2.1). Together with the initial condition

$$P(x,0) = P_0(x) \quad \forall x \in \overline{\Omega}\,, \tag{3.25}$$

where $P_0(x) = (p_0(x),\gamma_0(x))$ is given, we can formulate the classical formulation of the elastoplastic problem with hardening:

Classical Formulation I of Plasticity with Isotropic Hardening

Let f, g, u_D, and $P_0 = (p_0, \gamma_0)$ be given. Find u, $P = (p, \gamma)$, and $\Sigma = (\sigma, \alpha)$, which satisfy

$$\begin{aligned}
-\operatorname{div}\sigma(x,t) &= f(x,t) && (x,t) \in \Omega \times \Theta\,, \\
\sigma &= \mathbb{C}\left(\varepsilon(u) - p\right)\,, \\
\alpha &= -\gamma\,, \\
\varepsilon(u) &= \tfrac{1}{2}\left(\nabla u + \nabla u^T\right)\,, \\
\Sigma(x,t) &\in K && (x,t) \in \Omega \times \Theta\,, \\
\dot{P}(x,t) &\in \mathcal{N}_K(\Sigma) && (x,t) \in \Omega \times \Theta\,, \\
u(x,t) &= u_D(x,t) && (x,t) \in \Gamma_D \times \overline{\Theta}\,, \\
\sigma(x,t)\, n(x,t) &= g(x,t) && (x,t) \in \Gamma_N \times \overline{\Theta}\,, \\
P(x,0) &= P_0(x) && x \in \overline{\Omega}\,.
\end{aligned} \tag{3.26}$$

Here, the sets K and $\mathcal{N}_K(\sigma)$ are defined in (3.22), (3.23), and (3.24).

According to what we learned in Subsection 3.1.2, due to Theorem 2.2 and Theorem 2.3 there holds for $\Sigma = (\sigma, \alpha) \in \mathbb{R}^{3\times3}_{\mathrm{sym}} \times \mathbb{R}$ and $P = (p, \gamma) \in \mathbb{R}^{3\times3}_{\mathrm{sym}} \times \mathbb{R}$

$$\left[\Sigma \in K \ \wedge \ \dot{P} \in \mathcal{N}_K(\Sigma)\right] \ \Leftrightarrow \ \Sigma \in \partial {\mathcal{X}_K}^*(\dot{P})\,, \tag{3.27}$$

where the set $\partial {\mathcal{X}_K}^*(\dot{P})$ reads

$$\partial {\mathcal{X}_K}^*(\dot{P}) = \{\mathcal{T} \in \mathbb{R}^{3\times3}_{\mathrm{sym}} \times \mathbb{R} \mid {\mathcal{X}_K}^*(Q) \geq {\mathcal{X}_K}^*(\dot{P}) + \langle \mathcal{T}\,,\, Q - \dot{P}\rangle \quad \forall\, Q \in \mathbb{R}^{3\times3}_{\mathrm{sym}} \times \mathbb{R}\}\,. \tag{3.28}$$

The system (3.26) may thus be equivalently formulated in the following way:

Classical Formulation of Plasticity II with Isotropic Hardening

Let f, g, u_D, and $P_0 = (p_0, \gamma_0)$ be given. Find u, $P = (p, \gamma)$, and $\Sigma = (\sigma, \alpha)$, which satisfy

$$\begin{aligned}
-\operatorname{div}\sigma(x,t) &= f(x,t) && (x,t) \in \Omega \times \Theta\,, \\
\sigma &= \mathbb{C}\left(\varepsilon(u) - p\right)\,, \\
\alpha &= -\gamma\,, \\
\varepsilon(u) &= \tfrac{1}{2}\left(\nabla u + \nabla u^T\right)\,, \\
\Sigma(x,t) &\in \partial \mathcal{X}_K{}^*(\dot{P}) && (x,t) \in \Omega \times \Theta\,, \\
u(x,t) &= u_D(x,t) && (x,t) \in \Gamma_D \times \overline{\Theta}\,, \\
\sigma(x,t)\,n(x,t) &= g(x,t) && (x,t) \in \Gamma_N \times \overline{\Theta}\,, \\
P(x,0) &= P_0(x) && x \in \overline{\Omega}\,.
\end{aligned} \tag{3.29}$$

Here, the set $\partial\mathcal{X}_K{}^*(\dot{P})$ is defined in (3.28).

The explicit form of the dissipation functional $\mathcal{X}_K{}^*$ is presented in the following Lemma:

Lemma 3.2. *Let the functional $\mathcal{X}_K{}^* : \mathbb{R}^{3\times3}_{sym} \times \mathbb{R} \to \overline{\mathbb{R}}$ be defined according to Definition 2.5 and Definition 2.7, and let the convex set K be defined as in* (3.22) *by the yield functional ϕ in* (3.23) *for a certain choice of $\sigma_y \in \mathbb{R}^+$ and $H \in \mathbb{R}^+$.*

Then, there holds

$$\mathcal{X}_K{}^*(\dot{P}) = \mathcal{X}_K{}^*(\dot{p}, \dot{\gamma}) = \begin{cases} \sigma_y\,\|\dot{p}\|_F\,, & \textit{if } [\ \operatorname{tr}\dot{p} = 0\ ] \wedge [\ \dot{\gamma} + H\,\sigma_y\,\|\dot{p}\|_F \le 0\ ]\,, \\ +\infty\,, & \textit{else}\,. \end{cases} \tag{3.30}$$

Proof. The proof is analogue to the proof of Lemma 3.1. The definition of the conjugate functional in Definition 2.7 yields

$$\mathcal{X}_K{}^*(\dot{P}) = \sup_{\Sigma \in \mathbb{R}^{3\times3}_{\mathrm{sym}} \times \mathbb{R}} \Big(\langle \dot{P}\,,\,\Sigma\rangle - \mathcal{X}_K(\Sigma)\Big)\,,$$

which, due to the definition of the indicator functional $\mathcal{X}_K$ in Definition 2.5 is equivalent to

$$\mathcal{X}_K{}^*(\dot{P}) = \sup_{\Sigma \in K} \langle \dot{P}\,,\,\Sigma\rangle\,.$$

In the first instance we will show

$$\mathcal{X}_K{}^*(\dot{P}) = \mathcal{X}_K{}^*(\dot{p}, \dot{\gamma}) \ge \begin{cases} \sigma_y\,\|\dot{p}\|_F\,, & \text{if } [\ \operatorname{tr}\dot{p} = 0\ ] \wedge [\ \dot{\gamma} + H\,\sigma_y\,\|\dot{p}\|_F \le 0\ ]\,, \\ +\infty\,, & \text{else}\,, \end{cases} \tag{3.31}$$

and then finally,

$$[\ \operatorname{tr}\dot p = 0\ ] \wedge [\ \dot\gamma + H\,\sigma_y\,\|\dot p\|_F \le 0\ ] \ \Rightarrow\ [\ \mathcal{X}_K{}^*(\dot p) \le \sigma_y\,\|\dot p\|_F\ ]\,. \tag{3.32}$$

Since $\Sigma = (\sigma, \alpha) = (c\,I, 0)$, with $c \in \mathbb{R}$ and I denoting the identity, is in K, there holds

$$\mathcal{X}_K{}^*(\dot P) = \sup_{\Sigma\in K} \langle \dot P\,,\,\Sigma\rangle \ge \sup_{c\in\mathbb{R}} \langle c\,\dot p\,,\,I\rangle_F = \sup_{c\in\mathbb{R}} (c\,\operatorname{tr}\dot p) = \begin{cases} 0\,, & \text{if } \operatorname{tr}\dot p = 0\,,\\ +\infty\,, & \text{else}\,. \end{cases}$$

Let $\dot p$ be such, that $\operatorname{tr}\dot p = 0$, which implies $\operatorname{dev}\dot p = \dot p$. The specific choice of $\bar\Sigma = (\bar\sigma, \bar\alpha)$ with $\bar\sigma = \sigma_y\,(1 + H\,\bar\alpha)\,\dot p\,\|\dot p\|_F^{-1}$ and $\bar\alpha \in \mathbb{R}_0^+$ is in K, since

$$\|\operatorname{dev}\bar\sigma\|_F = \sigma_y\,(1 + H\,\bar\alpha)\,\|\operatorname{dev}\dot p\|_F \|\dot p\|_F^{-1} = \sigma_y\,(1 + H\,\bar\alpha)\,.$$

Moreover, if $\dot P = (\dot p, \dot\gamma)$ is such, that $\dot\gamma + H\,\sigma_y\,\|\dot p\|_F \le 0$, the choice of $\bar\Sigma$ yields

$$\mathcal{X}_K{}^*(\dot P) = \sup_{(\sigma,\alpha)\in K} (\langle \dot p\,,\,\sigma\rangle_F + \dot\gamma\,\alpha) \ge \langle \dot p\,,\,\bar\sigma\rangle_F + \dot\gamma\,\bar\alpha \ge \sigma_y\,\|\dot p\|_F + (\sigma_y\,H\,\|\dot p\|_F + \dot\gamma)\,\bar\alpha \ge \sigma_y\,\|\dot p\|_F\,,$$

whence there holds (3.31). It remains to show (3.32).

Let $\sigma_y\,H\,\|\dot p\|_F + \dot\gamma \le 0$ and $\dot p$ such, that $\operatorname{tr}\dot p = 0$, which implies

$$\langle \dot p\,,\,\sigma\rangle_F = \langle \operatorname{dev}\dot p\,,\,\sigma\rangle_F = \langle \dot p\,,\,\operatorname{dev}\sigma\rangle_F$$

for all $\sigma \in \mathbb{R}^{3\times3}_{\mathrm{sym}}$. Thus, there holds

$$\begin{aligned} \mathcal{X}_K{}^*(\dot P) &= \sup_{(\sigma,\alpha)\in K} (\langle \dot p\,,\,\sigma\rangle_F + \dot\gamma\,\alpha) \sup_{(\sigma,\alpha)\in K} (\|\dot p\|_F \|\operatorname{dev}\sigma\|_F + \dot\gamma\,\alpha) \\ &\le \sup_{\alpha\ge0} (\sigma_y\,(1 + H\,\alpha)\,\|\dot p\|_F + \dot\gamma\,\alpha) = \sigma_y\|\dot p\|_F + (\sigma_y\,H\,\|\dot p\|_F + \dot\gamma)\,\sup_{\alpha\ge0}\alpha = \sigma_y\|\dot p\|_F\,, \end{aligned}$$

which completes the proof. □

3.2 The Variational Formulation

The numerical solution of an elastoplastic problem requires a discretization scheme. In this thesis we focus on the implicit (backward) Euler method regarding the discretization in time, and the Finite Element Method for the spatial discretization. Hence, a variational formulation of the problem is required. Throughout the thesis we assume the given data to be sufficiently smooth and integrable. For shorter notation, we omit the dependency of stresses, strains, displacements, and forces on the spatial and temporal variables (x, t).

There are two different variational formulations popular in elastoplasticity [50]: first, the so called primal (variational) formulation, which is derived from the classical formulation in (3.29), and second, the dual (variational) formulation, derived from the classical formulation in (3.26). [1] We shall focus on the primal variational formulation in this work. The interested reader is referred to the monographs [96, 50] regarding the dual variational formulation.

[1] The study of perfect plasticity in the previous section, which lead to the classical formulations (3.16) and (3.12), was helpful for a better understanding of elastoplasticity with hardening. However, in this section the variational formulation is investigated for the case of elastoplasticity with hardening only.

3.2.1 Function Spaces

We utilize the Lebesgue space $Q := [L_2(\Omega)]^{3\times 3}_{\mathrm{sym}}$ and the Sobolev space $V := [H^1(\Omega)]^3$ with the associated scalar products and norms

$$
\begin{aligned}
\langle p\,,\,q\rangle_Q &= \int_\Omega \langle p\,,\,q\rangle_F \,\mathrm{d}x\,, & \|q\|_Q &:= \langle q\,,\,q\rangle_Q^{1/2}\,,\\
\langle u\,,\,v\rangle_V &= \int_\Omega \left(\langle u\,,\,v\rangle_F + \langle \nabla u\,,\,\nabla v\rangle_F\right)\,\mathrm{d}x\,, & \|v\|_V &:= \langle v\,,\,v\rangle_V^{1/2}\,.
\end{aligned}
$$

In order to incorporate Dirichlet boundary conditions in the variational formulation, we define the test space

$$V_0 = \{v \in V \mid v_{|\Gamma_D} = 0\}\,, \tag{3.33}$$

and the hyper plane

$$V_D = \{v \in V \mid v_{|\Gamma_D} = u_D\}\,. \tag{3.34}$$

Moreover, recall the pseudo time interval $\Theta =]0, T[$. We utilize the temporal Lebesgue space $L_2(\Theta\,;\,\bar{X})$ and the temporal Sobolev space $H^1(\Theta\,;\,\bar{X})$, where $\bar{X} \subset X$ is an arbitrary subspace of a Sobolev or Lebesgue subspace X (e.g., V, Q or V_0). The respective scalar products and norms read

$$
\begin{aligned}
\langle u\,,\,v\rangle_{L_2(\Theta\,;\,X)} &= \int_\Theta \langle u\,,\,v\rangle_X \,\mathrm{d}t\,, & \|v\|_{L_2(\Theta\,;\,X)} &= \langle v\,,\,v\rangle_{L_2(\Theta\,;\,X)}^{1/2}\,,\\
\langle u\,,\,v\rangle_{H^1(\Theta\,;\,X)} &= \int_\Theta \left(\langle u\,,\,v\rangle_X + \langle \dot{u}\,,\,\dot{v}\rangle_X\right)\,\mathrm{d}t\,, & \|v\|_{H^1(\Theta\,;\,X)} &= \langle v\,,\,v\rangle_{H^1(\Theta\,;\,X)}^{1/2}\,.
\end{aligned}
$$

Finally, let the temporal Sobolev subspace $H^1_0(\Theta\,;\,\bar{X})$ be defined by

$$H^1_0(\Theta\,;\,\bar{X}) = \{x \in H^1(\Theta\,;\,\bar{X}) \mid x_{|t=0} = 0\}\,,$$

where $x_{|t=0}$ denotes the trace of x on the boundary $\{0\}$ of the time interval Θ.

For simpler notation, we henceforth consider homogeneous initial conditions, and for the moment (as long as we discuss the modeling of time dependent variational formulations) also homogeneous Dirichlet boundary conditions, i. e.,

$$u_D(x,t) = 0 \quad \text{on } \overline{\Theta} \times \Gamma_D\,, \quad P_0(x) = (p_0(x), \gamma_0(x)) = 0 \quad \text{on } \overline{\Omega}\,.$$

The study of inhomogeneous cases is straightforward, but comes with a lot more of technical details which would blear the main ideas. In this scope, the interested reader is referred to the works [59, 58, 50]. As soon as we arrive at time discretized problems, inhomogeneous Dirichlet boundary conditions are again considered, so that the main contribution of this work (in Chapter 4) covers this case as well.

3.2.2 Discretization in Time

The numerical treatment requires a time discretization of the a time-dependent variational formulation. Therefore, let $N_\Theta \in \mathbb{N}$ denote the number of temporal subintervals, $\tau = T/N_\Theta$ the step size, and

$$\Theta_\tau = \{t_k = k\,\tau \;\mid\; k \in \{0,\dots,N_\Theta\}\} \tag{3.35}$$

be a uniform discretization of the closure of the time interval $\overline{\Theta} = [0,T]$. We approximate the respective quantities linearly, e. g., $p(x,t) = \sum_{k=1}^{N_\Theta} p_k(x)\varphi_k(t)$, where $\varphi_k(t)$ denote linear hat functions with $\varphi_k(t_j) = \delta_{jk}$, and the coefficients $p_k(x) = p(x,t_k)$. On each time interval $t \in (t_{k-1}, t_k]$, the temporal derivatives are approximated by the backward difference quotient, e. g.,

$$\dot{p}(x,t) \approx \frac{p_k(x) - p_{k-1}(x)}{\tau}\,.$$

This discretization of a time-dependent problem represents an implicit Euler scheme with fixed step size τ. We consider uniform time discretization in order to shorten the notation a bit. Nonuniform time discretization might be applied as well.

3.2.3 The Primal Formulation

The primal formulation is derived from the Classical Formulation II (3.29). Here, the governing equations are the equilibrium of forces (3.1),

$$-\operatorname{div}\sigma = f\,,$$

and the plastic flow law $\Sigma = (\sigma,\alpha) \in \partial\mathcal{X}_K{}^*(\dot{P})$, which (by definition) means, that the inequality

$$\sigma : (q - \dot{p}) + \alpha\,(\eta - \dot{\gamma}) + \mathcal{X}_K{}^*(\dot{p},\dot{\gamma}) \le \mathcal{X}_K{}^*(q,\eta) \quad \forall (q,\eta) \in \mathbb{R}^{3\times 3}_{\mathrm{sym}} \times \mathbb{R}\,, \tag{3.36}$$

holds, with $\mathcal{X}_K{}^*$ defined as in (3.30).

Concerning the equilibrium of forces, we substitute Hooke's law (3.4) and the additive splitting (3.3), multiply with an arbitrary test function $\bar{v} = (v - \dot{u})$ (where v is arbitrary, but has to vanish at the Dirichlet boundary Γ_D) and integrate over the spatial domain Ω and the temporal domain Θ. After partially integrating with respect to the spatial domain Ω, the equilibrium of forces (3.1) turns into the following variational equation: find $(u,p) \in H^1(\Theta\,;V_0) \times L_2(\Theta\,;Q)$ such that for all $v \in L_2(\Theta\,;V_0)$ there holds

$$\langle \mathbb{C}\,(\varepsilon(u) - p)\;,\,\varepsilon(v) - \varepsilon(\dot{u})\rangle_{L_2(\Theta\,;Q)} = \langle f\,,\,v - \dot{u}\rangle_{L_2(\Theta\,;L_2(\Omega))} + \langle g\,,\,v - \dot{u}\rangle_{L_2(\Theta\,;L_2(\Gamma_N))}\,. \tag{3.37}$$

We turn to the plastic flow rule (3.36), where we substitute Hooke's Law (3.4), the additive splitting of the strain (3.3), and the relation (3.20) between the internal variable γ and the internal force α. After integration over space and time we obtain the following variational inequality: find $(u,p,\gamma) \in L_2(\Theta\,;V_0) \times H_0^1(\Theta\,;Q) \times H_0^1(\Theta\,;L_2(\Omega))$ such that for all $(q,\eta) \in L_2(\Theta\,;Q) \times L_2(\Theta\,;L_2(\Omega))$ there holds

$$\langle \mathbb{C}\,(\varepsilon(u)-p)\ ,\ q-\dot{p}\rangle_{L_2(\Theta\,;Q)} + \langle -\gamma\ ,\ \eta-\dot{\gamma}\rangle_{L_2(\Theta\,;L_2(\Omega))} + \int_\Theta\int_\Omega \mathcal{X}_K{}^*(\dot{p},\dot{\gamma})\,\mathrm{d}x\,\mathrm{d}t \\ \leq \int_\Theta\int_\Omega \mathcal{X}_K{}^*(q,\eta)\,\mathrm{d}x\,\mathrm{d}t\,. \quad (3.38)$$

Summarizing, we are looking for $(u,p,\gamma) \in H_0^1(\Theta\,;V_0) \times H_0^1(\Theta\,;Q) \times H_0^1(\Theta\,;L_2(\Omega))$ such that for all $(v,q,\eta) \in L_2(\Theta\,;V_0) \times L_2(\Theta\,;Q) \times L_2(\Theta\,;L_2(\Omega))$ the equations (3.37) and (3.38) are satisfied. For a unified formulation, we collect the primal and the test variables

$$\begin{aligned} y=(u,p,\gamma) &\in Y = H_0^1(\Theta\,;V_0) \times H_0^1(\Theta\,;Q) \times H_0^1(\Theta\,;L_2(\Omega))\,, \\ z=(v,q,\eta) &\in Z = L_2(\Theta\,;V_0) \times L_2(\Theta\,;Q) \times L_2(\Theta\,;L_2(\Omega))\,, \end{aligned}$$

and define the bilinear forms $a : Y \times Z \to \mathbb{R}$, $b : Y \times Z \to \mathbb{R}$, $c : Y \times Z \to \mathbb{R}$, the linear form $l : Z \to \mathbb{R}$, and the convex functional $\psi : Z \to \overline{\mathbb{R}}$ by

$$\begin{aligned} b(y,z) &= \langle \mathbb{C}\,(\varepsilon(u)-p)\ ,\ \varepsilon(v)\rangle_{L_2(\Theta\,;Q)}\,, \\ c(y,z) &= \langle \mathbb{C}\,(\varepsilon(u)-p)\ ,\ q\rangle_{L_2(\Theta\,;Q)} + \langle -\gamma\ ,\ \eta\rangle_{L_2(\Theta\,;L_2(\Omega))}\,, \\ a(y,z) &= c(y,z)-b(y,z)\,, \\ l(z) &= \langle f\ ,\ v\rangle_{L_2(\Theta\,;L_2(\Omega))} + \langle g\ ,\ v\rangle_{L_2(\Theta\,;L_2(\Gamma))}\,, \\ \psi(z) &= \begin{cases} \int_\Theta\int_\Omega \sigma_y\,\|q\|_F\,\mathrm{d}x\,\mathrm{d}t & \text{if a. e.: } [\operatorname{tr} q = 0] \wedge [\eta + H\,\sigma_y\,\|q\|_F \leq 0]\,, \\ +\infty & \text{else.} \end{cases} \end{aligned}$$

Then we obtain the following variational formulation:

Problem 3.1. Find $y \in Y$, such that for all $z \in Z$ there hold

$$b(y,z-\dot{y}) = l(z-\dot{y})\,, \quad (3.39)$$

$$c(y,z-\dot{y}) + \psi(\dot{y}) \leq \psi(z)\,, \quad (3.40)$$

or, equivalently the subtraction (3.40) - (3.39),

$$a(y,z-\dot{y}) + l(z-\dot{y}) + \psi(\dot{y}) \leq \psi(z)\,. \quad (3.41)$$

Remark 3.1. C. Johnson shows in [58], that this Problem 3.1 is uniquely solvable, if the modulus of hardening H is positive, and if the given data is sufficiently smooth.

After the discretization of Problem 3.1 with respect to time, i. e., after the application of an implicit Euler method with uniform step size τ as discussed in Section 3.2.2, and after some laborious, but elementary calculation, a one-time step problem is obtained, which reads: [2]

[2] Notice, that here we consider the inhomogeneous Dirichlet boundary condition $u_{|\Gamma_D} = u_D$ again.

Problem 3.2. Let Θ_τ denote the set of time steps defined in (3.35). For an arbitrary time step $t_k \in \Theta_\tau$, let the body load $f_k \in L_2(\Omega)$, the surface load $g_k \in L_2(\Gamma_N)$, the previous plastic strain $p_{k-1} \in Q$ and the previous hardening parameter $\gamma_{k-1} \in L_2(\Omega)$ be given. Find the combination of displacement, plastic strain, and hardening parameter $y_k = (u_k, p_k, \gamma_k) \in V_D \times Q \times L_2(\Omega)$, such that for all test functions $z = (v, q, \eta) \in V_D \times Q \times L_2(\Omega)$ there holds

$$a_k(y_k, y_k - z) + l_k(y_k - z) + \psi_k(y_k) \le \psi_k(z)\,. \tag{3.42}$$

Here, the following definitions are used:

$$\begin{aligned} a_k(y_k, z) &= \langle \mathbb{C}\,(\varepsilon(u_k) - p_k)\ ,\ \varepsilon(v) - q\rangle_Q + \langle \gamma_k\ ,\ \eta\rangle_{L_2(\Omega)}\,, && (3.43)\\ l_k(z) &= -\langle f_k\ ,\ v\rangle_{L_2(\Omega)} - \langle g_k\ ,\ v\rangle_{L_2(\Gamma_N)}\,, && (3.44)\\ \psi_k(z) &= \sigma_y\,\|q - p_{k-1}\|_{L_1(\Omega)} + \mathcal{X}_{M_k}(q, \eta)\,, && (3.45) \end{aligned}$$

where $\mathcal{X}_{M_k}(q, \eta)$ denotes the indicator functional (see Definition 2.5) of the set

$$M_k = \{(q, \eta) \in Q \times L_2(\Omega)\ \mid\ a.\ e.: [\mathrm{tr}(q - p_{k-1}) = 0] \wedge [\eta + H\,\sigma_y\,\|q - p_{k-1}\|_F \le \gamma_{k-1}]\}\,.$$

Equation (3.42) is a so called variational inequality of the second kind, and it is known [37, 50], that there exists a unique solution to Problem 3.2. Moreover, it is elementary to show, that Problem 3.2 is equivalent to the following minimization problem [50]:

Problem 3.3. Let Θ_τ denote the set of time steps defined in (3.35). For an arbitrary time step $t_k \in \Theta_\tau$, let the body load $f_k \in L_2(\Omega)$, the surface load $g_k \in L_2(\Gamma_N)$, the previous plastic strain $p_{k-1} \in Q$ and the previous hardening parameter $\gamma_{k-1} \in L_2(\Omega)$ be given. Find the combination of displacement, plastic strain, and hardening parameter $y_k = (u_k, p_k, \gamma_k) \in V_D \times Q \times L_2(\Omega)$, such that for all test functions $z = (v, q, \eta) \in V_D \times Q \times L_2(\Omega)$ there holds

$$\bar{J}_k(y_k) \le \bar{J}_k(z)\,. \tag{3.46}$$

Here, the minimization functional $\bar{J}_k : V_D \times Q \times L_2(\Omega) \to \overline{\mathbb{R}}$ is defined

$$\bar{J}_k(z) = \frac{1}{2}\,a_k(z, z) + \psi_k(z) - l_k(z)\,, \tag{3.47}$$

with the bilinear form a_k, the convex functional ψ_k, and the linear functional l_k from (3.43)–(3.45).

The convex functional $\bar{J}_k$ in Problem 3.3 expresses the mechanical energy of the deformed system at the $k-$th time step. The goal is to find a displacement u_k, a plastic strain p_k, and the hardening parameter γ_k, such that the energy $\bar{J}_k$ is minimized. The minimization with respect to the hardening parameter $\gamma_k \in L_2(\Omega)$ can be calculated analytically, which is due to the simple minimization of the quadratic term η^2 in the energy functional $\bar{J}_k$ under the restriction $(p_k, \eta) \in M_k$. The minimizer $\gamma_k = \tilde{\gamma}_k(p_k)$ depends on the plastic strain p_k, where, $\tilde{\gamma}_k : Q \to L_2(\Omega)$ reads [21]

$$\tilde{\gamma}_k(q) = \gamma_{k-1} - \sigma_y H \|q - p_{k-1}\|_F\,. \tag{3.48}$$

Of course (cf. (3.20)), a minimization with respect to the internal variable γ_k may identified by the minimization with respect to the internal force $\alpha_k = \tilde{\alpha}_k(p_k)$, which is the preferred use in literature. Here the minimizer $\tilde{\alpha}_k : Q \to L_2(\Omega)$ reads

$$\tilde{\alpha}_k(q) = \alpha_{k-1} + \sigma_y H \|q - p_{k-1}\|_F \,. \tag{3.49}$$

By substitution, we end up with the following (equivalent) minimization problem in two variables:

Problem 3.4. Let $k \in \{1, \ldots, N_\Theta\}$ denote a given time step, $p_{k-1} \in Q$ and $\alpha_{k-1} \in L_2(\Omega)$ be given such, that $\alpha_{k-1} \geq 0$ almost everywhere. Define $\bar{J}_k : V \times Q \to \overline{\mathbb{R}}$ by $\bar{J}_k(v, q) := +\infty$ if $\operatorname{tr} q \neq \operatorname{tr} p_{k-1}$, else

$$\begin{aligned} \bar{J}_k(v, q) := \frac{1}{2} \int_\Omega & \langle \mathbb{C}(\varepsilon(v) - q) \,, \varepsilon(v) - q \rangle_F + (\alpha_{k-1} + \sigma_y H \|q - p_{k-1}\|_F)^2 \, \mathrm{d}x \\ & + \int_\Omega \sigma_y \|q - p_{k-1}\|_F \, \mathrm{d}x - \int_\Omega f_k \cdot v \, \mathrm{d}x - \int_{\Gamma_N} g_k \cdot v \, \mathrm{d}s \,. \end{aligned} \tag{3.50}$$

Find $(u_k, p_k) \in V_D \times Q$ such that $\bar{J}_k(u_k, p_k) \leq \bar{J}_k(v, q)$ holds for all $(v, q) \in V_D \times Q$.

Notice, that $\bar{J}_k$ is smooth with respect to the displacements v, but not with respect to the plastic strains q.

Chapter 4

A New Solver for the Primal Formulation

4.1 Deriving a new Minimization Problem

Various strategies have been introduced to solve the Minimization Problem 3.4. C. Carstensen investigated a separated minimization with respect to the displacement v and the plastic strain q alternately and proved the linear convergence of the resulting method in [21]. Another interesting technique is to reduce Problem 3.4 to a minimization problem with respect to the displacements v only. We will make the important observation that such a reduced minimization problem is smooth with respect to the displacements v and its derivative is explicitly computable. To discuss this issue, let us first introduce a more abstract formulation of (3.50). Therefore, we define the $\mathbb{C}$-scalar product, the $\mathbb{C}$-norm, a convex functional ψ_k and a linear functional l_k by the relations

$$\langle q_1\,,\,q_2\rangle_{\mathbb{C}} \;:=\; \int_\Omega \langle \mathbb{C}\,q_1(x)\,,\,q_2(x)\rangle_F\,\mathrm{d}x\,, \qquad \|q\|_{\mathbb{C}} \;:=\; \langle q\,,\,q\rangle_{\mathbb{C}}^{1/2}\,, \tag{4.1}$$

$$\psi_k(q) \;:=\; \begin{cases} \int_\Omega \left(\frac{1}{2}\tilde{\alpha}_k(q)^2 + \sigma_y\|q - p_{k-1}\|_F\right)\,\mathrm{d}x & \text{if } \operatorname{tr} q = \operatorname{tr} p_{k-1}\,, \\ +\infty & \text{else}\,, \end{cases} \tag{4.2}$$

$$l_k(v) \;:=\; \int_\Omega f_k \cdot v\,\mathrm{d}x + \int_{\Gamma_N} g_k \cdot v\,\mathrm{d}s\,, \tag{4.3}$$

where $\tilde{\alpha}_k(q)$ is defined in (3.49). Then the functional $\bar{J}_k(v,q)$ in (3.50) can simply be rewritten as

$$\bar{J}_k(v,q) = \frac{1}{2}\|\varepsilon(v) - q\|_{\mathbb{C}}^2 + \psi_k(q) - l_k(v)\,. \tag{4.4}$$

The following results are formulated for functionals mapping from a Hilbert space $\mathcal{H}$ into the set of extended real numbers $\overline{\mathbb{R}} = \mathbb{R} \cup \{\pm\infty\}$. The Hilbert space $\mathcal{H}$ provides a scalar product $\langle \circ\,,\,\diamond\rangle_{\mathcal{H}}$ and the norm $\|\cdot\|_{\mathcal{H}} := \langle\cdot\,,\,\cdot\rangle_{\mathcal{H}}^{1/2}$. The topological dual space of $\mathcal{H}$ is denoted by $\mathcal{H}^*$. Further, if a function F is Fréchet differentiable, we will denote its derivative in a point x by $DF(x)$ and its differential into the direction y by $DF(x\,;\,y)$.

The following theorem can be seen as a generalization of a work of J. J. Moreau [77]. The precise difference is discussed later in Remark 4.1 on page 34.

Theorem 4.1. *Let $\Phi : \mathcal{H} \to \mathbb{R}$ be a convex and Fréchet differentiable function with the derivative $D\Phi \in \mathcal{H}^*$, and let $\Psi : \mathcal{H} \to \overline{\mathbb{R}}$ be a convex and proper function. We define the functions $f : \mathcal{H} \times \mathcal{H} \to \overline{\mathbb{R}}$ and $F : \mathcal{H} \to \mathbb{R}$ by*

$$f(x, y) := \Phi(x - y) + \Psi(x) \quad \textit{and} \quad F(y) := \inf_{x \in \mathcal{H}} f(x, y)\,. \tag{4.5}$$

Let us assume additionally, that the infimum $F(y)$ is attained for all $y \in \mathcal{H}$, that is, there exists a function $\tilde{x} : \mathcal{H} \to \mathcal{H}$ such that $F(y) = f(\tilde{x}(y), y)$. Then the following statements are valid:

1. *F is convex and continuous in $\mathcal{H}$. If either Φ is strictly convex in $\mathcal{H}$ or Ψ is strictly convex in its effective domain, then F is strictly convex in $\mathcal{H}$.*
2. *The subdifferential of F writes $\partial F(y) = \{-D\Phi(\tilde{x}(y) - y)\}$ for all $y \in \mathcal{H}$.*

Proof. Hence Φ is finite and Ψ is proper, the function $f(\cdot, y) = \Phi(\cdot - y) + \Psi(\cdot)$ is proper with respect to the first argument for all $y \in \mathcal{H}$. Due to the minimization property of $\tilde{x}$, there holds that $\Psi(\tilde{x}(y))$ and $F(y)$ are finite for all $y \in \mathcal{H}$. Thus, F in (4.5) is well defined as a mapping of $\mathcal{H}$ into $\mathbb{R}$. Moreover, we note that $f(\tilde{x}(y), z)$ is finite for all y and z in $\mathcal{H}$. For the convexity of F, we must check that

$$F(ty_1 + (1 - t)y_2) \le tF(y_1) + (1 - t)F(y_2)$$

for all $y_1 \in \mathcal{H}$, $y_2 \in \mathcal{H}$ and $t \in [0, 1]$. Let $\overline{y} := ty_1 + (1 - t)y_2$ and $\overline{x} := t\tilde{x}(y_1) + (1 - t)\tilde{x}(y_2)$. Utilizing the minimization property of $\tilde{x}$ we obtain

$$F(ty_1 + (1 - t)y_2) = F(\overline{y}) = f(\tilde{x}(\overline{y}), \overline{y}) \le f(\overline{x}, \overline{y}). \tag{4.6}$$

Using the structure $f(x, y) = \Phi(x - y) + \Psi(y)$ and the convexity of Φ and Ψ, elementary calculations yield

$$f(\overline{x}, \overline{y}) \le tf(\tilde{x}(y_1), y_1) + (1 - t)f(\tilde{x}(y_2), y_2) = tF(y_1) + (1 - t)F(y_2). \tag{4.7}$$

The substitution of (4.7) in (4.6) proves the convexity of F. If either Φ or $\Psi|_{\mathrm{dom}\,\Psi}$ was strictly convex, the inequality in (4.7) would hold strictly for $y_1 \ne y_2$ and $t \in \,]0, 1[$. As a result, F would be strictly convex. It remains to show, that F is continuous in $\mathcal{H}$. We arbitrarily fix $\hat{x} \in \mathrm{dom}\,\Psi$, $\hat{y} \in \mathcal{H}$, and $\epsilon > 0$. Then, obviously

$$F(y) = \inf_{x \in \mathcal{H}} (\Phi(x - y) + \Psi(x)) \le \Phi(\hat{x} - y) + \Psi(\hat{x}).$$

Since Φ is continuous in $\hat{x} - \hat{y}$, there exists $\delta > 0$, such that for all $y : \|y - \hat{y}\|_{\mathcal{H}} < \delta$ there holds $\Phi(\hat{x} - y) + \Psi(\hat{x}) \le \Phi(\hat{x} - \hat{y}) + \epsilon + \Psi(\hat{x})$. Thus, F is bounded above on the non-empty open set $U := \{y : \|y - \hat{y}\|_{\mathcal{H}} < \delta\}$ and Theorem 2.4 a) concludes the continuity of F in $\mathcal{H}$.

Note, that due to Theorem 2.4 b), the function F is subdifferentiable. Let $y \in \mathcal{H}$, and $G \in \partial F(y)$ be arbitrary. By the definition of the subdifferential, there holds

$$F(y+z) \geq F(y) + \langle G\,,\, z\rangle_{\mathcal{H}} \tag{4.8}$$

for all $z \in \mathcal{H}$. On the other hand, for all $z \in \mathcal{H}$, there holds

$$F(y+z) = f(\tilde{x}(y+z), y+z) \leq f(\tilde{x}(y), y+z)\,. \tag{4.9}$$

Since $f(x,y) = \Phi(x-y) + \Psi(x)$ and Φ is Fréchet differentiable, there exists a function $r : \mathcal{H} \to \mathbb{R}$ with the property $\lim_{z\to 0}|r(z)|/\|z\|_{\mathcal{H}} = 0$ such that

$$f(\tilde{x}(y), y+z) = \underbrace{f(\tilde{x}(y), y)}_{=F(y)} - \langle D\Phi(\tilde{x}(y)-y)\,,\, z\rangle_{\mathcal{H}} + r(z)\,. \tag{4.10}$$

Combining (4.9) and (4.10) we obtain

$$-F(y+z) \geq -F(y) + \langle D\Phi(\tilde{x}(y)-y)\,,\, z\rangle_{\mathcal{H}} - r(z)\,. \tag{4.11}$$

Summation of (4.8) and (4.11) yields $r(z) \geq \langle G + D\Phi(\tilde{x}(y)-y)\,,\, z\rangle_{\mathcal{H}} \geq -r(-z)$ for all $z \in \mathcal{H}$, and thus there holds

$$\lim_{z\to 0} \frac{\langle G + D\Phi(\tilde{x}(y)-y)\,,\, z\rangle_{\mathcal{H}}}{\|z\|_{\mathcal{H}}} = 0\,,$$

which implies $G = -D\Phi(\tilde{x}(y)-y)$. Since G was chosen arbitrarily in $\partial F(y)$, we end up with $\partial F(y) = \{-D\Phi(\tilde{x}(y)-y)\}$. □

Notice, the subdifferential $\partial F(y)$ does not necessarily contain one element only, but depends on the set of functions $\tilde{x}$ satisfying $F(y) = f(\tilde{x}(y), y)$. If $\tilde{x}$ was unique, then $\partial F(y)$ would contain only one subgradient identical to derivative $DF(y)$ according to Theorem 2.4 *c*). We formulate a sufficient condition for the (unique) existence of $\tilde{x}$ under the assumptions of coercivity and lower semicontinuity.

Corollary 4.1 (Moreau). *Let the function $f : \mathcal{H} \times \mathcal{H} \to \overline{\mathbb{R}}$ be defined*

$$f(x,y) = \frac{1}{2}\|x-y\|^2_{\mathcal{H}} + \psi(x) \tag{4.12}$$

where ψ is a convex, proper, l.s.c. and coercive function of $\mathcal{H}$ into $\overline{\mathbb{R}}$. Then $F(y) := \inf_{x\in\mathcal{H}} f(x,y)$ defines a mapping $F : \mathcal{H} \to \mathbb{R}$ and there exists a unique function $\tilde{x} : \mathcal{H} \to \mathcal{H}$ such, that $F(y) = f(\tilde{x}(y), y)$ for all $y \in \mathcal{H}$, and there holds:

1. *F is strictly convex and continuous in $\mathcal{H}$.*

2. *F is Fréchet differentiable with*

$$DF(y) = \langle y - \tilde{x}(y)\,,\, \cdot\rangle_{\mathcal{H}} \in \mathcal{H}^* \quad \textit{for all } y \in \mathcal{H}\,. \tag{4.13}$$

Proof. Let $y \in \mathcal{H}$ be fixed arbitrarily. Then, $f(\cdot, y)$ satisfies the assumptions of Theorem 2.5. Thus, there exists a unique element $\tilde{x}(y) \in \mathcal{H}$ such that $f(\tilde{x}(y), y) = F(y)$. Theorem 4.1 (by choosing $\Phi(z) := \frac{1}{2}\|z\|^2_{\mathcal{H}}$) states, that F is strictly convex, continuous and subdifferentiable with a unique subgradient $\langle y - \tilde{x}(y)\,,\,\cdot\rangle_{\mathcal{H}}$. Together with Theorem 2.4 c) we conclude that F is Fréchet differentiable with $DF(\cdot)$ as in (4.13). $\square$

Remark 4.1. This corollary was first formulated and proved in 1965 by J. J. Moreau [77, 7.d. Proposition], and can be interpreted as an immediate consequence of Theorem 4.1 and Theorem 2.5.

The following Proposition is crucial for the further investigation of elastoplastic problems. Due to Corollary 4.1 the existence of a minimizer with respect to the plastic strain is guaranteed. This induces the definition of a new minimization functional – thus, a new minimization problem for elastoplasticity – in (smooth) dependency on the displacements only.

Proposition 4.1. *Let $t_k \in \Theta_\tau$ from equation* (3.35) *denote the k-th time step, and let $\bar{J}_k$ be defined as in (3.50). Then there exists a unique mapping $\tilde{p}_k : Q \to Q$ satisfying*

$$\bar{J}_k\left(v, \tilde{p}_k\left(\varepsilon\left(v\right)\right)\right) = \inf_{q \in Q} \bar{J}_k\left(v, q\right) \quad \forall v \in V_D\,. \tag{4.14}$$

Let J_k be the mapping of V_D into $\mathbb{R}$ defined by the identity

$$J_k(v) := \bar{J}_k(v, \tilde{p}_k(\varepsilon(v))) \quad \forall v \in V_D\,. \tag{4.15}$$

Then, J_k is strictly convex and Fréchet differentiable. The associated Gâteaux differential reads

$$DJ_k(v\,;\,w) = \langle \varepsilon(v) - \tilde{p}_k(\varepsilon(v))\,,\,\varepsilon(w)\rangle_{\mathbb{C}} - l_k(w) \quad \forall w \in V_0 \tag{4.16}$$

with the scalar product $\langle \circ\,,\,\diamond\rangle_{\mathbb{C}}$ defined in (4.1) and l_k defined in (4.3).

Proof. Recall, that the functional $\bar{J}_k : V \times Q \to \overline{\mathbb{R}}$ defined in (4.4) using (4.1), (4.2), and (4.3) can be decomposed as $\bar{J}_k(v, q) = f_k(\varepsilon(v), q) - l_k(v)$, where the functional $f_k : Q \times Q \to \overline{\mathbb{R}}$ reads as

$$f_k(s, q) := \frac{1}{2}\|q - s\|^2_{\mathbb{C}} + \psi_k(q).$$

Then, Corollary 4.1 states an existence of a unique minimizer $\tilde{p}_k : Q \to Q$ which satisfies the condition $f_k(\varepsilon(v), \tilde{p}_k(\varepsilon(v))) = \inf_{q \in Q} f_k(\varepsilon(v), q)$, where the functional

$$F_k(\varepsilon(v)) := f_k(\varepsilon(v), \tilde{p}_k(\varepsilon(v)))$$

is strictly convex and differentiable with respect to $\varepsilon(v) \in Q$. Since $\varepsilon : v \to \varepsilon(v)$ is a Fréchet differentiable, linear and injective mapping of V_D into Q, the compound functional $F_k(\varepsilon(v))$ is Fréchet differentiable and strictly convex with respect to $v \in V_D$. Considering the Fréchet differentiability and linearity of l_k with respect to $v \in V_D$, we can conclude the strictly convexity and Fréchet differentiability (in V_D) of the functional J_k defined in (4.15). The explicit form of the Gâteaux differential $DJ_k(v\,;\,w)$ in (4.16) results from the linearity of the two mappings l_k and ε, and the Fréchet derivative $DF_k(\varepsilon(v)\,;\,\cdot) = \langle \varepsilon(v) - \tilde{p}_k(\varepsilon(v))\,,\,\cdot\rangle_{\mathbb{C}}$ as in (4.13), combined using the chain rule for functionals. $\square$

Proposition 4.1 tells us, that for each displacement v there exists exactly one plastic strain $\tilde{p}_k(\varepsilon(v))$, such that the energy functional $J(v,q)$ attains its minimum $J(v,\tilde{p}_k(\varepsilon(v)))$. By the definition of $\Delta\tilde{p}_k(\cdot) := \tilde{p}_k(\cdot) - p_{k-1}$, there holds that, for fixed $v \in V_D$, finding the minimizer $\tilde{p}_k(\varepsilon(v))$ of functional $\bar{J}_k(v,q)$ in (3.50) with respect to q is equivalent to finding the minimizer $\Delta\tilde{p}_k(\varepsilon(v))$ of the functional

$$\frac{1}{2}\left(2\mu + \sigma_y^2 H^2\right)\|q\|_Q^2 - \langle \mathbb{C}\left(\varepsilon(v) - p_{k-1}\right)\,,\, q\rangle_Q + \langle \sigma_y\left(1 + \alpha_{k-1}H\right)\,,\, \|q\|_F\rangle_{L_2} \tag{4.17}$$

amongst trace-free elements $q \in Q$.

The explicit form of $\Delta\tilde{p}_k$ is presented in the following theorem, which is a generalization of [5, Proposition 7.1] in the sense that we here analyze the plastic strain field instead of the pointwise value. The validity of the pointwise equalities and inequalities occurring there, has to be understood in accordance with Lebesgue spaces as almost everywhere (denoted a. e.), i.e. up to a set of a zero measure.

Theorem 4.2. *Let $Q = L_2(\Omega)^{3\times 3}_{sym}$, $A \in Q$, $b \in L_2(\Omega)$ with $b(x) > 0$ in Ω, and $\xi \in \mathbb{R}$ with $\xi > 0$. Then there exists exactly one $p \in Q$ with $\|\mathrm{tr}\, p\|_{L_2(\Omega)} = 0$, that satisfies*

$$\langle A - \xi p\,,\, q - p\rangle_Q \le \langle b\,,\, \|q\|_F - \|p\|_F\rangle_{L_2} \tag{4.18}$$

for all $q \in Q$ with $\|\mathrm{tr}\, q = 0\|_{L_2(\Omega)}$. This p is characterized as the minimizer of

$$\frac{\xi}{2}\|q\|_Q^2 - \langle A\,,\, q\rangle_Q + \langle b\,,\, \|q\|_F\rangle_{L_2} \tag{4.19}$$

amongst trace-free elements $q \in Q$, and reads

$$p = \frac{1}{\xi}\max\{0, \|\mathrm{dev}\, A\|_F - b\}\frac{\mathrm{dev}\, A}{\|\mathrm{dev}\, A\|_F} \qquad \text{on } \Omega. \tag{4.20}$$

The minimal value of (4.19), attained for the p given by (4.20), is

$$-\frac{1}{2\xi}\|\max\{0, \|\mathrm{dev}\, A\|_F - b\}\|_{L_2}^2\,. \tag{4.21}$$

Proof. According to Definition 2.8, expression (4.18) states that

$$A - \xi p \in b\,\partial\|\cdot\|_F(p) \tag{4.22}$$

where $\partial\|\cdot\|_F$ denotes the subgradient of the Frobenius norm, and only trace-free arguments are under consideration. The Frobenius norm $\|\cdot\|_F : Q \to \mathbb{R}$ is a convex functional and so is (4.19). The identity (4.22) is equivalent to 0 belonging to the subgradient of (4.19), which characterizes the minimizers of (4.19). Moreover, there holds $\langle A\,,\, q\rangle_Q = \langle \mathrm{dev}\, A\,,\, q\rangle_Q$ for all trace-free elements $q \in Q$, whence the matrix A can be replaced by the matrix $\mathrm{dev}\, A$ in (4.18) and (4.19).

Let us separate the domain Ω into three disjoint subdomains

$$\begin{aligned}\Omega_e &:= \{x \in \Omega \mid \exists \text{ open } \omega \subset \Omega : \; x \in \omega \wedge \|\operatorname{dev} A\|_F - b \leq 0 \text{ in } \omega\}\,,\\ \Omega_p &:= \Omega \setminus \overline{\Omega_e}\,, \quad \Gamma_{ep} := \Omega \setminus (\Omega_e \cup \Omega_p)\,.\end{aligned}$$

Note that Ω_e and Ω_p are open, and it holds $\|\operatorname{dev} A\|_F - b \leq 0$ on Ω_e and $\|\operatorname{dev} A\|_F - b > 0$ on Ω_p. Let us additionally assume, that Γ_{ep} has measure zero. Consequently, the minimization of (4.19) results in finding $p \in Q$ with $\|\operatorname{tr} p\|_{L_2(\Omega)} = 0$, such that the functionals

$$J_i(p) := \frac{\xi}{2}\int_{\Omega_i} \|p\|_F^2 \,\mathrm{d}x - \int_{\Omega_i} \langle \operatorname{dev} A\,,\, p\rangle_F \,\mathrm{d}x + \int_{\Omega_i} b\|p\|_F \,\mathrm{d}x \quad i \in \{e, p\} \tag{4.23}$$

are minimized, or equivalently the inequalities

$$\int_{\Omega_i} \langle \operatorname{dev} A - \xi p\,,\, q - p\rangle_F \,\mathrm{d}x \leq \int_{\Omega_i} b\left(\|q\|_F - \|p\|_F\right) \,\mathrm{d}x \quad i \in \{e, p\} \tag{4.24}$$

are satisfied for all $q \in Q$ with $\|\operatorname{tr} q\|_{L_2(\Omega)} = 0$.

We will show identity (4.20). An application of the pointwise Cauchy-Schwartz inequality $\langle \operatorname{dev} A\,,\, p\rangle_F \leq \|\operatorname{dev} A\|_F \|p\|_F$ yields

$$J_e(p) \geq \frac{\xi}{2}\int_{\Omega_e} \|p\|_F^2 \,\mathrm{d}x + \int_{\Omega_e} \underbrace{(b - \|\operatorname{dev} A\|_F)}_{\geq 0} \|p\|_F \,\mathrm{d}x \geq 0.$$

By choosing $p = 0$ on Ω_e we obtain $J_e(p) = 0$. Therefore,

$$p = 0 \qquad \text{on } \Omega_e \tag{4.25}$$

minimizes J_e in (4.23). Moreover, there holds $p(x) \neq 0$ on Ω_p which we show by contradiction. Choose $\Omega' \subset \Omega_p$ arbitrary and fix. Assuming, that $p = 0$ on Ω' and plugging it into (4.24) for $i = p$ would yield

$$\int_{\Omega'} \langle \operatorname{dev} A\,,\, q\rangle_F \,\mathrm{d}x \leq \int_{\Omega'} b\|q\|_F \,\mathrm{d}x$$

for all trace-free elements $q \in Q$, which satisfy $q = p$ on $\Omega_p \setminus \Omega'$. By the choice of $q = \operatorname{dev} A$ on Ω' one obtains $\int_{\Omega'} \|\operatorname{dev} A\|_F - b \,\mathrm{d}x \leq 0$ and this would be a contradiction to the definition of Ω_p.

Thus there holds $p(x) \neq 0$ and consequently $\partial\|\cdot\|_F(p) = \{p/\|p\|_F\}$ on Ω_p, whence (4.24) with $i = p$ rewrites

$$\int_{\Omega_p} \left(\operatorname{dev} A - \xi\, p - b\,\frac{p}{\|p\|_F}\right) : q \,\mathrm{d}x = 0 \qquad \forall q \in Q\,,\; \|\operatorname{tr} q\|_{L_2(\Omega)} = 0\,.$$

Necessarily, there must hold

$$\operatorname{dev} A - \xi\, p - b\,\frac{p}{\|p\|_F} = 0 \qquad \text{on } \Omega_p\,, \tag{4.26}$$

whence we conclude

$$\|p\|_F = \frac{1}{\xi}\left(\|\operatorname{dev} A\|_F - b\right) . \tag{4.27}$$

Plugging (4.27) into (4.26) yields

$$p = \frac{1}{\xi}\left(\|\operatorname{dev} A\|_F - b\right) \frac{\operatorname{dev} A}{\|\operatorname{dev} A\|_F} \text{ on } \Omega_p. \tag{4.28}$$

Combining the formulas (4.25) and (4.28) we obtain (4.20). Finally, plugging (4.20) into (4.19) yields (4.21). □

We define the trial stress $\tilde{\sigma}_k : Q \to Q$ at the kth time step and the yield function $\phi_{k-1} : Q \to \mathbb{R}$ (cf. (3.23)) at the previous time step by

$$\tilde{\sigma}_k(q) := \mathbb{C}(q - p_{k-1}) \quad \text{and} \quad \phi_{k-1}(\sigma) := \|\operatorname{dev}\sigma\|_F - \sigma_y(1 + H\,\alpha_{k-1})\,. \tag{4.29}$$

After using the substitution $\Delta\tilde{p}_k(\varepsilon(v)) = \tilde{p}_k(\varepsilon(v)) - p_{k-1}$, Theorem 4.2 tells us that for a fixed displacement $v \in V_D$ the minimizer $\tilde{p}_k(\varepsilon(v))$ of (3.50) reads

$$\tilde{p}_k(\varepsilon(v)) = \frac{1}{2\mu + \sigma_y^2 H^2} \max\{0, \phi_{k-1}(\tilde{\sigma}_k(\varepsilon(v)))\} \frac{\operatorname{dev}\tilde{\sigma}_k(\varepsilon(v))}{\|\operatorname{dev}\tilde{\sigma}_k(\varepsilon(v))\|_F} + p_{k-1}\,. \tag{4.30}$$

Therefore, if the minimizer $u_k \in V_D$ of the functional $J_k(\cdot) = \bar{J}_k(\cdot, \tilde{p}_k(\varepsilon(\cdot)))$ in (4.15) is known, then the plastic strain p_k at the time step k is provided by the formula (4.30) as $p_k = \tilde{p}_k(\varepsilon(u_k))$. Notice that the formula (4.30) also satisfies the necessary condition $\operatorname{tr} p_k = \operatorname{tr} p_{k-1}$ to guarantee the minimization property $J_k(u_k) = \bar{J}_k(u_k, p_k) < +\infty$ (cf. (4.4) and (4.2)).

At each time step k the domain Ω can be decomposed into three disjoint parts (see Figure 4.1), analogously to the decomposition we used in the proof to Theorem 4.2:

- $\Omega_k^e(v) := \{x \in \Omega \mid \exists \text{ open } \omega \subset \Omega : \ x \in \omega \wedge \phi_{k-1}(\tilde{\sigma}_k(\varepsilon(v))) \le 0 \ a.\ e. \text{ in } \omega\}$, which is the set of elastic increment points,
- the set of plastic increment points $\Omega_k^p(v) := \Omega \setminus \overline{\Omega_k^e}(v)$,
- and the set of elastoplastic interface points $\Gamma_k^{ep}(v) := \Omega \setminus (\Omega_k^p(v) \cup \Omega_k^e(v))$.

Obviously, both sets $\Omega_k^e(v)$ and $\Omega_k^p(v)$ are open, and there holds

$$\begin{aligned} \phi_{k-1}(\tilde{\sigma}_k(\varepsilon(v))) &\le 0 \quad \text{a. e. in } \Omega_k^e(v), \\ \phi_{k-1}(\tilde{\sigma}_k(\varepsilon(v))) &> 0 \quad \text{a. e. in } \Omega_k^p(v). \end{aligned} \tag{4.31}$$

For a one-time step problem, the sets $\Omega^e(v) := \Omega_1^e(v)$ and $\Omega^p(v) := \Omega_1^p(v)$ specify elastically and plastically deformed parts of the continuum, respectively.

We obtain a smooth minimization problem with respect to the displacement field u_k only:

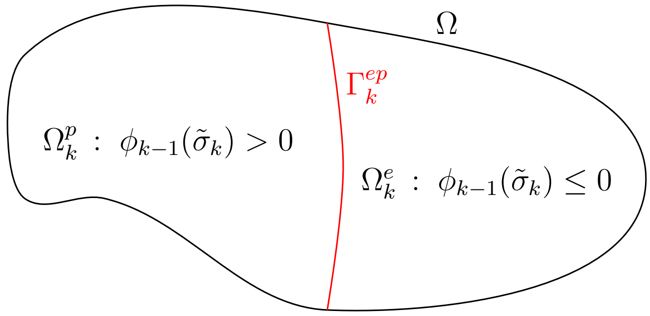

Figure 4.1: Domain decomposition of Ω at the kth time step, generated by the trial stress $\tilde{\sigma}_k(\varepsilon(v))(x)$ with $x \in \Omega$, as an argument of the yield functional ϕ_{k-1} (cf. 4.29). Up to the knowledge of the author, there is nothing known regarding the regularity of the elastoplastic interface $\Gamma_k^{ep}(v)$ in general. In this work, however, it is assumed to be sufficiently smooth and of measure zero.

Problem 4.1. Let $k \in \{1, \ldots, N_\Theta\}$ denote the time step. Let $p_{k-1} \in Q$ and $\alpha_{k-1} \in L_2(\Omega)$ be given, such that $\alpha_{k-1} \geq 0$ almost everywhere. Find $u_k \in V_D$ such that for all $v \in V_D$ there holds $J_k(u_k) \leq J_k(v)$ with the strictly convex and Fréchet differentiable functional J_k defined in (4.15) using $\tilde{p}_k$ as in (4.30). The Gâteaux differential of J_k is presented in (4.16).

Remark 4.2 (unique existence of a solution). We know, that there exists a unique solution (u_k, p_k) to Problem 3.4, and the second component p_k can be calculated by the identity $p_k = \tilde{p}_k(\varepsilon(u_k))$ explicitly. This implies that, due to the definition $J_k(\cdot) = \bar{J}_k(\cdot, \tilde{p}_k(\cdot))$, there holds $J_k(u_k) \leq J_k(v)$ for all $v \in V_D$. Thus, there exists a solution, namely $u_k \in V_D$, to Problem 4.1. The uniqueness of the solution follows from the strict convexity of the energy functional J_k, as it is shown in Proposition 4.1.

4.2 Solution by a Slant Newton Method

The minimizer $\tilde{p}_k$ in (4.30) is a continuous mapping of Q into Q. Thus, $DJ_k(v\,;w)$ in (4.16) is continuous with respect to v as well, and a gradient method could be used for a numerical solution. Instead, we investigate the existence of the second derivative of $J_k(v)$, which would allow the use of Newton's method or at least some Newton-like method.

4.2.1 Pointwise Smoothness results

The Gâteaux differential of DJ_k defined in (4.16) reads

$$D^2 J_k(v\,;\, w_1, w_2) = \langle \varepsilon(w_1) - D\tilde{p}_k(\varepsilon(v)\,;\, \varepsilon(w_1))\,,\, \varepsilon(w_2)\rangle_{\mathbb{C}} \quad \forall w_1, w_2 \in V_0$$

provided that the Gâteaux differential $D\tilde{p}_k : Q \to \mathcal{L}(Q, Q)$ of the plastic strain minimizer $\tilde{p}_k(\varepsilon(v))$ defined in (4.30) exists.

Remark 4.3. Throughout Subsection 4.2.1 we assume, that the total strain $\varepsilon(v)$ and the plastic strain p_{k-1} of the previous time step are piecewise continuous on the domain Ω. Thus, the mapping $\tilde{p}_k$ in (4.30) be seen as a piecewise continuous function on Ω. If so, we are able to discuss its pointwise Fréchet differentiability. The results of this discussion will give us candidates for slanting functions – a semismooth approach which will be discussed in the following two subsections.

Remark 4.4. Note, that the plastic strain minimizer $\tilde{p}_k$ is not Fréchet differentiable as a mapping from the Lebesgue space Q into Q, which is due to the nonlinearity of the mapping (see [69]).

In order to shorten the notation, let us, for the moment, omit the dependency of the strain ε on the displacement v, i. e. we write $\varepsilon(x)$ instead of $\varepsilon(v(x))$. Whenever appropriate, we also skip the dependency on the space variable, and write ε instead of $\varepsilon(x)$.

In the set of elastic increment points $x \in \Omega_k^e$, where we have $\phi_{k-1}(\tilde{\sigma}_k(\varepsilon(x))) \leq 0$, there holds

$$D\tilde{p}_k(\varepsilon(x)\,;\,q) = 0 \tag{4.32}$$

for all $q \in \mathbb{R}^{3\times3}_{\text{sym}}$. Notice, that if $\Omega_k^e = \Omega$, then we obtain the purely elastic case

$$D^2 J_k(v\,;\,w_1, w_2) = \langle \varepsilon(w_1)\,,\,\varepsilon(w_2)\rangle_{\mathbb{C}} \quad \forall w_1, w_2 \in V_0\,.$$

In the set of plastic increment points $x \in \Omega_k^p$, where we have $\phi_{k-1}(\tilde{\sigma}_k(\varepsilon(x))) > 0$, the plastic strain reads (cf. (4.30) and (4.31))

$$\tilde{p}_k(\varepsilon) = (2\mu + \sigma_y^2 H^2)^{-1} \phi_{k-1}(\tilde{\sigma}_k(\varepsilon))\,\frac{\operatorname{dev}\tilde{\sigma}_k(\varepsilon)}{\|\operatorname{dev}\tilde{\sigma}_k(\varepsilon)\|_F}\,.$$

By using the product and the chain rules, for every direction $q \in \mathbb{R}^{3\times3}_{\text{sym}}$ we obtain

$$\begin{aligned} D\tilde{p}_k(\varepsilon\,;\,q) = &\frac{1}{2\mu + \sigma_y^2 H^2}\,\Bigg(D\phi_{k-1}(\tilde{\sigma}_k(\varepsilon)\,;\,D\tilde{\sigma}_k(\varepsilon\,;\,q))\frac{\operatorname{dev}\tilde{\sigma}_k(\varepsilon)}{\|\operatorname{dev}\tilde{\sigma}_k(\varepsilon)\|_F} \\ &+ \phi_{k-1}(\tilde{\sigma}_k(\varepsilon))\; D\frac{(\cdot)}{\|\cdot\|_F}(\operatorname{dev}\tilde{\sigma}_k(\varepsilon)\,;\,D\operatorname{dev}\tilde{\sigma}_k(\varepsilon\,;\,q))\Bigg)\,. \end{aligned}$$

Using the derivatives rules (cf. (4.29))

$$D\tilde{\sigma}_k(\varepsilon\,;\,q) = D\tilde{\sigma}_k(\,q) = \mathbb{C}\,q, \quad D\operatorname{dev}\tilde{\sigma}_k(\varepsilon\,;\,q) = D\operatorname{dev}\tilde{\sigma}_k(\,q) = 2\mu\operatorname{dev} q$$

and

$$D\phi_{k-1}(\sigma\,;\,\tau) = \frac{\langle \operatorname{dev}\sigma\,,\,D\operatorname{dev}(\sigma\,;\,\tau)\rangle_F}{\|\sigma\|_F}\,, \qquad D\frac{(\cdot)}{\|\cdot\|_F}(\sigma\,;\,\tau) = \frac{\tau}{\|\sigma\|_F} - \frac{\sigma\langle\sigma\,,\,\tau\rangle_F}{\|\sigma\|_F^3},$$

we end up with the formula

$$\begin{aligned} D\tilde{p}_k(\varepsilon\,;\,q) \;=\; &\frac{2\mu}{2\mu + \sigma_y^2 H^2}\left(\frac{\phi_{k-1}(\varepsilon)}{\|\operatorname{dev}\tilde{\sigma}_k(\varepsilon)\|_F}\operatorname{dev} q\right. \\ &+ \left.\left(1 - \frac{\phi_{k-1}(\varepsilon)}{\|\operatorname{dev}\tilde{\sigma}_k(\varepsilon)\|_F}\right)\frac{\langle\operatorname{dev}\tilde{\sigma}_k(\varepsilon)\,,\,\operatorname{dev} q\rangle_F}{\|\operatorname{dev}\tilde{\sigma}_k(\varepsilon)\|_F^2}\operatorname{dev}\tilde{\sigma}_k(\varepsilon)\right)\,. \end{aligned} \tag{4.33}$$

The set of elastoplastic interface points Γ_k^{ep} represents the only part of Ω, where $\tilde{p}_k$ in (4.30), due to the term $\max\{0, \phi_{k-1}\}$, is not pointwise differentiable (see Figure 4.1). No matter that the elastoplastic interface is a set of measure zero, a classical Newton method is not applicable to Problem 4.1 - not even after a spatial discretization. However, the difficulties in differentiating the max-term may be overcome by the concept of slanting functions, as discussed in the following subsection.

4.2.2 The Concept of Slant Differentiability

Our goal is to solve Problem 4.1 by means of a Newton-like method which replaces the requirement of the second derivative $D^2 J_k(v)$ on the elastoplastic interface in a way that the local superlinear convergence rate can be shown.

The main tool in order to overcome the non-differentiability of DJ_k due to the mapping $\max\{0, \cdot\}$ is the concept of *slant differentiability*, which was introduced by X. Chen, Z. Nashed and L. Qi in [26]. Other concepts of semismoothness, e. g. [106], or the regularization (smoothing) of the non-differentiable terms, e. g. [63], are not discussed here and might be considered for alternate analysis of elastoplastic problems.

Henceforth, let X, Y, and Z be Banach spaces, and $\mathcal{L}(\circ, \diamond)$ denote the set of all linear mappings of the set $\circ$ into the set $\diamond$.

Definition 4.1 (slant differentiability pointwise)**.** Let $U \subseteq X$ be an open subset and $x \in U$. A function $F : U \to Y$ is said to be *slantly differentiable at* x if there exist

1. mappings $F^o : U \to \mathcal{L}(X, Y)$ and $r : X \to Y$ with $\lim_{h \to 0} \frac{\|r(h)\|}{\|h\|} = 0$ such, that

$$F(x + h) = F(x) + F^o(x + h)\, h + r(h)$$

   holds for all $h \in X$ satisfying $(x + h) \in U$, and

2. constants $\delta > 0$ and $C > 0$ such that for all $h \in X$ with $\|h\| < \delta$ there holds

$$\|F^o(x + h)\| := \sup_{y \in X \setminus \{0\}} \frac{\|F^o(x + h)\, y\|}{\|y\|} \leq C\,.$$

We say, that $F^o(x)$ is a *slanting function for* F *at* x.

Definition 4.2 (slant differentiability in an open set)**.** Let $U \subseteq X$ be an open subset. A function $F : U \to Y$ is said to be *slantly differentiable in* U if there exists $F^o : U \to \mathcal{L}(X, Y)$ such that F^o is a slanting function for F at every point $x \in U$. F^o is said to be a *slanting function for* F *in* U. The set of all functions which are slantly differentiable in U and map to Y is denoted by $\mathcal{S}(U, Y)$.

Remark 4.5. In analogy to the relation between Gâteaux differential and Gâteaux derivative, we define the *slanting differential for* F^o *at* x *along the direction* h by $\tilde{F}^o : U \times X \to Y$ with $\tilde{F}^o(x\,;\,h) := F^o(x)h$. Since the mappings F^o and $\tilde{F}^o$ are taking a different number of arguments, it is sufficient, if we characterize both by the same denomination F^o and forget about $\tilde{F}^o$. In other words, we shall write $F^o(\cdot)$ for a slanting function and $F^o(\circ\,;\diamond)$ for the appropriate slanting differential for F.

Theorem 4.3. *Let $U \subseteq X$ be an open subset, and $F : U \to Y$ be a slantly differentiable function with a slanting function $F^o : U \to \mathcal{L}(X,Y)$. We suppose, that $x^* \in U$ is a solution to the nonlinear problem $F(x) = 0$. If $F^o(x)$ is non-singular for all $x \in U$ and $\{\|F^o(x)^{-1}\| : x \in U\}$ is bounded, then the Newton-like iteration*

$$x^{j+1} = x^j - F^o(x^j)^{-1}F(x^j) \tag{4.34}$$

converges super-linearly to x^*, provided that $\|x^0 - x^*\|$ is sufficiently small.

Proof. See [26, Theorem 3.4] or [52, Theorem 1.1]. □

Our goal is to solve the smooth minimization problem in the displacement (Problem 4.1) by finding $u_k \in V_D$ such, that $DJ_k(u_k;w) = 0$ for all $w \in V_0$ with DJ_k as in (4.16). Therefore, we use the Newton-like method (4.34) with the choice

$$X = V\,, \qquad Y = {V_0}^*\,, \qquad U = V_D\,, \qquad F = DJ_k\,, \qquad x^j = v^j\,, \qquad \text{and} \qquad x^* = u_k\,.$$

The iteration scheme for the Newton-like method is formulated either as an operator equation in ${V_0}^*$ or in variational form: find v^{j+1} in V_D such that there holds

$$(DJ_k)^o\,(v^j\,;\,v^{j+1} - v^j) = -DJ_k(v^j)\,, \tag{4.35}$$

or equivalently,

$$(DJ_k)^o\,(v^j\,;\,v^{j+1} - v^j\,,\,w) = -DJ_k(v^j\,;\,w) \quad \forall w \in V_0\,. \tag{4.36}$$

It is still unclear, if a slanting function $(DJ_k)^o$ for the residual DJ_k exists. If it exists, the super-linear convergence of the Newton-like iteration scheme (4.35) or (4.36) can be shown by Theorem 4.3.

4.2.3 Slanting Functions in Elastoplasticity

It will turn out in this subsection, that a slanting function $(DJ_k)^o$ for the mapping DJ_k, defined in (4.16), does - in general - not exist. We will outline the difficulties in detail, and formulate an assumption, under which a slanting function can be found. However, in the spatially discretized case (see Chapter 5) the existence and the explicit form of a slanting function can be proven rigorously without any assumptions by the results of this subsection.

The motivation, to study the slant differentiability of DJ_k in the spatially continuous case, is the following: If there existed a slanting function for DJ_k, then the resulting slant Newton method (4.36) converges locally super-linear to the solution of the elastoplastic Problem 4.1 with a certain number $N \in \mathbb{N}$ of iteration steps. It would follow, that the number of iteration steps for the spatially discretized problems is bounded from above by N (see [16]).

Let us now calculate candidates for a slanting function $(DJ_k)^o$ for DJ_k in V_D, which uses the minimizer $\tilde{p}_k : Q \to Q$ defined as in (4.30). Notice, that a Fréchet differentiable function is slantly differentiable, with the Fréchet derivative serving as a slanting function, and the Gâteaux differential serving as a slanting differential. Due to the chain rule for slanting functions (Theorem A.1 in the Appendix) we obtain, that

$$(DJ_k)^o\,(v\,;\,w_1, w_2) = \int_\Omega \mathbb{C}\,[\varepsilon(w_1) - \tilde{p_k}^o(\varepsilon(v)\,;\,\varepsilon(w_1))] : \varepsilon(w_2)\,\mathrm{d}x \tag{4.37}$$

for all w_1 and w_2 in V_0 serves as a slanting function for DJ_k in (4.16), if $\tilde{p_k}^o$ serves as a slanting function for $\tilde{p}_k$.

Due to the chain rule and the product rule for slanting functions (Theorem A.1 and Theorem A.2 in the Appendix), and under the assumption, that all subterms are slantly differentiable (note, that a Fréchet derivative serves as a slanting function), a possible candidate for a slanting function $\tilde{p}_k^o$ for $\tilde{p}_k$ would have to satisfy

$$\tilde{p_k}^o(\varepsilon(v)\,;\,q) = \begin{cases} 0 & \text{in } \Omega_k^e(v)\,, \\ \xi\left(\beta_k \operatorname{dev} q + (1-\beta_k)\,\frac{\langle \operatorname{dev}\tilde{\sigma}_k\,,\,\operatorname{dev} q\rangle_F}{\|\operatorname{dev}\tilde{\sigma}_k\|_F^2}\operatorname{dev}\tilde{\sigma}_k\right) & \text{in } \Omega_k^p(v)\,, \end{cases} \tag{4.38}$$

for all $q \in Q$. Here, the abbreviations

$$\xi := \frac{2\mu}{2\mu + \sigma_y^2 H^2}, \quad \beta_k := \frac{\phi_{k-1}(\tilde{\sigma}_k)}{\|\operatorname{dev}\tilde{\sigma}_k\|_F}, \quad \tilde{\sigma}_k := \tilde{\sigma}_k(\varepsilon(v(x))) \tag{4.39}$$

with the mappings ϕ_{k-1} and $\tilde{\sigma}_k$ defined in (4.29) are used. Since the modulus of hardening H, the yield stress σ_y, and the Lamé parameter μ are positive and due to (3.49), (4.29) and (4.31), we always have

$$\xi \in \,]0,1[\qquad \text{and} \qquad \beta_k : \Omega_k^p(v) \to \,]0,1[\;. \tag{4.40}$$

M. Hintermüller, K. Ito and K. Kunisch discuss the slant differentiability of the mapping $\max\{0, y\}$ for certain Banach spaces, that is, for the finite dimensional case $y \in \mathbb{R}^n$ in [52, Lemma 3.1], and the infinite dimensional case $y \in L_q(\Omega)$ in [52, Proposition 4.1]. Let us summarize their results in the following two theorems.

Theorem 4.4 (The finite dimensional case)**.** *Let $n \in N$ be arbitrary, and F be a mapping of $\mathbb{R}^n$ into $\mathbb{R}^n$ defined as $F(y) := \max\{0, y\}$. Then, F is slantly differentiable, and, for all $\gamma = (\gamma_1, \dots, \gamma_n)^T \in \mathbb{R}^n$, the matrix valued function*

$$F^o(y) := \operatorname{diag}\left(f_i(y_i)\right)_{i=1}^n \quad \textit{with} \quad f_i(z) = \begin{cases} 0 & \textit{if } z < 0\,, \\ 1 & \textit{if } z > 0\,, \\ \gamma_i & \textit{if } z = 0\,, \end{cases} \tag{4.41}$$

serves as a slanting function.

The next theorem addresses the slant differentiability of the mapping $\max\{0, y\}$ in the infinite dimensional case $y \in L_q(\Omega)$. Therefore we require a decomposition of the domain Ω into three distinct subspaces $\Omega = \Omega_{\leq} \cup \Gamma_{|} \cup \Omega_{>}$, where $\Omega_{>}$ denotes the union of all open subsets of Ω satisfying $y(x) > 0$ a. e., $\Omega_{\leq}$ is the interior of the complement of $\Omega_{>}$ with respect to Ω, and $\Gamma_{|}$ denotes the interface between $\Omega_{>}$ and $\Omega_{\leq}$.

Theorem 4.5 (The infinite dimensional case)**.** *Let p and q in $\mathbb{R}$ be fixed arbitrarily such that $1 \leq p \leq q \leq +\infty$ is satisfied, and let F be a mapping of $L_q(\Omega)$ into $L_p(\Omega)$ defined as $F(y) := \max\{0, y\}$. Then there holds, that for γ fixed arbitrarily in $\mathbb{R}$, the function*

$$F^o(y)(x) := \begin{cases} 0 & \text{on } \Omega_{\leq}\,, \\ 1 & \text{on } \Omega_{>}\,, \\ \gamma & \text{on } \Gamma_{|}\,, \end{cases} \tag{4.42}$$

serves as a slanting function for F if $p < q$, but F^o does in general not serve as a slanting function for F if $p = q$.

Theorem 4.5 is a surprising result, since operators from one Lebesgue space into another Lebesgue space are Fréchet differentiable if and only if they are linear operators [69].

By the use of these results and the following assumption, we are able to find a slanting function for $\tilde{p}_k$ from (4.30), and thus for DJ_k from (4.16).

Assumption 4.1. For each time step $t_k \in \Theta_\tau$ (see (3.35)) there exists a positive number $\delta_k \in \mathbb{R}^+$, and a subset $V^k \subset V$, which induces the subsets

$$\begin{aligned} Q^k &= \{q \in Q \mid \exists v \in V^k : \varepsilon(v) = q\} \subset Q\,, \\ L_2^k(\Omega) &= \{\eta \in L_2(\Omega) \mid \exists q \in Q^k : \|q\|_F = \eta\} \subset L_2(\Omega)\,, \end{aligned}$$

such that for $\alpha_{k-1} \in L_2^{k-1}(\Omega)$ and $p_{k-1} \in Q^{k-1}$ the mapping $\phi_{k-1} \circ \tilde{\sigma}_k$, defined as in (4.29), is slantly differentiable as a mapping from Q^k into $L_{2+\delta}(\Omega)$, and the mapping $(\cdot)/\|\cdot\|_F$ is slantly differentiable from Q^k into $[L_\infty(\Omega)]^{3\times 3}_{\text{sym}}$.

Remark 4.6. Assumption 4.1 is not needed in the spatially discrete case, since there, the max-function is slantly differentiable from $\mathbb{R}$ to $\mathbb{R}$ without any extra assumptions (see Theorem 4.4), and the argument $\phi_{k-1} \circ \tilde{\sigma}_k$ of the max-function in formula (4.30) is continuously differentiable. In other words, all the following results of this subsection can be shown for the spatially discrete case (in Chapter 5) by the same techniques and without the use of Assumption 4.1.

Following, we shall denote $V_0^k = V_0 \cap V^k$ and $V_D^\delta = V_D \cap V^k$.

Corollary 4.2. *Let Assumption 4.1 be fulfilled, let $t_k \in \Theta_\tau$ as in* (3.35)*, let $v \in V_D^k$, $p_{k-1} \in Q^{k-1}$, and $\alpha_{k-1} \in L_2^k(\Omega)$ be fixed arbitrarily. Then, the mapping*

$$\tilde{p}_k : Q^k \to Q$$

defined as in (4.30) is slantly differentiable at $\varepsilon(v(x))$. *The mapping*

$$\tilde{p_k}^o(\varepsilon(v(x))\,;\,q) = \begin{cases} \xi\left(\beta_k\ \mathrm{dev}\, q + (1-\beta_k)\ \frac{\langle \mathrm{dev}\,\tilde{\sigma}_k\,,\,\mathrm{dev}\,q\rangle_F}{\|\mathrm{dev}\,\tilde{\sigma}_k\|_F^2}\,\mathrm{dev}\,\tilde{\sigma}_k\right) & \textit{in } \Omega_k^p(v)\,, \\ 0 & \textit{else}\,, \end{cases} \tag{4.43}$$

for all $q \in Q$ *serves as a slanting function for* $\tilde{p}_k$ *at* $\varepsilon(v(x))$, *wherein the abbreviations* (4.39) *together with the definitions* (4.29) *are used. Moreover, the functional* $DJ_k(v)$ *in (4.16) is slantly differentiable from* V_D^δ *into* ${V_0}^*$ *with the slanting function* $(DJ_k)^o\,(v)$ *defined as in (4.37).*

Proof. The result follows immediately by the application of the chain rule and the product rule (Theorem A.1 and Theorem A.2 in the Appendix), Theorem 4.5 (by setting $\gamma = 0$), and Assumption 4.1 to the explicit formula (4.30). □

4.2.4 Proof of Locally Superlinear Convergence

In order to apply Theorem 4.3, the existence and boundedness of the inverse operator $[(DJ_k)^o]^{-1}$ is required. It is proved in detail in Proposition 4.2 on page 46, which uses the boundedness and ellipticity of the bilinear form $(DJ_k)^o\,(v) := (DJ_k)^o\,(v\,;\,\diamond,\circ)$ from the following lemma.

Lemma 4.1. *Let* $k \in \{1,\ldots,N_\Theta\}$ *and* $v \in V_D$ *be fixed arbitrarily, and let the mapping* $(DJ_k)^o : V_D \to \mathcal{L}(V_0, {V_0}^*)$ *be defined* $(DJ_k)^o\,(v) := (DJ_k)^o\,(v\,;\,\diamond,\circ)$ *as in (4.37) with the mapping* $\tilde{p_k}^o$ *as in (4.43). Then there exist positive constants* κ_1 *and* κ_2 *which satisfy*

$$(DJ_k)^o\,(v\,;\,w,w) \;\geq\; \kappa_1\|w\|_V^2 \quad \forall w \in V_0 \quad \textit{(ellipticity)}\,, \tag{4.44}$$

$$(DJ_k)^o\,(v\,;\,w,\overline{w}) \;\leq\; \kappa_2\|w\|_V\|\overline{w}\|_V \quad \forall w,\overline{w} \in V_0 \quad \textit{(boundedness)}\,. \tag{4.45}$$

Proof. Let us recall the definition of $(DJ_k)^o$ in (4.37), i.e.,

$$(DJ_k)^o\,(v\,;\,w,w) = \langle \varepsilon(w) - \tilde{p_k}^o(\varepsilon(v)\,;\,\varepsilon(w))\,,\,\varepsilon(w)\rangle_{\mathbb{C}}\,. \tag{4.46}$$

First, we prove the contractivity of the operator ${p_k}^o(\varepsilon(v),\cdot)$ defined in (4.43) with respect to its second argument: There holds

$$\begin{aligned}
\|\tilde{p_k}^o(\varepsilon(v)\,;\,q)\|_{\mathbb{C}}^2 &= \int_\Omega \langle \mathbb{C}{p_k}^o(\varepsilon(v)\,;\,q)\,,\,{p_k}^o(\varepsilon(v)\,;\,q)\rangle_F\,\mathrm{d}x = 2\mu\int_\Omega \|{p_k}^o(\varepsilon(v)\,;\,q)\|_F^2\,\mathrm{d}x \\
&= \xi^2\,2\mu\int_{\Omega_k^p(v)} \|\beta_k\,\mathrm{dev}\,q + (1-\beta_k)\ \frac{\langle \mathrm{dev}\,\tilde{\sigma}_k\,,\,\mathrm{dev}\,q\rangle_F}{\|\mathrm{dev}\,\tilde{\sigma}_k\|_F^2}\,\mathrm{dev}\,\tilde{\sigma}_k\|_F^2\,\mathrm{d}x \\
&\leq \xi^2\,2\mu\int_\Omega \|\mathrm{dev}\,q\|_F^2 = \xi^2\int_\Omega \langle \mathbb{C}\,\mathrm{dev}\,q\,,\,\mathrm{dev}\,q\rangle_F\,\mathrm{d}x \\
&\leq \xi^2\int_\Omega \langle \mathbb{C}q\,,\,q\rangle_F\,\mathrm{d}x = \xi^2\|q\|_{\mathbb{C}}^2
\end{aligned}$$

for all $q \in Q$, where ξ, β_k, and $\tilde{\sigma}_k$ are defined in (4.39). Then the substitution of this estimate to (4.46) yields

$$(DJ_k)^o\,(v\,;\,w,w) \geq (1-\xi)\|\varepsilon(w)\|_{\mathbb{C}}^2\,,$$

which together with Korn's inequality (there exists a constant $\kappa_1^{\mathrm{e}} > 0$ such, that $\|\varepsilon(w)\|_{\mathbb{C}}^2 \geq \kappa_1^{\mathrm{e}}\|w\|_V^2$ holds for all w in V_0) already provides the ellipticity with the constant

$$\kappa_1 := (1-\xi)\,\kappa_1^{\mathrm{e}}.$$

We show the boundedness (4.45). The Cauchy-Schwartz inequality implies

$$(DJ_k)^o\,(v\,;\,w,\overline{w}) \leq \|\varepsilon(w) - \tilde{p_k}^o(\varepsilon(v)\,;\,\varepsilon(w))\|_{\mathbb{C}}\|\varepsilon(\overline{w})\|_{\mathbb{C}} \quad \forall w,\overline{w} \in V_0\,. \tag{4.47}$$

Then the triangle inequality and the contractivity of $\tilde{p_k}^o$ provide the estimate

$$(DJ_k)^o\,(v\,;\,w,\overline{w}) \leq (1+\xi)\,\|\varepsilon(w)\|_{\mathbb{C}}\|\varepsilon(\overline{w})\|_{\mathbb{C}} \quad \forall w,\overline{w} \in V_0. \tag{4.48}$$

It is well know from linear elasticity, that there exists a constant κ_2^{e}, which satisfies

$$\|\varepsilon(w)\|_{\mathbb{C}}\,\|\varepsilon(\overline{w})\|_{\mathbb{C}} \leq \kappa_2^{\mathrm{e}}\,\|w\|_V\,\|\overline{w}\|_V\,.$$

Thus, (4.45) holds with

$$\kappa_2 = (1+\xi)\,\kappa_2^{\mathrm{e}}. \tag{4.49}$$

□

Remark 4.7. By exploiting the structure of the slanting function $\tilde{p_k}^o(\varepsilon(v);\varepsilon(w))$ the boundedness constant κ_2 from (4.49) can be further improved to

$$\kappa_2 = \kappa_2^{\mathrm{e}}. \tag{4.50}$$

Let us check that for all $w \in V_0$ there holds a. e. in $\Omega_k^p(v)$:

$$\begin{aligned}
\|\tilde{p_k}^o(\varepsilon(v)\,;\,\varepsilon(w))\|_F^2 &= \xi^2\left(\beta_k^2\|\operatorname{dev}\varepsilon(w)\|_F^2 + (1+\beta_k)(1-\beta_k)\frac{\langle \operatorname{dev}\tilde{\sigma}_k\,,\,\operatorname{dev}\varepsilon(w)\rangle_F^2}{\|\operatorname{dev}\tilde{\sigma}_k\|_F^2}\right)\\
&\leq \xi\left(\beta_k\|\operatorname{dev}\varepsilon(w)\|_F^2 + 2(1-\beta_k)\frac{\langle \operatorname{dev}\tilde{\sigma}_k\,,\,\operatorname{dev}\varepsilon(w)\rangle_F^2}{\|\operatorname{dev}\tilde{\sigma}_k\|_F^2}\right)\\
&\leq 2\xi\left(\beta_k\|\operatorname{dev}\varepsilon(w)\|_F^2 + (1-\beta_k)\frac{\langle \operatorname{dev}\tilde{\sigma}_k\,,\,\operatorname{dev}\varepsilon(w)\rangle_F^2}{\|\operatorname{dev}\tilde{\sigma}_k\|_F^2}\right)\\
&= 2\langle \operatorname{dev}\varepsilon(w)\,,\,\tilde{p_k}^o(\varepsilon(v)\,;\,\varepsilon(w))\rangle_F\,,
\end{aligned}$$

where ξ, β_k, and $\tilde{\sigma}_k$ are defined in (4.39). This inequality holds trivially a. e. in $\Omega_k^e(v)$, where $\tilde{p_k}^o(\varepsilon(v)\,;\,\cdot) \equiv 0$. Using the scalar product $\langle \circ\,,\,\diamond\rangle_Q = \int_\Omega \langle \circ\,,\,\diamond\rangle_F\,\mathrm{d}x$, we obtain

$$\|\tilde{p_k}^o(\varepsilon(v)\,;\,\varepsilon(w))\|_Q^2 \leq 2\,\langle \operatorname{dev}\varepsilon(w)\,,\,\tilde{p_k}^o(\varepsilon(v)\,;\,\varepsilon(w))\rangle_Q,$$

which is equivalent thanks to Lemma A.1 to

$$\|\tilde{p_k}^o(\varepsilon(v)\,;\,\varepsilon(w))\|_{\mathbb{C}}^2 \leq 2\,\langle \varepsilon(w)\,,\,\tilde{p_k}^o(\varepsilon(v)\,;\,\varepsilon(w))\rangle_{\mathbb{C}}. \tag{4.51}$$

Due to (4.51), there holds $\|\varepsilon(w) - \tilde{p_k}^o(\varepsilon(v)\,;\,\varepsilon(w))\|_{\mathbb{C}}^2 \leq \|\varepsilon(w)\|_{\mathbb{C}}^2$, which applied to the inequality (4.47) improves the inequality (4.48) and provides the sharper constant (4.50).

Proposition 4.2. *Let $k \in \{1, \dots, N_\Theta\}$ be fixed and the assumptions of Corollary 4.2 be fulfilled. Let the mapping $DJ_k : V_D^k \to {V_0}^*$ be defined by $DJ_k(v) := DJ_k(v\,;\circ)$ as in (4.16), the mapping $(DJ_k)^o : V_D^k \to \mathcal{L}(V_0, {V_0}^*)$ be defined $(DJ_k)^o(v) := (DJ_k)^o(v\,;\diamond,\circ)$ as in (4.37), and let the solution u_k to Problem 4.1 be in $V_D^k \subset V_D$ (see Assumption 4.1). Then the Newton-like iteration*

$$v^{j+1} = v^j - \left[(DJ_k)^o(v^j)\right]^{-1} DJ_k(v^j)$$

converges superlinearly to the solution u_k, provided that $\|v^0 - u_k\|_V$ is sufficiently small.

Proof. We check the assumptions of Theorem 4.3 for the choice $F = DJ_k$. Let $v \in V_D^k$ be arbitrarily fixed. The mapping $(DJ_k)^o(v) : V_0 \to {V_0}^*$ serves as a slanting function for DJ_k at v. Moreover, $(DJ_k)^o(v) : V_0 \to {V_0}^*$ is bijective if and only if there exists a unique element w in V_0 such, that for arbitrary but fixed $f \in {V_0}^*$ there holds

$$(DJ_k)^o(v\,;\, w, \overline{w}) = f(\overline{w}) \quad \forall \overline{w} \in V_0\,. \tag{4.52}$$

Since the bilinear form $(DJ_k)^o(v)$ is elliptic and bounded (Lemma 4.1), we apply the Lax-Milgram Theorem to ensure the existence of a unique solution to (4.52). Finally, the uniform boundedness of $[(DJ_k)^o(\cdot)]^{-1}$ follows from the estimate

$$\begin{aligned}
\|[(DJ_k)^o(v)]^{-1}\|_{L({V_0}^*,V_0)} &= \sup_{w^*\in {V_0}^*} \frac{\|[(DJ_k)^o(v)]^{-1}\, w^*\|_V}{\|w^*\|_{{V_0}^*}} \\
&= \sup_{w\in V_0} \frac{\|w\|_V}{\|(DJ_k)^o(v\,;\,w,\cdot)\|_{{V_0}^*}} = \sup_{w\in V_0} \inf_{\overline{w}\in V_0} \frac{\|w\|_V \|\overline{w}\|_V}{|(DJ_k)^o(v\,;\,w,\overline{w})|} \\
&\qquad\qquad \le \sup_{w\in V_0} \frac{\|w\|_V^2}{|(DJ_k)^o(v\,;\,w,w)|} \le \frac{1}{\kappa_1}\,,
\end{aligned}$$

with κ_1 denoting the v-independent ellipticity constant of Lemma 4.1. □

Summarizing, Problem 4.1 can be iteratively solved by a slant Newton method:

Problem 4.2. Let $t_k \in \Theta_\tau$, defined in (3.35), denote the time step, and let Assumption 4.1 be fulfilled. Let $p_{k-1} \in Q^{k-1}$ and $\alpha_{k-1} \in L_2^{k-1}(\Omega)$ be given, such that $\alpha_{k-1} \ge 0$ almost everywhere. For a given initial value $v^0 \in V_D^k$, iterate $v^j \in V_D^k$ such that

$$(DJ_k)^o(v^j\,;\, v^{j+1} - v^j\,,\, w) = -DJ_k(v^j\,;\, w) \quad \forall w \in V_0\,, \tag{4.53}$$

where DJ_k and $(DJ_k)^o$ are defined in (4.16) and (4.37) using $\tilde{p}_k$ as in (4.30) and $\tilde{p}_k^o$ as in (4.43).

Remark 4.8. The slanting function $(DJ_k)^o$ is the spatially continuous counterpart of the *consistent tangential stiffness matrix* proposed by Simo and Hughes [96].

4.3 Vector Representation

Throughout the following chapters we use a vector representation of the stress and strain tensors of the following kind:

$$\sigma = \begin{pmatrix} \sigma_{11} & \sigma_{12} & \sigma_{13} \\ \sigma_{12} & \sigma_{22} & \sigma_{23} \\ \sigma_{13} & \sigma_{23} & \sigma_{33} \end{pmatrix} \quad \rightarrow \quad \boldsymbol{\sigma} = \begin{pmatrix} \sigma_{11} & \sigma_{22} & \sigma_{33} & \sigma_{23} & \sigma_{13} & \sigma_{12} \end{pmatrix}^T ,$$

$$\varepsilon = \begin{pmatrix} \varepsilon_{11} & \varepsilon_{12} & \varepsilon_{13} \\ \varepsilon_{12} & \varepsilon_{22} & \varepsilon_{23} \\ \varepsilon_{13} & \varepsilon_{23} & \varepsilon_{33} \end{pmatrix} \quad \rightarrow \quad \boldsymbol{\varepsilon} = \begin{pmatrix} \varepsilon_{11} & \varepsilon_{22} & \varepsilon_{33} & 2\,\varepsilon_{23} & 2\,\varepsilon_{13} & 2\,\varepsilon_{12} \end{pmatrix}^T ,$$

$$p = \begin{pmatrix} p_{11} & p_{12} & p_{13} \\ p_{12} & p_{22} & p_{23} \\ p_{13} & p_{23} & p_{33} \end{pmatrix} \quad \rightarrow \quad \mathbf{p} = \begin{pmatrix} p_{11} & p_{22} & p_{33} & 2\,p_{23} & 2\,p_{13} & 2\,p_{12} \end{pmatrix}^T .$$

Hooke's Law (3.4) may then be realized by the matrix-vector multiplication

$$\boldsymbol{\sigma} = C\,(\boldsymbol{\varepsilon} - \mathbf{p}) \ , \quad C = \begin{pmatrix} 2\,\mu + \lambda & \lambda & \lambda & 0 & 0 & 0 \\ \lambda & 2\,\mu + \lambda & \lambda & 0 & 0 & 0 \\ \lambda & \lambda & 2\,\mu + \lambda & 0 & 0 & 0 \\ 0 & 0 & 0 & \mu & 0 & 0 \\ 0 & 0 & 0 & 0 & \mu & 0 \\ 0 & 0 & 0 & 0 & 0 & \mu \end{pmatrix} .$$

The main benefit of using this representation is its comfortable use in the implementation of the numerical solver. Moreover, there are two special cases, where the dimensionality of the problems may be reduced – resulting in a higher efficiency of the numerical solver:

4.3.1 The Plane Strain Model

If the domain Ω is long and has a constant cross section with respect to one of the three space dimensions, and if no body forces, surface forces, or displacements are prescribed in that direction, then the solution u_k will vanish in one, let's say the last, component. Therefore it is sufficient to look for a solution u_k in the space $\left[H^1(\Omega)\right]^2$ instead of $\left[H^1(\Omega)\right]^3$. The domain Ω still has to be considered as a three dimensional object, though.

Consequently, the displacement u and the strain ε, due to (3.2), read (the time- or load-step index k is now omitted)

$$u = \begin{pmatrix} u_1(x) \\ u_2(x) \\ 0 \end{pmatrix} , \quad \varepsilon = \begin{pmatrix} \varepsilon_{11} & \varepsilon_{12} & 0 \\ \varepsilon_{12} & \varepsilon_{22} & 0 \\ 0 & 0 & 0 \end{pmatrix} ,$$

and the stress σ and plastic strain p, due to (3.4) and (4.30), read

$$\sigma = \begin{pmatrix} \sigma_{11} & \sigma_{12} & 0 \\ \sigma_{12} & \sigma_{22} & 0 \\ 0 & 0 & \sigma_{33} \end{pmatrix} , \quad p = \begin{pmatrix} p_{11} & p_{12} & 0 \\ p_{12} & p_{22} & 0 \\ 0 & 0 & p_{33} \end{pmatrix} ,$$

where σ_{33} can be calculated by using σ_{11}, σ_{22}, and σ_{12} (see Table 4.1), as well as p_{33}, since p is trace free, can be calculated by $p_{33} = -(p_{11}+p_{22})$. Therefore, it is sufficient to represent u, ε, p and σ by the vectors

$$\mathbf{u} = \begin{pmatrix} u_1 \\ u_2 \end{pmatrix}, \quad \boldsymbol{\varepsilon} = \boldsymbol{\varepsilon}(\mathbf{u}) = \begin{pmatrix} \varepsilon_{11}(u_1, u_2, 0) \\ \varepsilon_{22}(u_1, u_2, 0) \\ 2\varepsilon_{12}(u_1, u_2, 0) \end{pmatrix}, \quad \mathbf{p} = \begin{pmatrix} p_{11} \\ p_{22} \\ p_{12} \end{pmatrix}, \quad \boldsymbol{\sigma} = \begin{pmatrix} \sigma_{11} \\ \sigma_{22} \\ \sigma_{12} \end{pmatrix}. \tag{4.54}$$

Analogously to the 3D-case, Hooke's Law may be formulated as the matrix-vector multiplication

$$\boldsymbol{\sigma} = C\ (\boldsymbol{\varepsilon} - \mathbf{p})\ , \quad C = \begin{pmatrix} 2\,\mu + \lambda & \lambda & 0 \\ \lambda & 2\,\mu + \lambda & 0 \\ 0 & 0 & \mu \end{pmatrix}.$$

A detailed collection of analogous operations in classical or vector representation – such as norms, traces and deviators – is presented in Table 4.1.

4.3.2 The Plane Stress Model

If the domain Ω is very thin with respect to one of the three space dimensions, and if no body forces, surface forces, or displacements are prescribed in that direction, then the components of the stress tensor with respect to this component, will vanish:

$$\sigma = \begin{pmatrix} \sigma_{11} & \sigma_{12} & 0 \\ \sigma_{12} & \sigma_{22} & 0 \\ 0 & 0 & 0 \end{pmatrix}.$$

Hooke's Law says

$$0 = \sigma_{33} = 2\,\mu\,(\varepsilon_{33} - p_{33}) + \lambda\ \mathrm{tr}\,(\varepsilon - p)\ ,$$

which implies

$$\lambda\ \mathrm{tr}\,(\varepsilon - p) = \frac{2\,\mu\,\lambda}{2\,\mu + \lambda}\,(\varepsilon_{11} - p_{11} + \varepsilon_{22} - p_{22})\ .$$

Hence, by using the representation (4.54), we end up with

$$\boldsymbol{\sigma} = C\ (\boldsymbol{\varepsilon} - \mathbf{p})\ , \quad C = \begin{pmatrix} 2\,\mu + \tilde{\lambda} & \tilde{\lambda} & 0 \\ \tilde{\lambda} & 2\,\mu + \tilde{\lambda} & 0 \\ 0 & 0 & \mu \end{pmatrix},$$

with

$$\tilde{\lambda} = \frac{2\,\mu\,\lambda}{2\,\mu + \lambda}\,.$$

Up to this rescaling of λ, the variational formulation in the plane stress case is identical to the one in the plane strain case, and a slightly modified version Table 4.1 can be used.

Note, that in vector representation (no matter if we consider the plane strain, plane stress, or the full 3D-case), there always holds $\langle \sigma\,,\,\varepsilon\rangle_F = \boldsymbol{\sigma}^T\boldsymbol{\varepsilon}$. For simplicity, we shall consider the plane strain model in vector representation throughout the remaining part of this work. As matter of fact, we no more indicate the use of the vector representation by bold letters.

Classical Representation	Vector Representation
$\varepsilon := \begin{pmatrix} \varepsilon_{11} & \varepsilon_{12} & 0 \\ \varepsilon_{12} & \varepsilon_{22} & 0 \\ 0 & 0 & 0 \end{pmatrix}$	$\boldsymbol{\varepsilon} := \begin{pmatrix} \varepsilon_{11} \\ \varepsilon_{22} \\ 2\,\varepsilon_{12} \end{pmatrix}$
$\sigma_\varepsilon := \mathbb{C}\,\varepsilon = \begin{pmatrix} \sigma_{\varepsilon,11} & \sigma_{\varepsilon,12} & 0 \\ \sigma_{\varepsilon,12} & \sigma_{\varepsilon,22} & 0 \\ 0 & 0 & \sigma_{\varepsilon,33} \end{pmatrix}$ with $\quad \mathbb{C}\,\varepsilon = 2\mu\,\varepsilon + \lambda\ \mathrm{tr}\,\varepsilon\, I$	$\boldsymbol{\sigma}_\varepsilon := \begin{pmatrix} \sigma_{\varepsilon,11} \\ \sigma_{\varepsilon,22} \\ \sigma_{\varepsilon,12} \end{pmatrix} = \underbrace{\begin{pmatrix} \lambda + 2\,\mu & \lambda & 0 \\ \lambda & \lambda + 2\,\mu & 0 \\ 0 & 0 & \mu \end{pmatrix}}_{=:C} \boldsymbol{\varepsilon}\,,$ $\sigma_{\varepsilon,33} = \underbrace{\dfrac{\lambda}{2\ (\lambda+\mu)}}_{=\nu}\ (1 \quad 1 \quad 0)\ \boldsymbol{\sigma}_\varepsilon,\ \ \mathrm{tr}\,\sigma_\varepsilon = \frac{\nu+1}{\nu}\,\sigma_{\varepsilon,33}$
$\mathrm{dev}\,\sigma_\varepsilon = \sigma_\varepsilon - \frac{\mathrm{tr}\,\sigma_\varepsilon}{3}\, I$	$\mathbf{dev}\boldsymbol{\sigma}_\varepsilon := \begin{pmatrix} (\mathrm{dev}\,\sigma_\varepsilon)_{11} \\ (\mathrm{dev}\,\sigma_\varepsilon)_{22} \\ (\mathrm{dev}\,\sigma_\varepsilon)_{12} \end{pmatrix} = \boldsymbol{\sigma}_\varepsilon - \frac{\mathrm{tr}\,\sigma_\varepsilon}{3} \begin{pmatrix} 1 \\ 1 \\ 0 \end{pmatrix},$ thus, $\ \mathbf{dev}\boldsymbol{\sigma}_\varepsilon = \underbrace{\left(I - \dfrac{\nu+1}{3} \begin{pmatrix} 1 & 1 & 0 \\ 1 & 1 & 0 \\ 0 & 0 & 0 \end{pmatrix} \right)}_{=:K} \boldsymbol{\sigma}_\varepsilon$
$p = \begin{pmatrix} p_{11} & p_{12} & 0 \\ p_{12} & p_{22} & 0 \\ 0 & 0 & -(p_{11}+p_{22}) \end{pmatrix}$	$\mathbf{p} := \begin{pmatrix} p_{11} \\ p_{22} \\ p_{12} \end{pmatrix},\ \ \Vert\mathbf{p}\Vert_N^2 := \mathbf{p}^T \underbrace{\begin{pmatrix} 2 & 1 & 0 \\ 1 & 2 & 0 \\ 0 & 0 & 2 \end{pmatrix}}_{=:N} \mathbf{p}\,,$ then: $\quad \Vert\mathbf{p}\Vert_N = \Vert p\Vert_F$
$\sigma_p := \mathbb{C}\,p = \begin{pmatrix} \sigma_{\varepsilon,11} & \sigma_{\varepsilon,12} & 0 \\ \sigma_{\varepsilon,12} & \sigma_{\varepsilon,22} & 0 \\ 0 & 0 & \sigma_{\varepsilon,33} \end{pmatrix}$ with $\quad \mathbb{C}\,p = 2\,\mu\,p + \lambda\,\underbrace{\mathrm{tr}\,p}_{=0}\,I = 2\,\mu\,p$	$\boldsymbol{\sigma}_p := \begin{pmatrix} \sigma_{p,11} \\ \sigma_{p,22} \\ \sigma_{p,12} \end{pmatrix} = 2\,\mu\,\mathbf{p}$ and $\quad \sigma_{p,33} = -\,(1 \quad 1 \quad 0)\ \boldsymbol{\sigma}_p$
$\sigma = \mathbb{C}\ (\varepsilon - p) = \sigma_\varepsilon - \sigma_p$	$\boldsymbol{\sigma} = \boldsymbol{\sigma}_\varepsilon - \boldsymbol{\sigma}_p \quad$ and $\quad \sigma_{33} = \sigma_{\varepsilon,33} - \sigma_{p,33}$
$\mathrm{dev}\,\sigma = \mathrm{dev}\,\sigma_\varepsilon - \underbrace{\mathrm{dev}\,\sigma_p}_{=\sigma_p}\,,$ $\Vert\mathrm{dev}\,\sigma\Vert_F^2 = \sum_{i,j} (\mathrm{dev}\,\sigma)_{ij}^2$	$\mathbf{dev}\boldsymbol{\sigma} = \mathbf{dev}\boldsymbol{\sigma}_\varepsilon - \boldsymbol{\sigma}_p\,,\ \ \Vert\mathrm{dev}\,\sigma\Vert_F = \Vert\mathbf{dev}\boldsymbol{\sigma}\Vert_N\,,$ $(\mathrm{dev}\,\sigma)_{33} = -\,(1 \quad 1 \quad 0)\ \mathbf{dev}\boldsymbol{\sigma}$

Table 4.1: Classical vs. Vector Representation in case of the Plane Strain Model.

Chapter 5

Spatial Discretization

In this chapter, we discuss the spatial discretization of the (elastoplastic) Problem 4.1. Therefore, in order to shorten the notation, we assume, that the domain Ω is a polygonal domain, and that the Dirichlet boundary condition (3.5) is homogeneous ($u_D = 0$).

5.1 Galerkin Scheme

We approximate the space $V = [H^1(\Omega)]^2$ by a sequence of finite dimensional subspaces

$$V_{\mathrm{FE}}^1 \subset V_{\mathrm{FE}}^2 \subset \ldots \subset V_{\mathrm{FE}}^{l-1} \subset V_{\mathrm{FE}}^{l} \subset V_{\mathrm{FE}}^{l+1} \subset \ldots \subset V \tag{5.1}$$

with the property

$$\lim_{l\to\infty} \inf_{w \in V_{\mathrm{FE}}^l} \|v - w\|_V = 0\,, \quad \forall v \in V\,. \tag{5.2}$$

Here, V_{FE}^l is called the subspace of V at level l. Since V_{FE}^l is finite dimensional, there exists $N_l \in \mathbb{N}$ and a basis $\{\psi_1, \ldots, \psi_{N_l}\}$ with $\psi_i \in V$ for all $i \in \{1, \ldots, N_1\}$, such that

$$V_{\mathrm{FE}}^l = \mathrm{span}\{\psi_1, \ldots, \psi_{N_l}\}\,, \quad N_l = \dim V_{\mathrm{FE}}^l\,.$$

Further, we define the subspace

$$V_{\mathrm{FE},0}^l = V_{\mathrm{FE}}^l \cap V_0\,.$$

The finite dimensional approximation spaces regarding the plastic strains and the hardening parameter are defined as

$$\begin{aligned} Q_{\mathrm{FE}}^l &= \{q \in Q \mid \exists v \in V_{\mathrm{FE}}^l : q = \boldsymbol{\varepsilon}(v)\}\,, \\ L_{\mathrm{FE}}^l &= \{\eta \in L_2(\Omega) \mid \exists q \in Q_{\mathrm{FE}}^l : \eta = \|q\|_F\}\,, \end{aligned}$$

where the strain $\boldsymbol{\varepsilon}$ (in vector representation) is defined in (4.54). In this way, the solution to Problem 4.1 is approximated by a solution to

Problem 5.1. Let $t_k \in \Theta_\tau$, defined as in (3.35), denote the time step, and let $l \in \mathbb{N}$ be the level of spatial discretization. Let $p_{k-1} \in Q^l_{\text{FE}}$ and $\alpha_{k-1} \in L^l_{\text{FE}}$ be given, such that $\alpha_{k-1} \geq 0$ almost everywhere. Find $u_k \in V^l_{\text{FE},0}$ such that for all $v \in V^l_{\text{FE},0}$ there holds $J_k(u_k) \leq J_k(v)$ with the strictly convex and Fréchet differentiable functional J_k defined in (4.15) using $\tilde{p}_k$ as in (4.30). The Gâteaux differential of J_k is presented in (4.16).

This problem is solved by the slant Newton scheme (4.53), where the explicit form of the residual DJ_k and the stiffness matrix $(DJ_k)^o$ in the discrete case depends on the special choice of the approximation spaces V^l_{FE}, Q^l_{FE}, and L^l_{FE}. In case of using a low order Finite Element Method (Section 5.2) the explicit formulas are given in (5.9) and (5.10) by using the minimizer with respect of the plastic strain (5.6) and its slanting function (5.11). The respective formulas in the case of high order Finite Elements (Section 5.3) may be obtained analogously.

Remark 5.1. Unlike in the infinite dimensional case, no more assumptions are needed in the finite dimensional case (cf. Assumption 4.1) in order to obtain a slanting function for the residual DJ_k or the plastic strain p_k, respectively. This is because the special choice of discrete spaces V^l_{FE} in the following subsections will be such, that the plastic strain p_k is piecewise continuous on Ω, and therefore a slanting function (cf. Remark 4.8) may be derived pointwise. Hence, the slant Newton method for the elastoplastic problem is well defined and the local super-linear convergence is guaranteed.

5.2 Low Order FEM (h-FEM)

In this section, the reader is assumed to already know the basics of h-FEM (for an introduction on this topic, see [27]). Utilizing this method, we are going to derive the discrete formulas of DJ_k and $(DJ_k)^o$, by which Problem 4.2 finally may be implemented and solved on the computer. The notation in this section is based on the work [4]. In order to keep things simple, we consider the plane strain model only (see Section 4.3). The plane stress case or the fully 3D case can be treated analogously.

Let $\mathcal{T}$ be a γ-shape regular triangulation of Ω, where all elements $T \in \mathcal{T}$ are triangles. The term γ-shape regular means, that the ratio of diameter versus radius of the inscribed circle is uniformly bounded from below by a constant $\gamma > 0$ for all elements $T \in \mathcal{T}$.

Let $\mathcal{E} = \{E\}$ denote the set of all edges and $\mathcal{E}_N = \mathcal{E} \cap \Gamma_N$ be its intersection with the Neumann boundary Γ_N. The vertices of all triangles are collected in the set

$$\mathcal{N} = \{\mathbf{x} \in \mathbb{R}^2 \mid \exists T \in \mathcal{T} : \mathbf{x} \text{ is vertex of } T\}\,.$$

Let $\psi_i : \Omega \to \mathbb{R}$ be an affine linear function on each element $T \in \mathcal{T}$ such that for an arbitrary node $\mathbf{x}_l$ the condition $\psi_i(\mathbf{x}_l) = \delta_{il}$ is satisfied for all $i, l \in \{1, \ldots, |\mathcal{N}|\}$. Further, let e_j denote the j-th unit vector. Then, u_{FE} can be expressed by

$$u_{\text{FE}}(x) := \sum_{i=1}^{|\mathcal{N}|} \sum_{j=1}^{2} u_{i,j} \psi_i(x) e_j\,,$$

where $u_{i,j} := (u(\mathbf{x}_i))_j$, or for short, we can write

$$u_{\mathrm{FE}}(x) = \Psi(x)^T \mathbf{u}$$

by defining

$$\Psi(x) := (\psi_i(x)\, e_j)_{i\in\{1,\ldots,|\mathcal{N}|\},j\in\{1,2\}} \in \mathbb{R}^{2|\mathcal{N}|}$$

and

$$\mathbf{u} := (u_{i,j})_{i\in\{1,\ldots,|\mathcal{N}|\},j\in\{1,2\}} \in \mathbb{R}^{2|\mathcal{N}|}\,.$$

Recalling the notation of Section 5.1, the space V is approximated by the subspace

$$V_{\mathrm{FE}}^l := \{\Psi^T \mathbf{u} \mid \mathbf{u} \in \mathbb{R}^{2|\mathcal{N}|}\}\,.$$

Note, that the dimension of the approximation space is $2|\mathcal{N}|$, which is related to the mesh size h by $h \approx |\mathcal{N}|^{-2}$ in 2D. The term l in V_{FE}^l means, that we have a mesh size of $h = h_0 * 0.5^l$, where h_0 denotes the initial mesh size. In this way, the level l controls the dimension of the approximation space.

Let R_T and R_E be operators which restrict the global vector $\mathbf{u}$ onto a local element T by

$$\mathbf{u}_T = R_T \mathbf{u}\,, \quad \mathbf{u}_E = R_E \mathbf{u}\,. \tag{5.3}$$

Let the fixed triangle $T \in \mathcal{T}$ have the vertices $(\mathbf{x}_\alpha, \mathbf{x}_\beta, \mathbf{x}_\gamma)$ with the coordinates

$$((x_{\alpha,1}, x_{\alpha,2})\,, (x_{\beta,1}, x_{\beta,2})\,, (x_{\gamma,1}, x_{\gamma,2}))\,.$$

Then $\boldsymbol{\varepsilon}(u_{\mathrm{FE}})$ can be calculated on T by

$$\boldsymbol{\varepsilon}(u_h)(\mathbf{x})_{|T} = \begin{pmatrix} \partial_1\psi_\alpha & 0 & \partial_1\psi_\beta & 0 & \partial_1\psi_\gamma & 0 \\ 0 & \partial_2\psi_\alpha & 0 & \partial_2\psi_\beta & 0 & \partial_2\psi_\gamma \\ \partial_2\psi_\alpha & \partial_1\psi_\alpha & \partial_2\psi_\beta & \partial_1\psi_\beta & \partial_2\psi_\gamma & \partial_1\psi_\gamma \end{pmatrix} \begin{pmatrix} u_{\alpha,1} \\ u_{\alpha,2} \\ u_{\beta,1} \\ u_{\beta,2} \\ u_{\gamma,1} \\ u_{\gamma,2} \end{pmatrix},$$

or in a more compact way,

$$\boldsymbol{\varepsilon}(u_h)(x)_{|T} = B\,\mathbf{u}_T\,, \tag{5.4}$$

where the partial derivatives of ψ_α, ψ_β, and ψ_γ can be obtained by

$$\nabla \begin{pmatrix} \psi_\alpha \\ \psi_\beta \\ \psi_\gamma \end{pmatrix} = \begin{pmatrix} 1 & 1 & 1 \\ x_{\alpha,1} & x_{\beta,1} & x_{\gamma,1} \\ x_{\alpha,2} & x_{\beta,2} & x_{\gamma,2} \end{pmatrix}^{-1} \begin{pmatrix} 0 & 0 \\ 1 & 0 \\ 0 & 1 \end{pmatrix}.$$

Integration over body and surface forces may be realized by the midpoint rule. We approximate f_k and g_k by $f_T := f_k(\overline{x}_T)$ and $g_E := g_k(\overline{x}_E)$, where $\overline{x}_T$ and $\overline{x}_E$ denote the center of mass of the element T, and the edge E, respectively. Defining

$$\mathbf{f}_T := \frac{|T|}{3}\, R_T^T\, f_T\,, \quad \text{and} \quad \mathbf{g}_E := \frac{|E|}{2}\, R_E^T\, g_E\,,$$

on each $T \in \mathcal{T}$ and on each $E \in \mathcal{E}_N$ there hold

$$\int_T f^T v_h \, \mathrm{d}x \approx \mathbf{f}_T^T \mathbf{v} \,, \quad \text{and} \quad \int_E g^T v_h \, \mathrm{d}s \approx \mathbf{g}_E^T \mathbf{v} \,. \tag{5.5}$$

The whole integral over Ω can be split into a sum of integrals on single elements $T \in \mathcal{T}$. Therefore, by combining (5.3), (5.4) and (5.5) we obtain from (4.16) the discrete formulation of the energy functional's Gâteaux-differential

$$DJ_k^{\mathrm{FE}}(\mathbf{u}\,;\,\mathbf{v}) := \sum_{T\in\mathcal{T}} \left[|T| \; \left(C\, B\, \mathbf{u}_T - 2\mu\, \tilde{\mathbf{p}}_k(B\, \mathbf{u}_T)\right)^T B\, R_T - \mathbf{f}_T^T \right] \mathbf{v} - \sum_{E\in\mathcal{E}_N} \mathbf{g}_E^T \mathbf{v}$$

with

$$\tilde{\mathbf{p}}_k(B\, \mathbf{u}_T) := \frac{\max\{0, \phi_{k-1}(\mathbf{dev}\tilde{\boldsymbol{\sigma}}_k(B\, \mathbf{u}_T))\}}{2\mu + \sigma_y^2 H^2} \frac{\mathbf{dev}\tilde{\boldsymbol{\sigma}}_k(B\, \mathbf{u}_T)}{\|\mathbf{dev}\tilde{\boldsymbol{\sigma}}_k(B\, \mathbf{u}_T)\|_N} + \mathbf{p}_{k-1}\,, \tag{5.6}$$

where

$$\begin{aligned} \mathbf{dev}\tilde{\boldsymbol{\sigma}}_k(B\, \mathbf{u}_T) \;&:=\; KCB\, \mathbf{u}_T - 2\, \mu\, \mathbf{p}_{k-1}\,, & (5.7)\\ \phi_{k-1}(\mathbf{dev}\tilde{\boldsymbol{\sigma}}_k(B\, \mathbf{u}_T)) \;&:=\; \|\mathbf{dev}\tilde{\boldsymbol{\sigma}}_k(B\, \mathbf{u}_T)\|_N - \sigma_y(1 + H\alpha_{k-1})\,. & (5.8) \end{aligned}$$

Since $DJ_k^{\mathrm{FE}}(\mathbf{u}\,;\,\mathbf{v})$ is a finite dimensional mapping, there exists the Fréchet-derivative

$$DJ_k^{\mathrm{FE}}(\mathbf{u}) = \sum_{T\in\mathcal{T}} \Big(|T| \; \left(CB\, \mathbf{u}_T - 2\mu\, \tilde{\mathbf{p}}_k(B\, \mathbf{u}_T)\right)^T B\, R_T - \mathbf{f}_T \Big) - \sum_{E\in\mathcal{E}_N} \mathbf{g}_E\,. \tag{5.9}$$

Moreover (see Corollary 4.2 and Remark 5.1), the mapping DJ_k^{FE} is slantly differentiable with

$$\left(DJ_k^{\mathrm{FE}}\right)^o(\mathbf{u}) = \sum_{T\in\mathcal{T}} |T|\, R_T^T\, B^T \left(C - 2\mu\, \tilde{\mathbf{p}}_k^o(B\, \mathbf{u}_T)\right)^T B\, R_T \,, \tag{5.10}$$

where due to Theorem 4.4, and the fact, that a Fréchet derivative also is a slanting function (a result from [26]), the mapping

$$\tilde{\mathbf{p}}_k^o(B\, \mathbf{u}_T) = \begin{cases} \xi\, \left((1-\beta_k)\, \frac{\mathbf{dev}\tilde{\boldsymbol{\sigma}}_k \mathbf{dev}\tilde{\boldsymbol{\sigma}}_k^T N}{\|\mathbf{dev}\tilde{\boldsymbol{\sigma}}_k\|_N^2} + \beta_k I \right) KC & \text{if } \phi_k(\tilde{\boldsymbol{\sigma}}_k) > 0\,,\\ 0 & \text{else}\,. \end{cases} \tag{5.11}$$

serves as a slanting function for $\tilde{\mathbf{p}}_k$ defined in (5.6). Here, the definitions $\xi := \frac{1}{2\mu+\sigma_y^2 H^2}$ and $\beta_k := \frac{\phi_{k-1}(\mathbf{dev}\tilde{\boldsymbol{\sigma}}_k)}{\|\mathbf{dev}\tilde{\boldsymbol{\sigma}}_k\|_N}$, and the abbreviation $\mathbf{dev}\tilde{\boldsymbol{\sigma}}_k$ for $\mathbf{dev}\tilde{\boldsymbol{\sigma}}_k(B\, \mathbf{u}_T)$ as in (5.7) are used.

The slant Newton method (see Theorem 4.3) is applied for the calculation of $\mathbf{u} \in \mathbb{R}^{2|\mathcal{N}|}$ such that $DJ_k^{\mathrm{FE}}(\mathbf{u}) = 0$ and $\mathbf{u}$ satisfies the Dirichlet boundary condition:

$$\mathbf{u}^{i+1} = \mathbf{u}^i + \Delta\mathbf{u}^{i+1} \qquad (\forall i \in \mathbb{N}_0), \tag{5.12}$$

where $\Delta\mathbf{u}^{i+1}$ solves

$$\left(DJ_k^{\mathrm{FE}}\right)^o(\mathbf{u}^i)\; \Delta\mathbf{u}^{i+1} = -DJ_k^{\mathrm{FE}}(\mathbf{u}^i)\,. \tag{5.13}$$

Remark 5.2. Note, that the slant Newton iterates (5.12) with (5.13) converge locally super linear to the discrete solution, if the initial error $\|\mathbf{u} - \mathbf{u}_0\|_F$ is sufficiently small. This result can be shown by using Theorem 4.3, since $\left(DJ_k^{\mathrm{FE}}\right)^o(\mathbf{u}^i)$ is positively definite, as can be shown analogously to Lemma 4.1, and the uniform boundedness of the inverse $\left[\left(DJ_k^{\mathrm{FE}}\right)^o(\mathbf{u}^i)\right]^{-1}$ can be shown analogously to Proposition 4.2.

5.3 High Order FEM (p-FEM)

In this section, we will briefly mention the most important definitions and results of high order Finite Element Methods (p-FEM). For more detailed information, the interested reader is referred to the pioneering work [10], and the monograph [93]. Same as in h-FEM, also in p-FEM a γ-shape regular mesh is used, but in contrast to h-FEM, the accuracy of the approximate solution is increased, i. e., the dimension of the finite element space V_{FE}^l is enlarged, by increasing the polynomial degree of the shape functions instead of refining the mesh by the partitioning of elements. The big advantage of a high order method is the faster convergence [9], whereas the major drawback of a high order method is the expensive assembling of the system matrix. As long as this handicap can be settled (e.g., by finding recurrences via symbolic computation [11, 14, 15]), the application of such methods are definitely worth their price. We turn to the basic definition of hierarchic basis functions in p-FEM. Let be mentioned, that in this paper, we concentrate on the Karniadakis-Sherwin polynomials [61]. Before defining the discretization of the vector valued displacement field $u \in [H^1(\Omega)]^2$, the scalar case $u \in H^1(\Omega)$ is discussed.

Let the reference triangle $\hat{K}$ and the reference square $\hat{Q}$ be defined by

$$\hat{K} := \{(x, y) \mid x > -1,\ y > -1,\ x + y < 0\} \quad \text{and} \quad \hat{Q} = (-1, 1)^2 . \tag{5.14}$$

The Duffy transformation $D : \mathbb{R}^2 \to \mathbb{R}^2$, defined by

$$D(\eta_1, \eta_2) = \left(\frac{1}{2}(1 + \eta_1)(1 - \eta_2) - 1\ ,\ \eta_2\right) , \tag{5.15}$$

maps $\hat{Q}$ onto $\hat{K}$. The inverse maps $\hat{K}$ onto $\hat{Q}$ and is given by

$$D^{-1}(\xi_1, \xi_2) = \left(2\frac{1 + \xi_1}{1 - \xi_2} - 1\ ,\ \xi_2\right) .$$

The further proceeding is to define local shape functions Φ on $\hat{Q}$ and then, by the application of the inverse Duffy transformation $\Psi = \Phi \circ D^{-1}$, to obtain local shape functions on the reference triangle $\hat{K}$.

Definition 5.1. Let $\alpha > -1$, $\beta > -1$, and $n \in \mathbb{N} \cup \{0\}$ be given. The polynomial $P_n^{(\alpha,\beta)} : [-1, 1] \to \mathbb{R}$ defined by

$$P_n^{(\alpha,\beta)}(\eta) := \frac{(-1)^n}{2^n\, n!}\,(1 - \eta)^{-\alpha}(1 + \eta)^{-\beta}\,\frac{d^n}{d\eta^n}\left((1 - \eta)^{\alpha+n}(1 + \eta)^{\beta+n}\right) \tag{5.16}$$

is called nth *Jacobi Polynomial with respect to the weight* $(1 - \eta)^\alpha(1 + \eta)^\beta$.

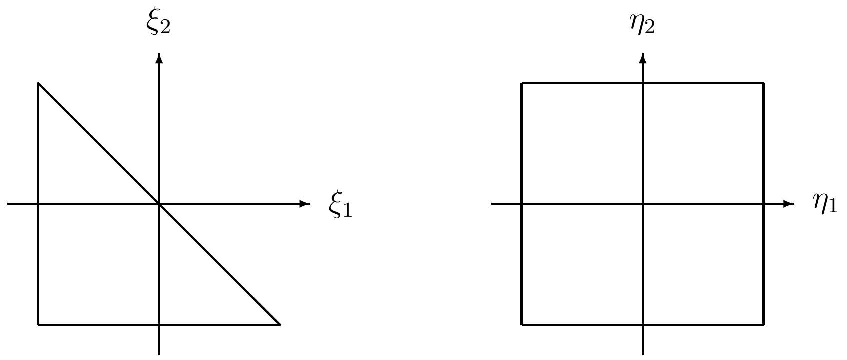

Figure 5.1: The reference elements $\hat{K}$ and $\hat{Q}$ defined in equation (5.14).

Definition 5.2. Let the reference elements $\hat{K}$ and $\hat{Q}$ be given by (5.14) and let the transformation $D : \mathbb{R}^2 \to \mathbb{R}^2$ be defined as in (5.15). For a given polynomial degree $p \in \mathbb{N}$ we define the set $\Psi = \bigcup_{B=1}^{5} \Psi^B$ of local shape functions by

$$\Psi^B := \Phi^B \circ D^{-1} = \{\phi \circ D^{-1} \mid \phi \in \Phi^B\} \quad B = 1, \dots, 5\,, \tag{5.17}$$

where Φ^B is given by:

$$\begin{aligned}
\Phi^1 &= \{\frac{(1-\eta_1)}{2}\frac{(1-\eta_2)}{2}, \frac{(1+\eta_1)}{2}\frac{(1-\eta_2)}{2}, \frac{(1+\eta_2)}{2}\},\\
\Phi^2 &= \{\frac{(1-\eta_1)}{2}\frac{(1+\eta_1)}{2}\frac{(1-\eta_2)}{2}P_{i-1}^{(1,1)}(\eta_1) \mid i = 1, \dots, p-1\},\\
\Phi^3 &= \{\frac{(1+\eta_1)}{2}\frac{(1-\eta_2)}{2}\frac{(1+\eta_2)}{2}P_{i-1}^{(1,1)}(\eta_2) \mid i = 1, \dots, p-1\},\\
\Phi^4 &= \{\frac{(1-\eta_1)}{2}\frac{(1-\eta_2)}{2}\frac{(1+\eta_2)}{2}P_{i-1}^{(1,1)}(\eta_2) \mid i = 1, \dots, p-1\},\\
\Phi^5 &= \{\frac{(1-\eta_1^2)}{4}\frac{(1+\eta_2)}{2}\frac{(1-\eta_2)^{i+1}}{2^{i+1}}P_{i-1}^{(1,1)}(\eta_1)P_{j-1}^{(2i+1,1)}(\eta_2)\\
&\qquad\qquad\qquad\qquad \mid i, j = 1, \dots, p-1\}.
\end{aligned}$$

The subdivision of the shape functions is as follows: The set Φ^1 contains vertex shape functions, which vanish on all vertices, except on one, where the value one is attained. The set Φ^5 contains the interior bubble functions, which vanish on all edges, and the remaining sets Φ^2, Φ^3, Φ^4 contain edge bubble functions, which vanish on all but one edge. In [61] it is shown, that Ψ is a set of linear independent polynomial functions, and that the span of Ψ contains all polynomials of degree p on the reference triangle $\hat{K}$.

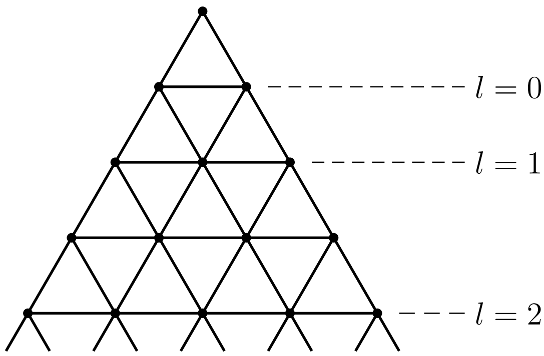

Figure 5.2: Degrees of freedom in case of h-refinement.

In this way we approximate $u \in H^1(\Omega)$ by $u_{\mathrm{FE}} \in S^p(\Omega, \mathcal{T})$ with

$$S^p(\Omega, \mathcal{T}) := \{u \in H^1(\Omega) \mid u \circ F_K \in \operatorname{span}\Psi \text{ for all } K \in \mathcal{T}\}, \tag{5.18}$$

where F_K denotes the mapping from the reference triangle $\hat{K}$ to the local element K. In case of vector valued problems, such as in elastoplasticity, each shape function $\psi \in \Psi$ is replaced by a set of d vector valued shape functions $\{\psi\, e_i \mid i = 1, \ldots, d\}$, where e_i denotes the ith unit vector. Speaking in the notation of Section 5.1, we have $V_{FE}^l = S^{p_l}(\Omega, \mathcal{T})$, where p_l denotes the polynomial degree of level l. In order to keep the property (5.1), one has to guarantee $p_l \geq p_{l-1}$.

When using p-FEM with $p_l = l$, only

$$|V_{\mathrm{FE}}^l| = O(p_l^2) = O(l^2)$$

degrees of freedom have to be computed. Compared to this (compare Figure 5.2), the growth of unknowns in the case of h-FEM with $h_l = 2^{-l}$ is

$$|V_{\mathrm{FE}}^l| = O(2^{1/h_l}) = O(4^l)\,.$$

The a priori error analysis of the high order Finite Element Method [9] states the convergence (for space dimension $d = 2$)

$$\|u - u_{\mathrm{FE}}\|_{H^1(\Omega)} \leq C\, p^{-s}\, \|u\|_{H^{s+1}(\Omega)}$$

if $u \in H^{s+1}(\Omega)^2$, and in the case of singular behavior of the type $u \approx r^\alpha$, $\alpha > 0$, where r is the distance from the singularity, we obtain

$$\|u - u_{\mathrm{FE}}\|_{H^1(\Omega)} \leq C\, p^{-2\alpha}\,,$$

which is logarithmically twice the rate of the h-version [93].

5.4 Combining Low and High Order FEM (*hp*-FEM)

The concept of *hp*-FEM is the adaptive combination *h*-FEM and *p*-FEM. The key idea is to increase the polynomial degree locally on elements, where the solution has high regularity. On such elements we can expect locally up to exponential convergence (see [7, 93]) of the approximate towards the solution. On other elements, where the regularity of the solution is low, mesh refinement, i. e. *h*-FEM, is applied, which locally yields algebraic convergence. Globally, the convergence of *hp*-approximations is much faster than the convergence in *h*-FEM or *p*-FEM, under certain conditions up to exponential convergence can be achieved. The price we pay is, that the method is much harder to implement than *h*- or *p*-FEM. We turn to the definition of the approximation space, which actually will be very much the same as in *p*-FEM.

Let a polynomial degree $p_K \in \mathbb{N}$ be associated with each element $K \in \mathcal{T}$ and the polynomial degree p_e with each edge e by

$$p_e = \min\{p_K \mid e \text{ is an edge of } K\}\,.$$

The information of polynomial degree distribution is collected in a vector $\mathbf{p} = (p_K)_{K\in\mathcal{T}}$, which is called (polynomial) degree vector.

With p_{Ke1}, p_{Ke2}, p_{Ke3}, and p_K denoting the polynomial degree on the edges e_1, e_2, e_3, and in the interior of element K, the set of shape functions Ψ is defined as in Definition 5.2, where Φ^1,…,Φ^5 are given by:

$$\begin{aligned}
\Phi^1 &= \{\frac{(1-\eta_1)}{2}\frac{(1-\eta_2)}{2}, \frac{(1+\eta_1)}{2}\frac{(1-\eta_2)}{2}, \frac{(1+\eta_2)}{2}\},\\
\Phi^2 &= \{\frac{(1-\eta_1)}{2}\frac{(1+\eta_1)}{2}\frac{(1-\eta_2)}{2}P_{i-1}^{(1,1)}(\eta_1) \mid i = 1,\ldots,p_{AB}-1\},\\
\Phi^3 &= \{\frac{(1+\eta_1)}{2}\frac{(1-\eta_2)}{2}\frac{(1+\eta_2)}{2}P_{i-1}^{(1,1)}(\eta_2) \mid i = 1,\ldots,p_{BC}-1\},\\
\Phi^4 &= \{\frac{(1-\eta_1)}{2}\frac{(1-\eta_2)}{2}\frac{(1+\eta_2)}{2}P_{i-1}^{(1,1)}(\eta_2) \mid i = 1,\ldots,p_{CA}-1\},\\
\Phi^5 &= \{\frac{(1-\eta_1^2)}{4}\frac{(1+\eta_2)}{2}\frac{(1-\eta_2)^{i+1}}{2^{i+1}}P_{i-1}^{(1,1)}(\eta_1)P_{j-1}^{(2i+1,1)}(\eta_2)\\
&\qquad\qquad \mid i,j = 1,\ldots,p_K-1\}.
\end{aligned}$$

The approximation space reads

$$S^{\mathbf{p}}(\Omega,\mathcal{T}) := \{u \in H^1(\Omega) \mid u \circ F_K \in \operatorname{span}\Psi \text{ for all } K \in \mathcal{T}\}\,, \tag{5.19}$$

where Ψ depends on p_{Ke1}, p_{Ke2}, p_{Ke3}, and p_K. Referring to Section 5.1, in *hp*-FEM the approximation space is defined $V_{FE}^l = S^{\mathbf{p}_l}(\Omega,\mathcal{T})$, where $\mathbf{p}_l$ denotes the polynomial degree vector of level l. In order to keep the property (5.1), one has to guarantee $\mathbf{p}_l \geq \mathbf{p}_{l-1}$ component wise.

As already mentioned, the *hp*-method is expensive, but the approximate solutions converge very fast. It is even possible to achieve exponential convergence, if the solution is analytic up to point-wise singularities on the boundary (if $\Omega \in \mathbb{R}^2$). Therefore the construction of ideal geometric meshes and the use of linear degree vectors (see Definitions 5.3 and 5.4), is assumed. However, in such cases the convergence rate is globally even exponential ([8], [93, Theorem 4.63])

$$\|u - u_{FE}\|_{H^1(\Omega)} \leq C \exp(-bN^{1/3}), \tag{5.20}$$

where C and b denote some positive constants, and $N = \dim(S^{\mathbf{p}}(\Omega, \mathcal{T}))$ denotes the dimension of the used finite element space.

In elastoplasticity, the solution in each time step is known to be in $H^2_{\mathrm{loc}}(\Omega)$, and analytic in balls where the plastic strain p vanishes [65, 12]. These, so called elastic zones, typically cover the major part of the domain Ω, thus, the application of an hp-FEM is a natural choice. In those parts of the interior domain, where the material reacts purely elastic, the polynomial degree of the shape functions is increased, whereas the mesh is being h-refined in plastic areas and towards rough boundary data or geometry.

Whenever plastic zones are small compared to elastic zones, the application of hp-FEM is worth the cost. However, since the plastic zones are a set of non-zero measure, we cannot expect an exponential convergence rate as in (5.20), but some algebraic convergence which is faster than in both h-FEM and p-FEM.

The basic hp-adaptive algorithm reads as presented in Algorithm 1.

Algorithm 1 The hp-adaptive Algorithm:

Require: A mesh $\mathcal{T}$, a polynomial degree vector $(p_K)_{K\in\mathcal{T}}$, a Finite Element Solution u_{FE}.
Ensure: A refined mesh $\mathcal{T}_{\mathrm{ref}}$, a new polynomial degree vector $(p_K)_{K\in\mathcal{T}_{\mathrm{ref}}}$.

1: Determine which elements to refine $\rightarrow \mathcal{T}_h$.
2: Determine where the polynomial degree should be increased $\rightarrow \mathcal{T}_p$.
3: Obtain a preliminary refined mesh $\rightarrow \mathcal{T}'_{\mathrm{ref}}$.
4: Elimination of hanging nodes $\rightarrow \mathcal{T}_{\mathrm{ref}}$.
5: Increase the polynomial degree $p_K = p_K + 1$ for all elements $K \in \mathcal{T}_{\mathrm{ref}} \cap \mathcal{T}_p$. In particular: Elements to which an h-refinement is applied inherit the polynomial degree from their father.

Note, that Items 3–5 are straight forward, whereas, one still has to decide on the exact realization of Items 1 and 2. In general, the set of all adaptive strategies divides into two classes: strategies which are problem dependent, and those which are not. In problem dependent strategies, the decision whether to refine in h, or in p, or not at all, relies on the evaluation of problem dependent quantities, typically the error estimator. Strategies of this type can be found in [83, 30, 1].

Since the reliability and efficiency of error estimators for elastoplasticity is strongly depending on the amount of hardening (i. e., the size of the hardening module H, which was introduced in (3.23)), the use of problem independent algorithms is a natural choice, wherever the hardening module H is small. Methods as in [32, 33], estimate the regularity of the solution without using problem dependent quantities. The main idea of these strategies is to minimize a local error projection of a reference solution, that is obtained by a uniformly h-refined mesh intermediately. In this way an optimal hp-mesh is produced adaptively. The big advantage of such method is, that no knowledge about the problem has to be passed to the mesh generation, the drawback is to cope with different meshes at the same time, which often is hard to implement on the computer in Finite Element frameworks.

In this paper we choose a strategy of hp-refinement, which is presented in [38]. This strategy was first discussed in [71] for the spectral element method, and later used in [57] for hp-FEM in one dimension (or in more dimensions, where elements have tensor structure). T. Eibner and M. Melenk [38] present the extension of the strategy to hp-FEM for the Poisson problem in more dimensions, i. e., where elements have the shape of triangles and tetrahedrons. Especially two advantages are covered by this approach: First, the algorithm is problem independent (see Remark 5.3), and second, there is no need to handle more than one FE-mesh in the implementation. The algorithm is based on estimating the Sobolev regularity of the solution by a certain L_2-orthogonal polynomial expansion:

Proposition 5.1. *Define on the reference triangle $\hat{K}$ the $L_2(\hat{K})$-orthogonal basis ψ_{pq}, $p, q \in \mathbb{N}_0$ by*

$$\psi_{pq} = \tilde{\psi}_{pq} \circ D^{-1}\,, \quad \tilde{\psi}_{pq} = P_p^{(0,0)}(\eta_1)\left(\frac{1-\eta_2}{2}\right)^p P_q^{(2p+1,0)}(\eta_2)\,,$$

where $P_p^{(\alpha,\beta)}$ is the (well known) p-th Jacobi polynomial with respect to the weight $\eta \mapsto (1-\eta)^\alpha(1+\eta)^\beta$ and D the Duffy transformation. Let $u \in L_2(\hat{K})$ be written as

$$u = \sum_{p,q\in\mathbb{N}_0} u_{pq}\psi_{pq}\,. \tag{5.21}$$

Then u is analytic on $\overline{\hat{K}}$ if and only if there exist constants $C, b > 0$ such that $|u_{pq}| \leq C\,e^{-b(p+q)}$ for all $p, q \in \mathbb{N}_0$.

Proof. See [72]. □

Since the true solution u is not available, the idea for an hp-adaptive algorithm is to estimate the decay of the coefficients u_{pq} of the L_2 conforming expansion of the finite element solution $u_{FE|K} \circ F_K = \sum_{p,q} u_{pq}\psi_{pq}$ instead. If the decay is exponentially, then the polynomial degree p will be increased, otherwise, the mesh will be refined, see Algorithm 2.

Remark 5.3. Note, that in the above algorithm, the use of an a-posteriori error estimator can be switched off by setting $\sigma = 0$, which is recommended for materials without, or small, hardening effects. The crucial part of the algorithm is testing the approximated slope of the expansion coefficients versus a given critical slope b. In this sense, the algorithm is problem independent. However, the use of an a-posteriori error estimator (say the ZZ-error estimator [29]) may nevertheless be of advantage. Particularly if the material shows hardening effects, i. e., if the modulus of hardening H in (3.23) is large.

Algorithm 2 Items 1 and 2 in Algorithm 1:

Require: A mesh $\mathcal{T}$; a polynomial degree vector $(p_K)_{K\in\mathcal{T}}$; parameters $b > 0$ and $\sigma \geq 0$; a Finite Element Solution u_{FE}; a reliable, efficient, and localizable a posteriori error estimator $\eta(u_{\mathrm{FE}})$.

Ensure: The marked elements $\mathcal{T}_p$ and $\mathcal{T}_h$.

1: Compute the mean error $\bar{\eta}^2 = |\mathcal{T}|^{-1} \sum_{K\in\mathcal{T}} \eta_K^2$

2: For elements $K \in \mathcal{T}$ with $\eta_K^2 \geq \sigma\bar{\eta}^2$ compute the expansion coefficients

$$u_{ij,K} = \|\psi_{ij}\|_{L_2(\hat{K})}^{-2} \, \langle u_{\mathrm{FE}|K} \circ F_K \, , \, \psi_{ij}\rangle_{L_2(\hat{K})}$$

for $0 \leq i + j \leq p_K$.

3: Estimate the decay coefficient b_K by a least squares fit of

$$\ln|u_{ij,K}| \approx C_K - b_K(i + j) \, .$$

4: Determine

$$\mathcal{T}_p = \{K \in \mathcal{T} \mid \eta_K^2 \geq \sigma \, \bar{\eta}^2 \wedge b_K \geq b\} \, ,$$
$$\mathcal{T}_h = \{K \in \mathcal{T} \mid \eta_K^2 \geq \sigma \, \bar{\eta}^2 \wedge b_K < b\} \, .$$

In Chapter 6 we compare Algorithm 2 with a standard *hp*-adaptive approach, which is proposed a Series of papers by L. Demkowicz, T. Oden, W. Rachowicz, and coworkers [31, 82, 87] and also used in *hp*-BEM, e. g., [51]. This approach, summarized in Algorithm 3, puts the decision of whether refining in h or in p solely on the local evaluation of an a-posteriori-error-estimator $\eta_K(u_{\mathrm{FE}})$.

Algorithm 3 Items 1 and 2 in Algorithm 1:

Require: A mesh $\mathcal{T}$; parameters $0 < \sigma_1 < \sigma_2 < 1$; a localizable a-posteriori error estimator $\eta(u_{\mathrm{FE}})$.

Ensure: The marked elements $\mathcal{T}_p$ and $\mathcal{T}_h$.

1: Compute the maximum error $\eta_{\max} = \max_{K\in\mathcal{T}} \eta_K$

2: Determine

$$\mathcal{T}_p = \{K \in \mathcal{T} \mid \sigma_1 \, \eta_{\max} < \eta_K \leq \sigma_2 \, \eta_{\max}\} \, ,$$
$$\mathcal{T}_h = \{K \in \mathcal{T} \mid \sigma_2 \, \eta_{\max} < \eta_K\} \, .$$

5.5 The Zone Concentrated FEM

In addition to the *hp*-adaptive strategy in Algorithm 1, we investigate also another approach, which we call a Zone Concentrated FEM (ZC-FEM). For this technique we use the knowledge from Boundary Concentrated FEM (BC-FEM), introduced by B. N. Khoromskij and J. M. Melenk [62]).[1] This approach is still of an *hp*-adaptive Finite Element type, but with a slightly different aim. Let us start with a short review on BC-FEM. Considering the regularity of the solution to be low at the boundary and high in the interior of the domain, the parameters h and p are chosen to be small in a neighborhood of the boundary and to be growing towards the interior of the domain. This growth is based on the use of *geometric meshes* and *linear polynomial degree vectors*, which are defined as follows:

Definition 5.3. A γ-shape-regular mesh $\mathcal{T}$ is called a geometric mesh with boundary mesh size h if there exist constants c_1, $c_2 > 0$ such that for all $K \in \mathcal{T}$ with diameter h_K the following hold:

1. $h \leq h_K \leq c_2 h$ at the boundary, and
2. $c_1 \inf_{x\in K} \overline{(x,\Gamma)} \leq h_K \leq c_2 \sup_{x\in K} \overline{(x,\Gamma)}$.

Here, $\overline{(x,\Gamma)}$ denotes the shortest distance of point x to the boundary $\Gamma = \partial\Omega$.

Definition 5.4. A polynomial degree vector $\mathbf{p} := (p_K)_{K\in\mathcal{T}}$ is said to be *linear* with slope $\alpha > 0$ if there exist positive constants c_1 and c_2, such that

$$1 + \alpha\, c_1 \, \log \frac{h_K}{h} \leq p_K \leq 1 + \alpha\, c_2 \, \log \frac{h_K}{h}\,.$$

holds for all $K \in \mathcal{T}$.

In BC-FEM, a *hp*-FEM discretization is performed, which uses a geometric mesh $\mathcal{T}$ and a linear polynomial degree vector $\mathbf{p}$. If the slope α of Definition 5.4 is chosen large enough, then the convergence rate of BC-FEM is of the same order as in h-FEM, namely in 2D

$$\|u - u_{FE}\|_{H^1(\Omega)} \leq \|u\|_{H^{1+s}(\Omega)} h^s\,,$$

where u is assumed to have global Sobolev regularity $u \in \left[H^{1+s}(\Omega)\right]^2$ with $s \in (0,1)$, and h denotes the mesh size on the boundary - see [62].

Note, that the number of unknowns is significantly smaller than in h-FEM. For the 2D case, in BC-FEM the number of unknowns is proportional to the number of unknowns on the boundary (such as in BEM), whereas in a classical h-FEM the number of degrees of freedom is proportional to the *square* of the number of unknowns on the boundary. This is why the method is called a Boundary Concentrated Finite Element Method (BC-FEM) [62]. And this is the conceptional difference to other *hp*-adaptive strategies: The method

[1] Similarly to a Zone Conzentrated FEM, one could also think of applying an Interface Concentrated Finite Element Method (IC-FEM), see [13], to Elastoplasticity.

exploits the knowledge about the regularity of the solution in a way, that it searches for the smallest (and sparse) system which allows for the same convergence rate as is obtained in a uniform h-FEM.

Here we come to the extension of BC-FEM, which we call ZC-FEM: In elastoplasticity, BC-FEM can be applied for the purely elastic region, since the solution is known to be analytic in the interior of the purely elastic region [12], whereas the plastic region, where the solution is known to be just in $H^2_{\text{loc}}(\Omega)$ [65], is discretized by using a classical h-FEM. Usually, when applying BC-FEM, the geometric mesh $\mathcal{T}$, and the linear polynomial degree vector $\mathbf{p}$ can be constructed in advance, since the position of the boundary is known. This is different when using ZC-FEM for elastoplastic problems. The interface between plastic and elastic parts of the domain, which represents a part of the boundary of the elastic zone, is not known in advance. This is due to the fact that the calculation of the plastic strain field relies on the solution of the problem (the displacement field), as it is pointed out in equation (4.30). In other words, after every refinement step the interface will probably move. Thus, one has to estimate, which parts of the domain will be plastic at the next step of refinement. This task can be handled by two different strategies:

The first one is to estimate the analyticity of the FE-solution as presented in Algorithm 2 (with $\sigma = 0$). This would yield an optimal prediction of the plastic zones in the next step of refinement. Although, the prize we pay is a fairly high-dimensional test situation, since the polynomial degree of the shape functions has to be high (experimentally: greater than 4) in order to obtain a reasonable prediction of the plastic zones.

The second option is to mark all elements for h-refinement, if they behave plastic at this level of refinement, i. e., where the plastic strain p_k satisfies $\|p_k\|_{L_2(K)} > 0$, and additionally mark elements for h-refinement, which have a common vertex with those. This technique implicitly assumes, that the elastoplastic interface of the FE-solution after the refinement will move no further than at most one layer of elements from its former position, which can be acchieved by choosing the time step (or load step, respectively) sufficiently small.

The resulting method has the same accuracy as a classical h-FEM, i. e.,

$$\|u - u_{\text{FE}}\|_{H^1(\Omega)} = O(h)$$

where h denotes the mesh size at the boundary. However, the number of degrees of freedom of u_{FE} is significantly smaller compared to the classical h-FEM approach: Considering the classical h-FEM in two dimensions ($d = 2$), the number degrees of freedom is roughly $O(N^2)$, with $N = h^{-1}$ denoting the number of nodes on the boundary of the domain, whereas in ZC-FEM it is $O(N_E) + O(N_P^2)$, where N_E is the number of nodes on the boundary of the purely elastic sub-domain, and N_P the number of nodes on the boundary of the plastic sub-domain. Thus, this method pays off in situations, where the area of the plastic regions is small compared to the overall domain.

Let finally be mentioned, that the fastest expected convergence rate of the fully discrete scheme (no matter if h- or hp-FEM is used in space) assymptotically satisfies

$$\|u - u_{\text{FE}}\|_{H^1(\Theta\,;\,H^1(\Omega))} = O(\tau + h)\,,$$

where τ denotes the maximum step size of the pseudo-time variable, see [50].

Chapter 6

Implementation and Numerical Results

6.1 Software Development

The implementation was done in two software packages. First, the theoretical results of Chapter 4 were tested for the plane stain and plane stress case in Matlab. The full code is named `Epsilom` (Elastoplastic solver induced by the Lemma of Moreau). It is available for download at `http://www.numa.uni-linz.ac.at/Research/software.html`. Then, the code was transferred to the software package NETGEN/NGSolve [92], in which the 3D case, and especially the adaptive strategies for *hp*-FEM (see Section 5.4 and 5.5) were implemented. After laborious work on the implementation in NETGEN/NGSolve, it was finally visible, which strategies are of advantage for certain problems. The study of these tests is subject to the following Sections.

6.2 Uniform h-FEM

In this section, we show the computational success of the slant Newton method for a spatial discretization of uniform h-refinement and the constant polynomial degree $p = 1$. In all numerical examples, the scaled accuracy of the residual (cf. (5.12) and (5.13)) was used as the termination criterion, i. e., we tested

$$\|DJ_k^{\mathrm{FE}}(\mathbf{u}^i)\| \leq 10^{-8} \|DJ_k^{\mathrm{FE}}(\mathbf{u}^0)\| .$$

Example 6.1. This example is motivated by a benchmark problem for linear elasticity, where an L-shape domain (geometry and coarse grid triangulation are displayed in Figure 6.1) is deformed (due to a certain choice of surface traction) such, that the solution u

dof	10	66	...	20466	97282	391170
step 1	2.8383e-02	3.9827e-02	...	7.2243e-02	7.0236e-02	6.8321e-02
step 2	1.0467e-04	1.2352e-03	...	1.1004e-02	1.1063e-02	1.1022e-02
step 3	2.3781e-09	6.1409e-07	...	1.1453e-03	1.2746e-03	1.3552e-03
step 4	1.0944e-16	2.9589e-13	...	2.0826e-05	4.0743e-05	5.9611e-05
step 5			...	6.8005e-09	5.1957e-08	2.0693e-07
step 6			...	5.2211e-15	1.3866e-13	4.3361e-12
step 7			...			1.8774e-14
time	2.00537	2.25042	...	142.29	590.106	2692.87

Table 6.1: Convergence table in Example 6.1.

can be written in polar coordinates as

$$\begin{aligned} u_r(r,\theta) =& \frac{1}{2\mu} r^\alpha \left[-(\alpha+1)\cos((\alpha+1)\,\theta) + (C_2 - (\alpha+1))\,C_1 \cos((\alpha-1)\,\theta)\right], \\ u_\theta(r,\theta) =& \frac{1}{2\mu} r^\alpha \left[(\alpha+1)\sin((\alpha+1)\,\theta) + (C_2 + (\alpha-1))\,C_1 \sin((\alpha-1)\,\theta)\right], \end{aligned} \tag{6.1}$$

where $C_1 = -(\cos((\alpha+1)\omega))/\cos((\alpha-1)\omega)$, and $C_2 = (2(\lambda+2\mu))/(\lambda+\mu)$. This solution attains a singularity at the reentrant corner of the domain, when $\alpha \approx 0.544483737$. We now prescribe the solution (6.1) with $\alpha = 0.544483737$ at the whole boundary of the domain, and calculate the solution of the related elastoplastic problem. The material parameters are defined as

$$E = 1e5 \text{ MPa}, \quad \nu = 0.3, \quad \sigma_Y = 2.2 \text{ MPa}, \quad H = 1\,.$$

Figure 6.2 shows the yield function ϕ (3.23) on the right and the plastic zones on the left, where purely elastic zones are colored green (light gray in case of a non-color print respectively), and plastic zones are colored pink (dark grey respectively). For better visibility, the domain's displacement is multiplied by a factor of 3000. Table 6.1 reports on the convergence behavior of the Newton-like method for uniform mesh refinement. For various levels of refinement (dof: short for *degrees of freedom*) the table displays the $H^1(\Omega)$ seminorm of the error $|u^j - u^*|_1$, where u^* is the approximation after 20 Newton iteration steps. The total duration in the last line is measured in seconds.

Example 6.2. This example simulates the deformation of a screw-wrench under pressure. Problem geometry is shown in Figure 6.3: A screw-wrench *sticks* on a screw (homogeneous Dirichlet boundary condition) and a surface load g is applied to a part of the wrench's handhold in interior normal direction (Neumann boundary condition, cf. 6.3). The material parameters are set

$$E = 2e8 \text{ MPa}, \quad \nu = 0.3, \quad \sigma_Y = 2e6 \text{ MPa}, \quad H = 0.001\,,$$

and the surface load intensity amounts $|g| = 6e4$ MPa. Figure 6.4 shows the yield function ϕ (3.23) on the right and the plastic zones on the left, where purely elastic zones are colored

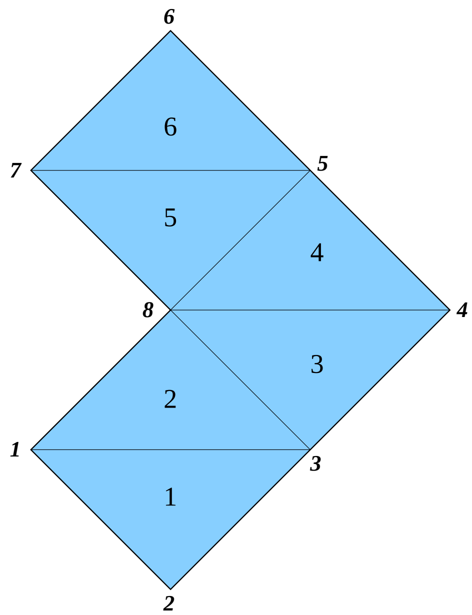

Figure 6.1: Problem geometry and the coarse triangulation of Example 6.1. The L-shape domain Ω is described by the polygon $(-1,-1)$, $(0,-2)$, $(2,0)$, $(0,2)$, $(-1,1)$, $(0,0)$.

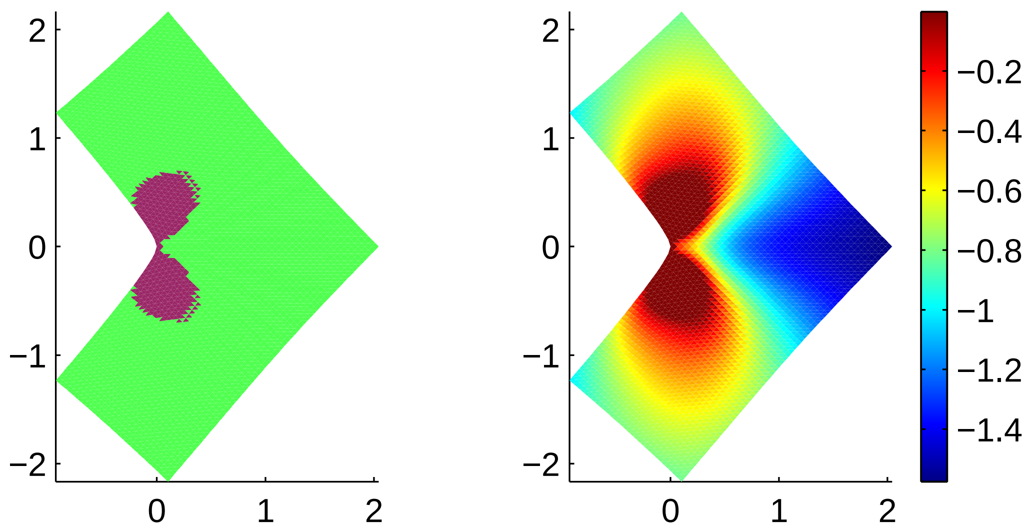

Figure 6.2: Plastic zones (left) and yield function (right) of the deformed domain in Example 6.1. The displacement is magnified by the factor 3000.

dof	60	202	...	41662	165246	658174
step 1	2.3834e-14	3.6169e-03	...	1.3194e-01	1.4872e-01	1.5846e-01
step 2		2.3598e-06	...	5.6966e-02	6.9302e-02	7.9603e-02
step 3		1.5324e-11	...	7.5805e-03	1.3223e-02	2.9909e-02
step 4		4.5752e-15	...	4.0307e-04	2.4344e-03	3.5626e-03
step 5			...	5.9665e-06	2.1840e-04	1.2013e-04
step 6			...	2.9485e-10	1.5089e-05	1.0364e-05
step 7			...	7.8696e-14	3.8914e-09	1.1642e-09
step 8			...		1.5508e-13	2.9988e-13
time	1.31385	2.58625	...	262.304	1177.64	4892

Table 6.2: Convergence table in Example 6.2.

green (light gray in case of a non-color print respectively), and plastic zones are colored pink (dark grey respectively). The displacement of the domain is multiplied by the factor 10, for a better visibility of the deformation. Table 6.2 reports on the convergence of the Newton-like method for graduated uniform meshes. Alike in Example 6.1, for various levels of refinement (dof: short for *degrees of freedom*) the table displays the $H^1(\Omega)$ seminorm of the error $|u^j - u^*|_1$, where u^* is the approximation after 20 Newton iteration steps. The total duration in the last line is measured in seconds.

Example 6.3. The example is taken from [100] and serves as a benchmark problem in computational plane strain plasticity (see [35]). In difference to the original problem setup, we choose H to be non-zero, thus hardening effects are considered. The calculation of the original perfect plastic problem can be found in [44]. We consider a thin plate represented by the square $(-10, 10) \times (-10, 10)$ with a circular hole of the radius $r = 1$ in the middle. A surface load g is applied on the plate's upper and lower edge with the intensity $|g| =$ 450 MPa. Due to the domain's symmetry, only the right upper quarter is discretized, as can be seen in Figure 6.41. Therefore it is necessary to incorporate homogeneous Dirichlet boundary conditions in the normal direction (gliding conditions) to both symmetry axes. The material parameters are set

$$E = 206900 \text{ MPa}\,, \quad \nu = 0.29\,, \quad \sigma_Y = \sqrt{\frac{2}{3}}\,450 \text{ MPa}\,, \quad H = \frac{1}{2}\,.$$

Figure 6.43 shows the yield function ϕ (3.23) and Figure 6.44 shows the plastic zones, where purely elastic zones are colored red, and plastic zones are colored blue. To obtain a better visibility, the deformation in Figure 6.42 is multiplied by a factor of 100. Table 6.3 reports on the convergence of the Newton-like method. For various levels of refinement (dof: short for *degrees of freedom*) the table displays the $H^1(\Omega)$ seminorm of the error $|u^j - u^*|_1$, where u^* is the approximation after 20 Newton iteration steps. The total duration in the last line is measured in seconds.

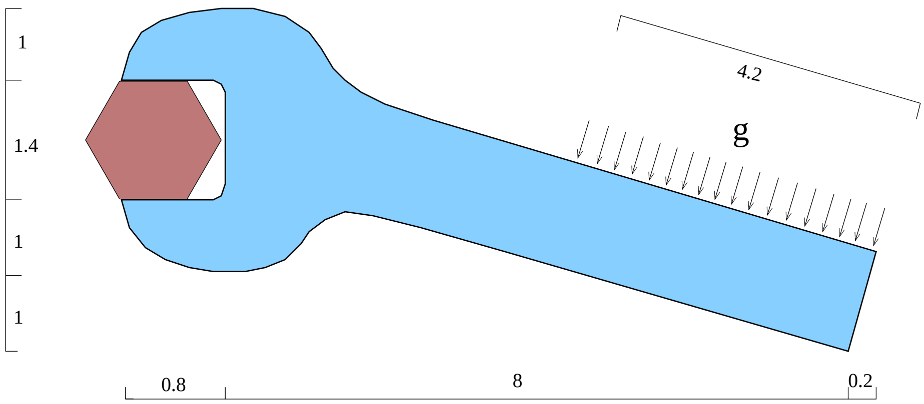

Figure 6.3: Problem geometry in Example 6.2.

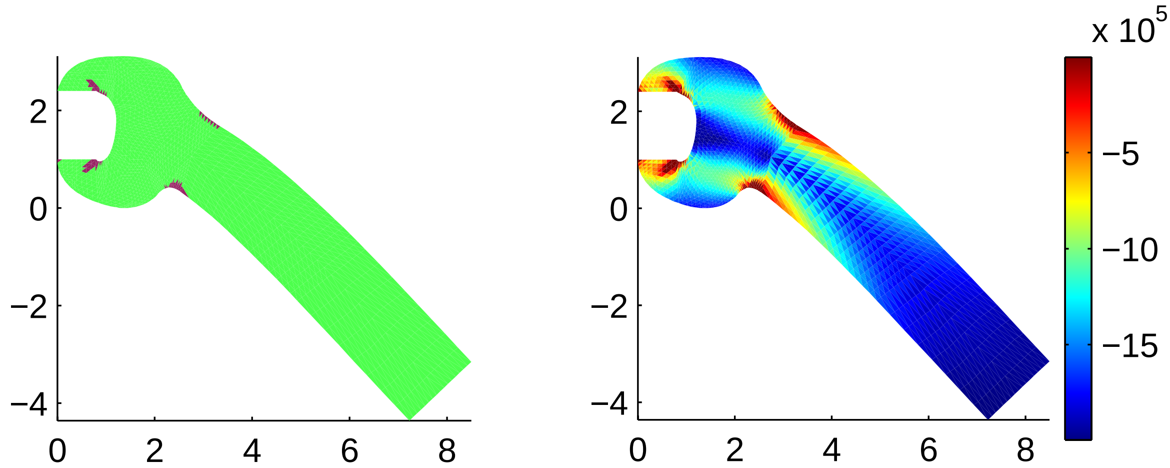

Figure 6.4: Plastic zones (left) and yield function (right) of the deformed domain in Example 6.2. The displacement is magnified by the factor 10.

dof	245	940	...	14560	57920	231040
step 1	2.1826e-02	3.5365e-02	...	4.5238e-02	4.6300e-02	4.6603e-02
step 2	2.2225e-03	5.8553e-03	...	8.0839e-03	8.3886e-03	8.5454e-03
step 3	1.0478e-04	1.6539e-04	...	3.4440e-04	4.0032e-04	4.1602e-04
step 4	1.4404e-08	3.9755e-08	...	1.5206e-05	1.2050e-05	1.3944e-05
step 5	7.2634e-16	6.9728e-15	...	2.4947e-07	7.2972e-07	3.2631e-07
step 6			...	3.5062e-13	5.3972e-12	1.6473e-12
step 7			...		7.2441e-15	1.4518e-14
time	2	4.6	...	64	286	1195

Table 6.3: Convergence table in Example 6.3.

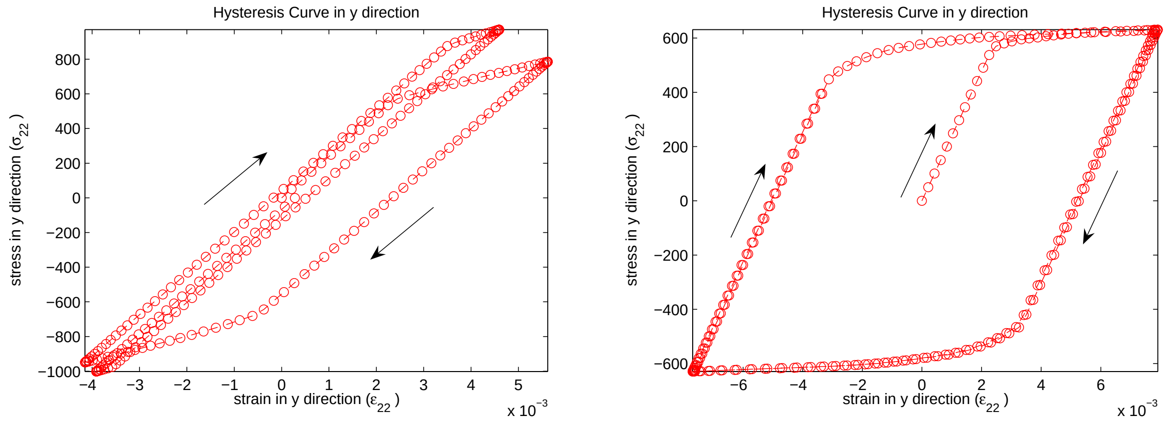

Figure 6.5: On the left, you see the hysteresis curve for Example 6.3 with respect to the time dependent surface load $g(t) = (0, \sin(\pi t))$ MPa for $t \in [0, 4]$. At the material point with coordinates roughly (2,2), the stress component σ_{22} is plotted versus the strain component ε_{22}. Both quantifiers are set to zero at $t = 0$. The time development takes place in direction of the arrows. On the right, you see the hysteresis curve for the same example, testing for $H = 0$ which models a perfect plastic material behaviour.

Example 6.4. The same problem as in Example 6.3 was calculated in 3D assuming the plate geometry $(-10, 10) \times (-10, 10) \times (0, 2)$. Figure 6.6 shows the norm of the plastic strain field p (right) and the coarsest refinement of the geometry (left), and Table 6.4 reports on the convergence of the slant Newton method. The implementation was done in C++ using the NETGEN/NGSolve software package developed in Linz [92].

6.3 Adaptive *hp*-FEM Strategies

We discuss three different numerical examples, for each of which four different *hp*-adaptive FEM strategies are tested versus a uniform *h*-refinement:

dof:	717	5736	45888	367104
step 1	1.013e-01	1.254e-01	1.367e-01	1.419e-01
step 2	7.024e-03	6.919e-03	7.159e-03	6.993e-03
step 3	1.076e-04	9.359e-05	1.263e-04	1.176e-04
step 4	2.451e-08	6.768e-07	1.744e-06	1.849e-06
step 5	7.149e-15	6.887e-12	4.874e-09	1.001e-08
step 6			4.298e-13	2.368e-14
time:	10	72	912	39200

Table 6.4: Convergence table of Example 6.4

.

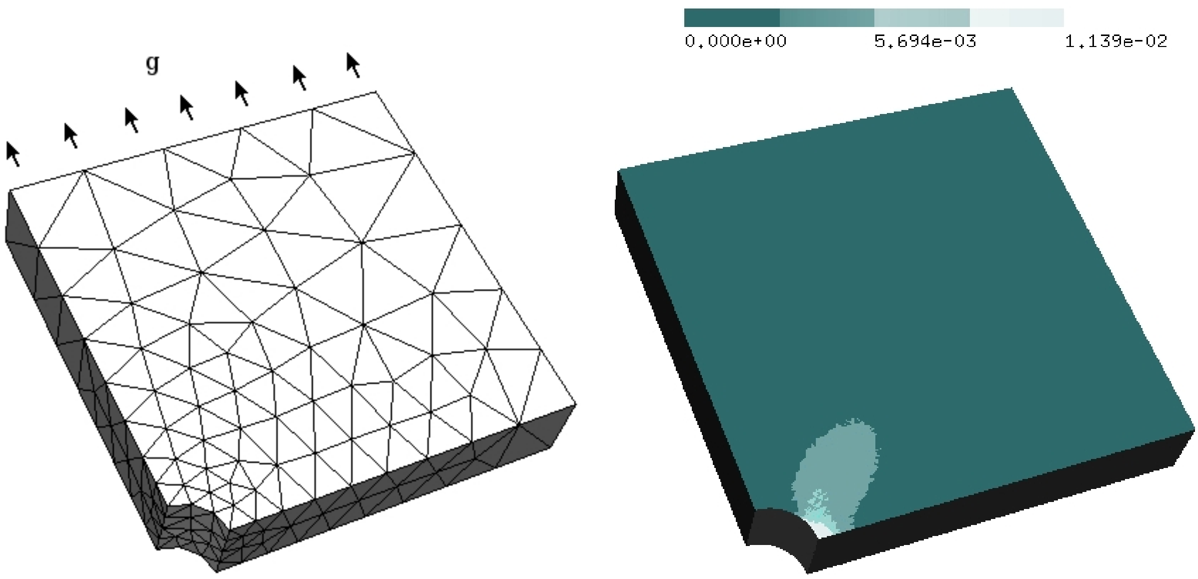

Figure 6.6: The two plots show the coarsest tetrahedal FE-mesh with the applied traction g (left), and the norm of the plastic strain field p (right) on a finer mesh of the three dimensional problem in Example 6.4.

- *Strategy 1* is a Zone Concentrated FEM as outlined in Section 5.5. It is the combination of a-priori h-refinement towards the boundary and the plastic zones. An element is treated as a part of the plastic zone, if one of its vertices belongs to an element, where the plastic strain is nonzero, $\|p_k\|_F \neq 0$. The remaining part of the domain, which reacts purely elastic, is discretized by a geometric mesh and a linear polynomial degree vector (see Definition 5.3 and 5.4).

- *Strategy 2* exactly covers Algorithm 2, where the parameters are set to $\sigma = 10^{-4}$ and $b = 3$. If the FE-solution is of too low order ($p < 5$) locally, then testing for analyticity is not reliable, and the element is marked for p-refinement.

- *Strategy 3* is almost identical to *Strategy 2*, and also using the same parameters. In difference to *Strategy 2*, plastic elements (where the plastic strain p_k yields $\|p_k\|_F \neq 0$) are marked for h-refinement in advance. Also elements, which have a common vertex with those, are marked for h-refinement, since the elastoplastic interface may move from refinement to refinement. This way, the polynomial degree of the FE-solution may kept low in elastoplastic zones.

- *Strategy 4* is the classical hp-adaptivity approach, as in Algorithm 3. The parameters are set to $\sigma_1 = 10^{-8}$ and $\sigma_2 = 10^{-4}$.

Remark 6.1. In all of the above Strategies, which rely on a-posteriori error-estimation, the ZZ-error-estimator [29]

$$\begin{aligned} \eta_K^2(u_{\mathrm{FE}}) &= \int_K (\sigma_{\mathrm{FE}} - \sigma_{\mathrm{FE}}^*) : \mathbb{C}^{-1}(\sigma_{\mathrm{FE}} - \sigma_{\mathrm{FE}}^*)\,\mathrm{d}x\,, \\ \eta^2(u_{\mathrm{FE}}) &= \frac{\sum_{K\in\mathcal{T}} \eta_K^2}{\sum_{K\in\mathcal{T}} \int_K \sigma_{\mathrm{FE}}^* : \mathbb{C}^{-1}\sigma_{\mathrm{FE}}^*\,\mathrm{d}x} \end{aligned} \tag{6.2}$$

is used. Here, the flux $\sigma_{\mathrm{FE}} = \mathbb{C}\,\varepsilon(u_{\mathrm{FE}})$ is the elastic part of the stress depending on the finite element solution u_{FE} (element wise), and σ_{FE}^* is the Clement Interpolation of σ_{FE}. This error estimator is known to be efficient and reliable for elastoplastic problems with hardening [22, 3, 24, 23]. However, the respective estimates are cruzially depending on the modulus of hardening H (see (3.23)) and do, particularly, not hold in the case of perfect plasticity, where $H = 0$.

All examples of this section were computed in the framework NETGEN/NGSolve [92].

Example 6.5. A beam $\Omega = (0,2)\times(-0.5,0.5)$ is fixed on the left boundary $\Gamma_D = \{(x,y)\in\partial\Omega \mid x = 0\}$ and stressed on the right boundary $\Gamma_N = \{(x,y)\in\partial\Omega \mid x = 2\}$ in positive x-direction with a traction of intensity $|g| = 1.35$ (see Figure 6.7). The material parameters are chosen as follows: Young's modulus $E = 1000$ MPa, Poisson ratio $\nu = 0.3$, yield stress $\sigma_y = 1$ MPa, and modulus of hardening $H = 10$. The graphical output after some steps of uniform refinement is as follows: The displacement is plotted in Figure 6.8, which also shows the deformation of the domain magnified by a factor 100. The yield function ϕ (3.23) is plotted in Figure 6.9. In Figure 6.10 the plastic zones (red) versus elastic zones (blue) are shown, whereas Figure 6.11 and Figure 6.12 report on the point-wise Frobenius-norm of the plastic strain. The estimated slope of the FE solution coefficients, as discussed in Algorithm 2, is plotted in Figure 6.13. We numerically tested uniform refinement (h-FEM) versus the hp-FE Strategies 1-4. Let be mentioned, that in all tests the super linear convergence of the Newton like method was observed. Figures 6.14-6.17 illustrate the polynomial order distribution after some steps of adaptive hp-refinement, whereas the resulting meshes are shown in Figures 6.18-6.21. The approximation error $\|u - u_{\mathrm{FE}}\|_{H^1(\Omega)}$ is estimated by the elastic ZZ-error estimator (6.2). Figures 6.22 and 6.23 show the convergence results graphically.

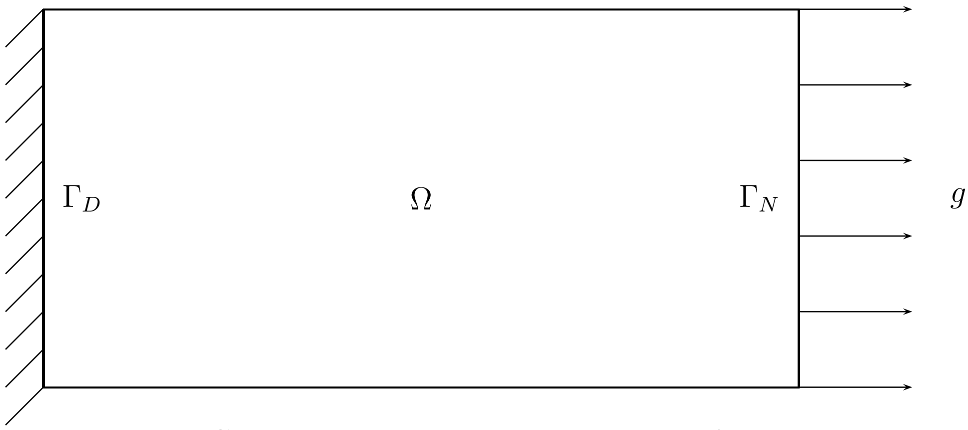

Figure 6.7: Geometry and problem description of Example 6.5.

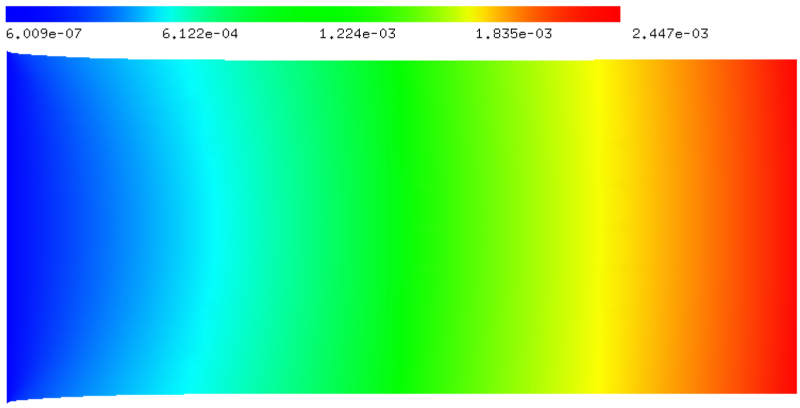

Figure 6.8: Displacement and deformed domain ($\times 100$) in Example 6.5.

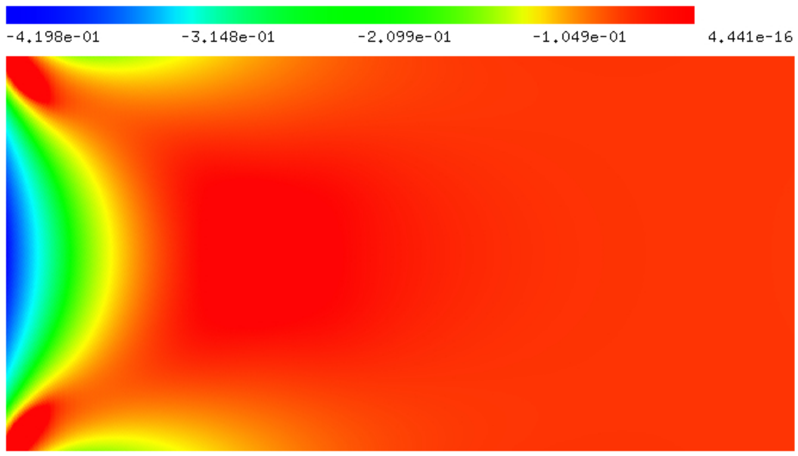

Figure 6.9: Yield function ϕ (3.23) in Example 6.5.

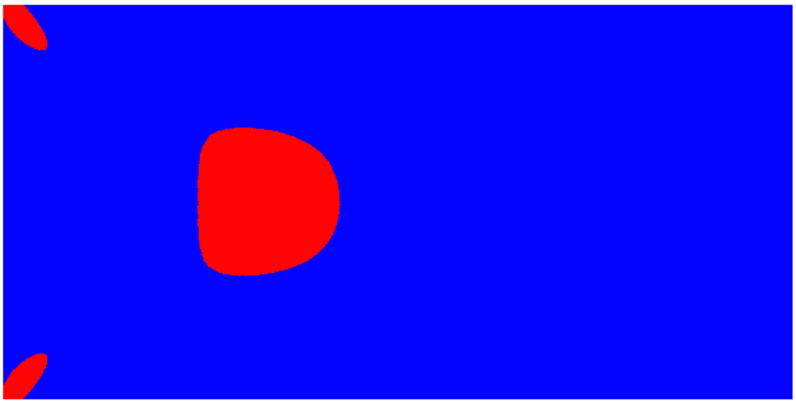

Figure 6.10: Plastic (red) and elastic (blue) zones in Example 6.5.

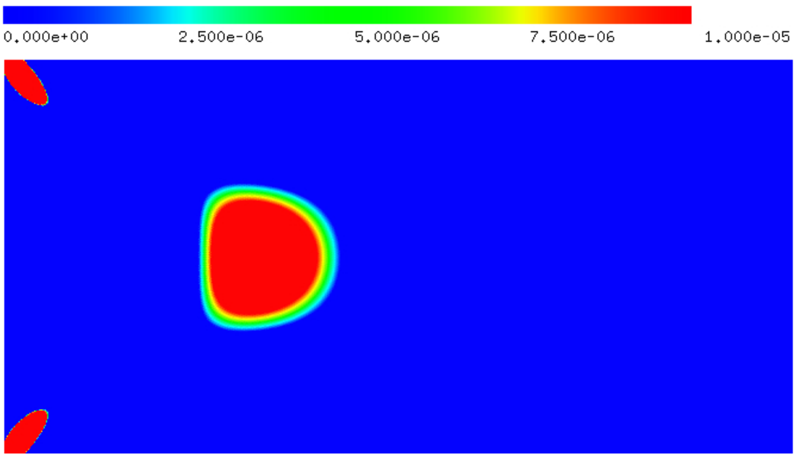

Figure 6.11: Frobenius norm of the plastic strain in Example 6.5.

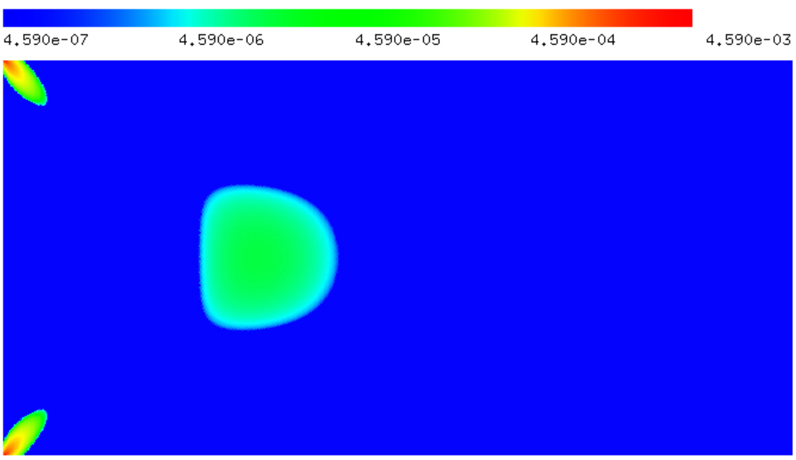

Figure 6.12: Logarithmic Frobenius norm of the plastic strain in Example 6.5.

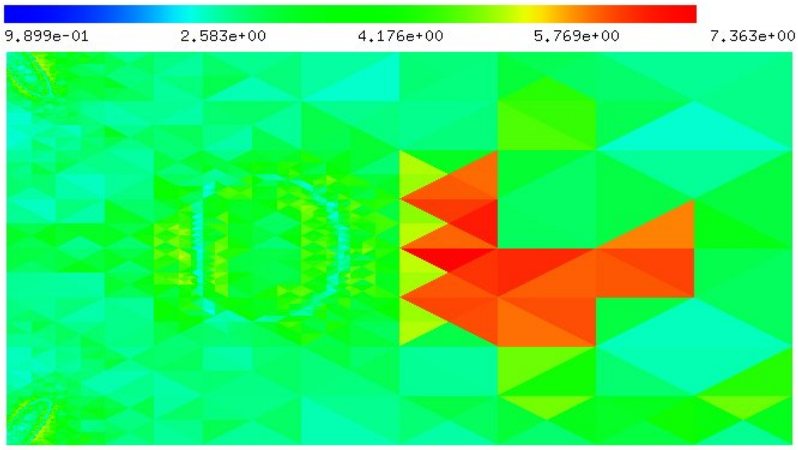

Figure 6.13: The estimated slope of coefficients (Algorithm 2) in Example 6.5.

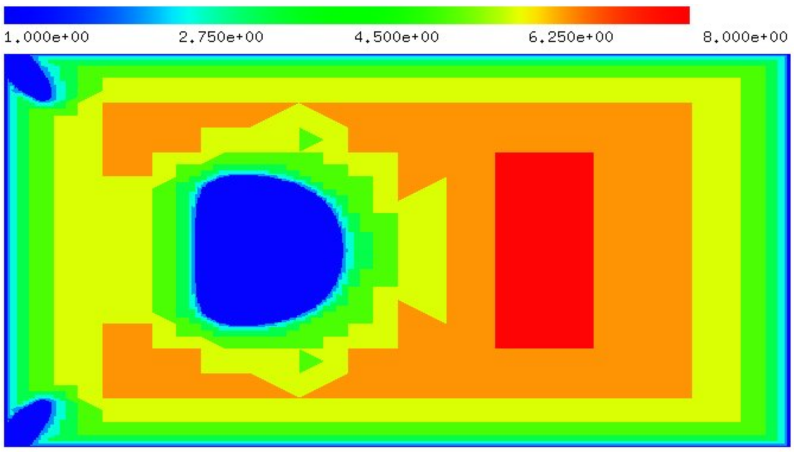

Figure 6.14: Polynomial order with Strategy 1 in Example 6.5.

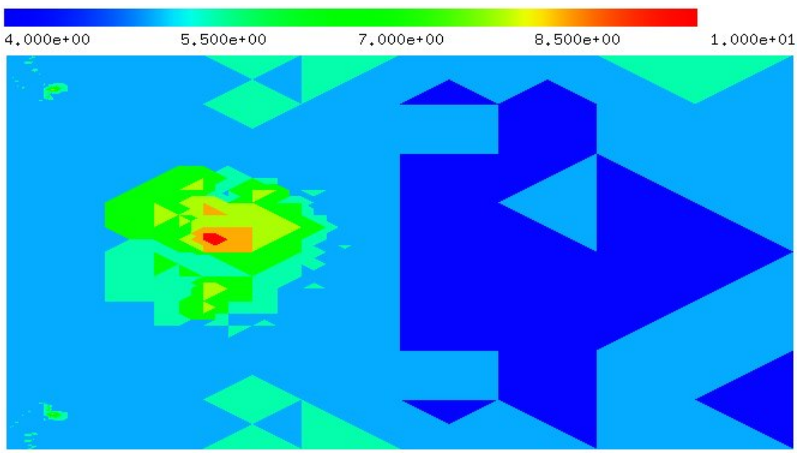

Figure 6.15: Polynomial order with Strategy 2 in Example 6.5.

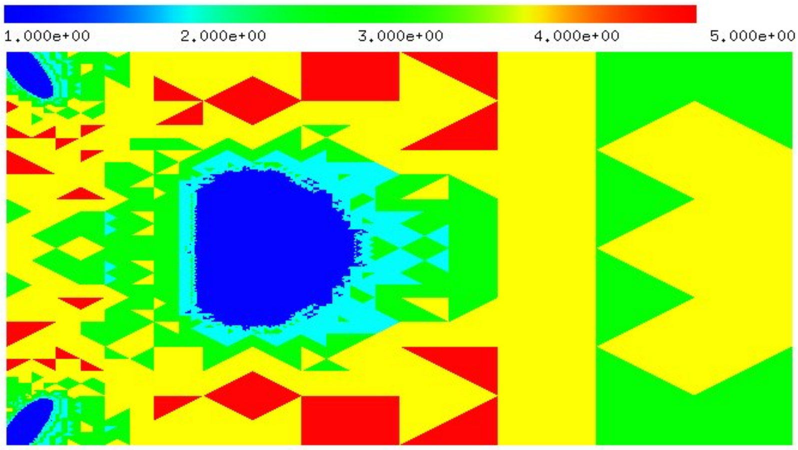

Figure 6.16: Polynomial order with Strategy 3 in Example 6.5.

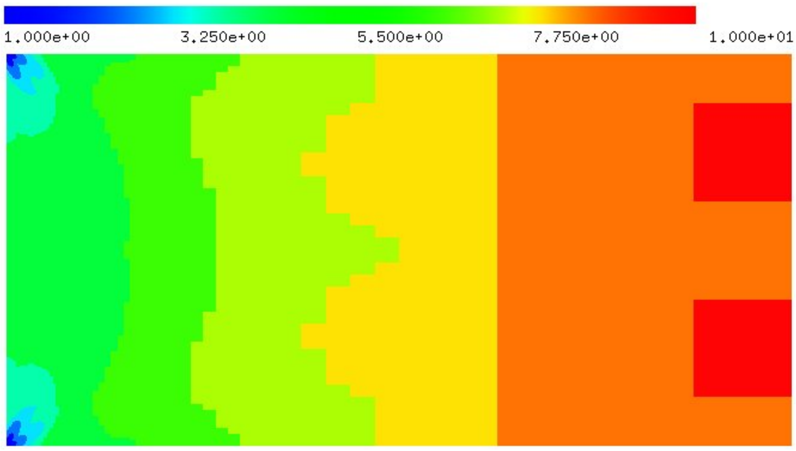

Figure 6.17: Polynomial order with Strategy 4 in Example 6.5.

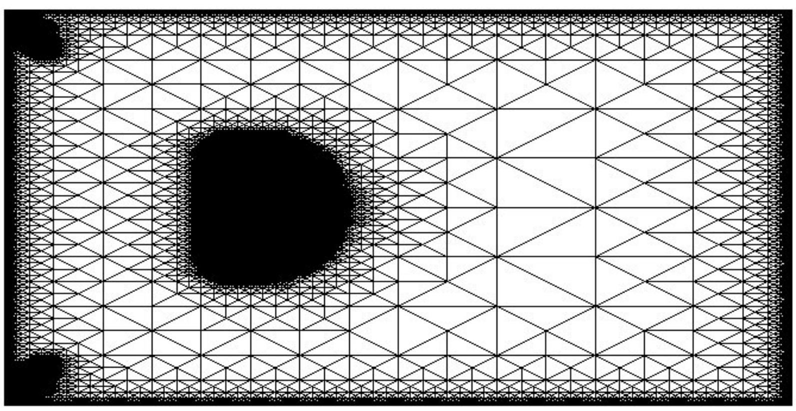

Figure 6.18: Adaptive mesh with Strategy 1 in Example 6.5.

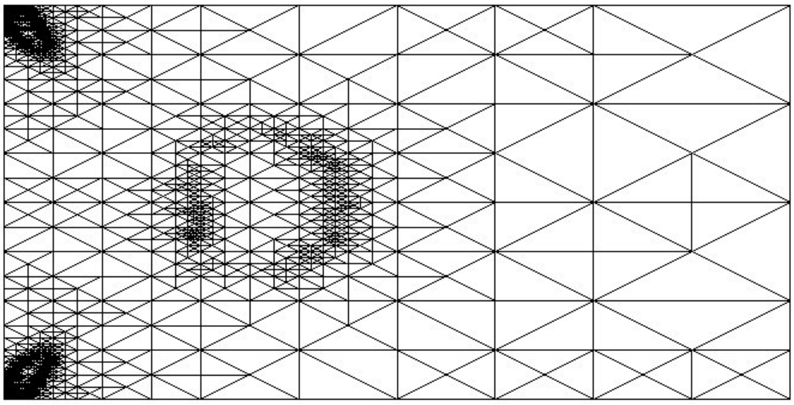

Figure 6.19: Adaptive mesh with Strategy 2 in Example 6.5.

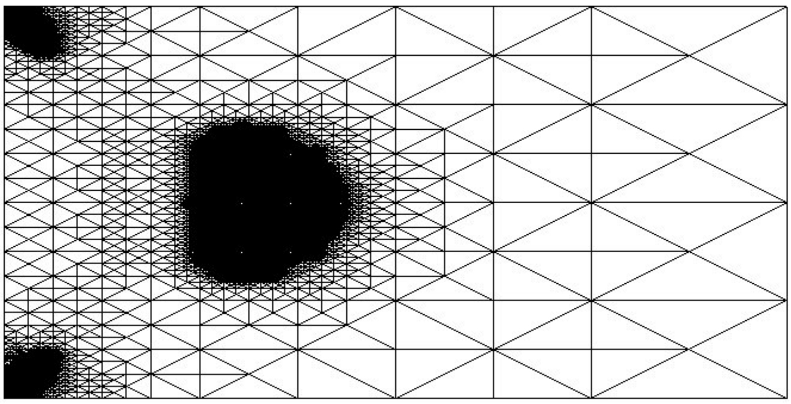

Figure 6.20: Adaptive mesh with Strategy 3 in Example 6.5.

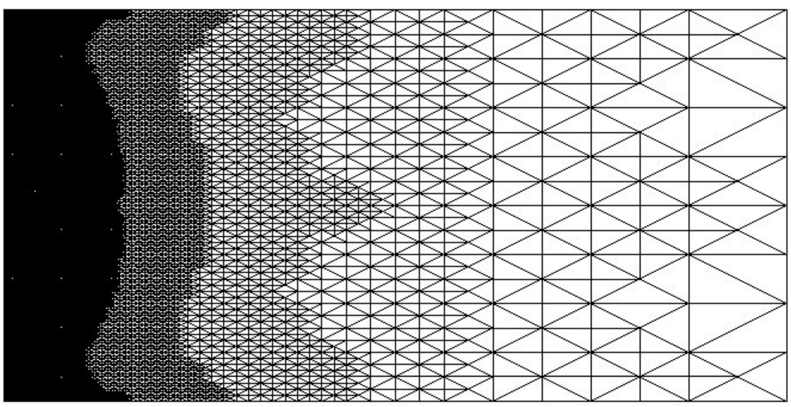

Figure 6.21: Adaptive mesh with Strategy 4 in Example 6.5.

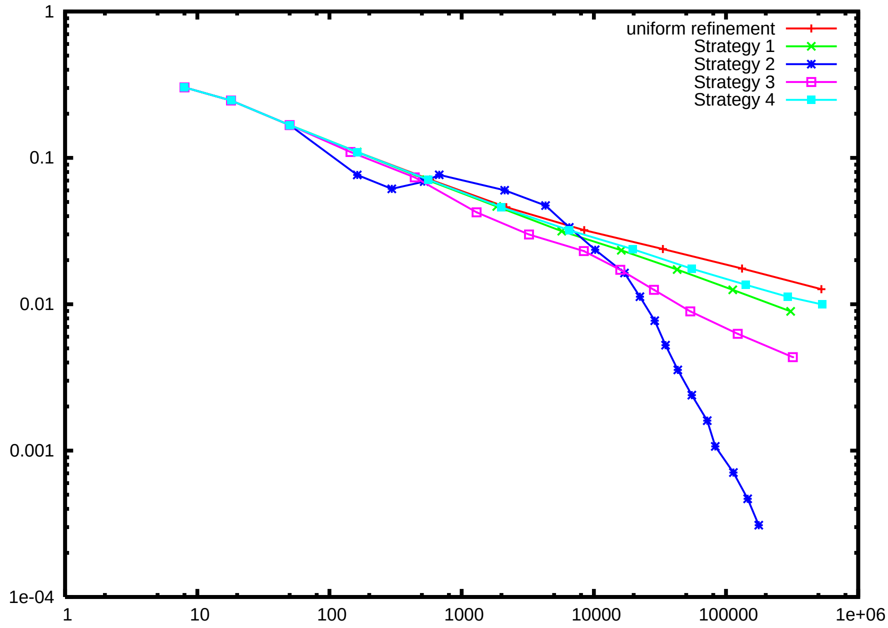

Figure 6.22: The global estimated error (6.2) versus degrees of freedom in Example 6.5.

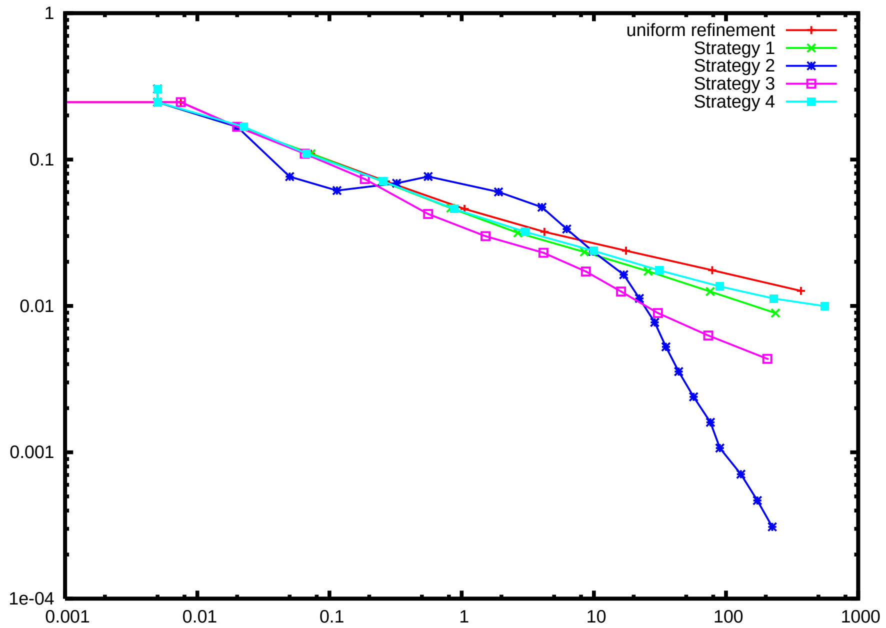

Figure 6.23: Here, the global estimated error (6.2) is plotted versus the time (in seconds) which was spent per Newton step in Example 6.5. One Newton step covers the assembling of the stiffness matrix and a sparse direct solver (PARDISO [90, 91]).

Example 6.6. A beam $\Omega = (0, 2) \times (-0.5, 0.5)$ is fixed on the boundary $\Gamma_D = \{(x, y) \in \partial\Omega \mid x \in (0, 0.5)\}$. On the boundary $\Gamma_N = \{(x, y) \in \partial\Omega \mid x \in (1.5, 2)\}$ a traction $g = (0.9, -\mathrm{sign}(y)\, 0.1)$ is applied (see Figure 6.24). The material parameters are chosen as follows: Young's modulus $E = 1000$ MPa, Poisson ratio $\nu = 0.3$, yield stress $\sigma_y = 1$ MPa, and modulus of hardening $H = 10$. The graphical output after some steps of uniform refinement is as follows: The displacement is plotted in Figure 6.25, which also shows the deformation of the domain magnified by a factor 50. The yield function ϕ (3.23) is plotted in Figure 6.26. In Figure 6.27 the plastic zones (red) versus elastic zones (blue) are shown, whereas Figure 6.28 and Figure 6.29 report on the point-wise Frobenius-norm of the plastic strain. The estimated slope of the FE solution coefficients, as discussed in Algorithm 2, is plotted in Figure 6.30. We numerically tested uniform refinement (h-FEM) versus the hp-FE Strategies 1-4. Let be mentioned, that in all tests the super linear convergence of the Newton like method was observed. Figures 6.31-6.33 illustrate the polynomial order distribution after some steps of adaptive hp-refinement, whereas the resulting meshes are shown in Figures 6.35-6.37. The approximation error $\|u - u_{\mathrm{FE}}\|_{H^1(\Omega)}$ is estimated by the elastic ZZ-error estimator (6.2). Figures 6.39 and 6.40 show the convergence results graphically.

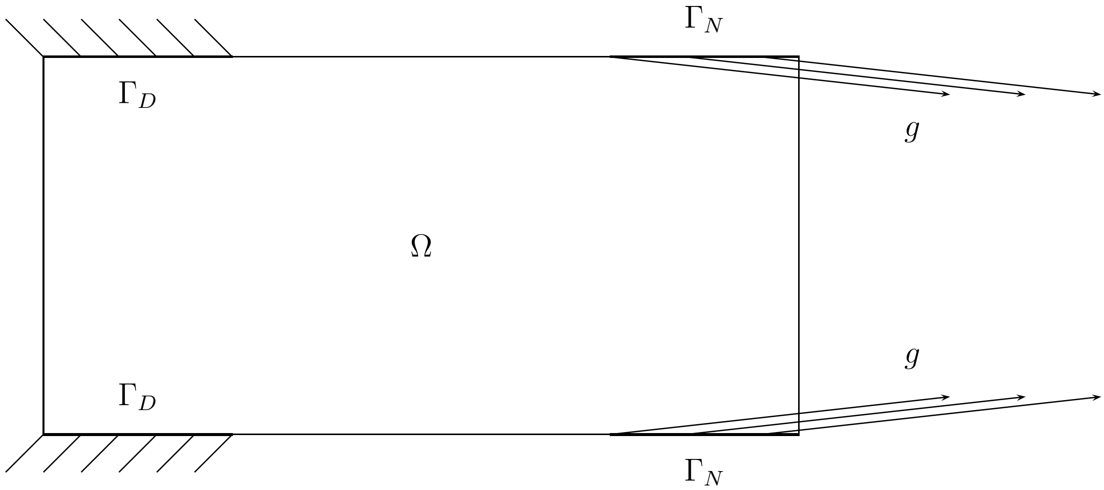

Figure 6.24: Geometry and problem description of Example 6.6.

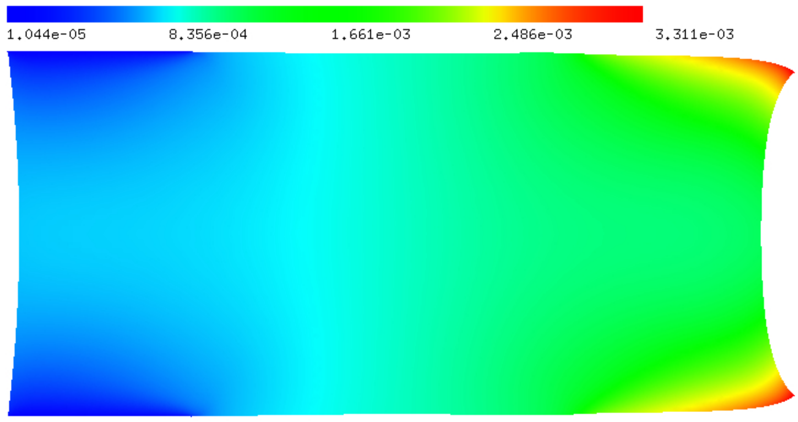

Figure 6.25: Displacement and deformed domain ($\times 50$) in Example 6.6.

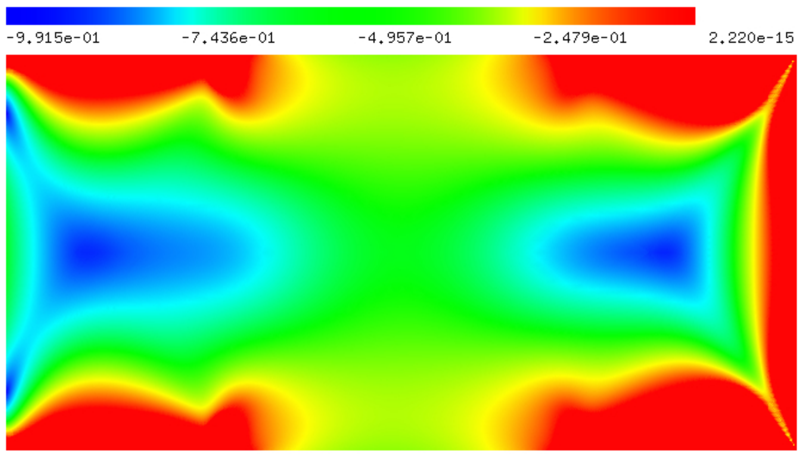

Figure 6.26: Yield function ϕ (3.23) in Example 6.6.

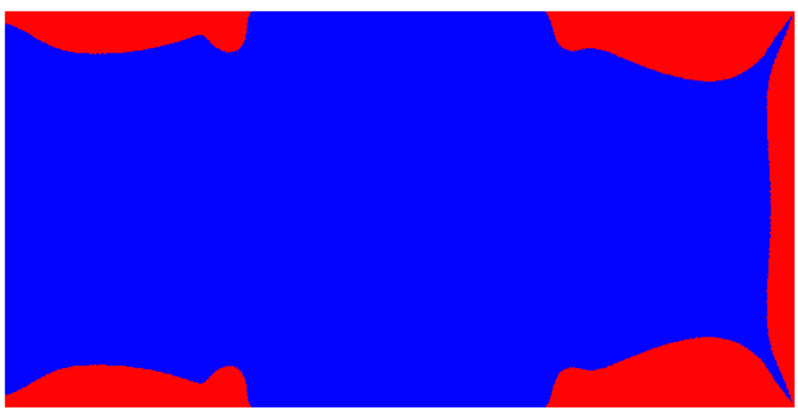

Figure 6.27: Plastic (red) and elastic (blue) zones in Example 6.6.

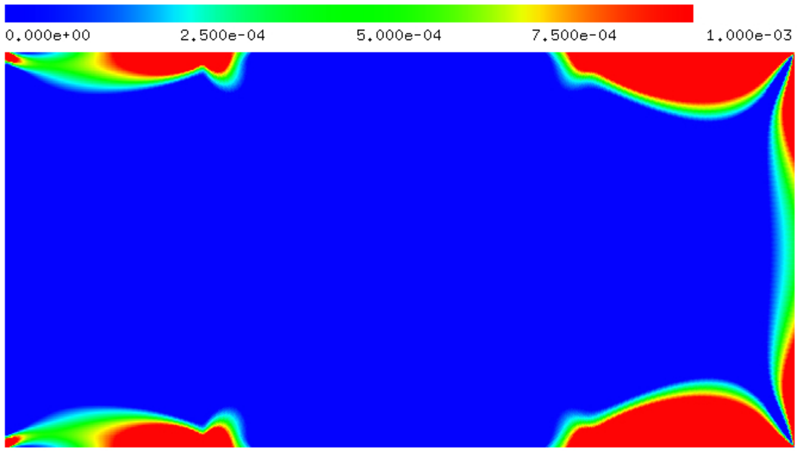

Figure 6.28: Frobenius norm of the plastic strain in Example 6.6.

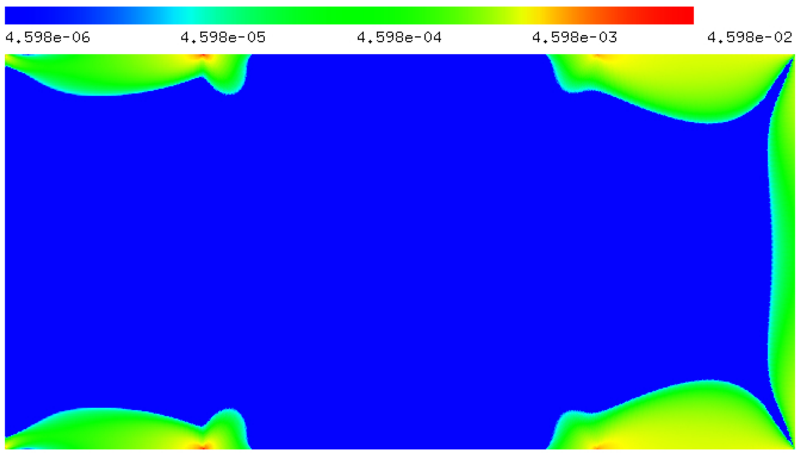

Figure 6.29: Logarithmic Frobenius norm of the plastic strain in Example 6.6.

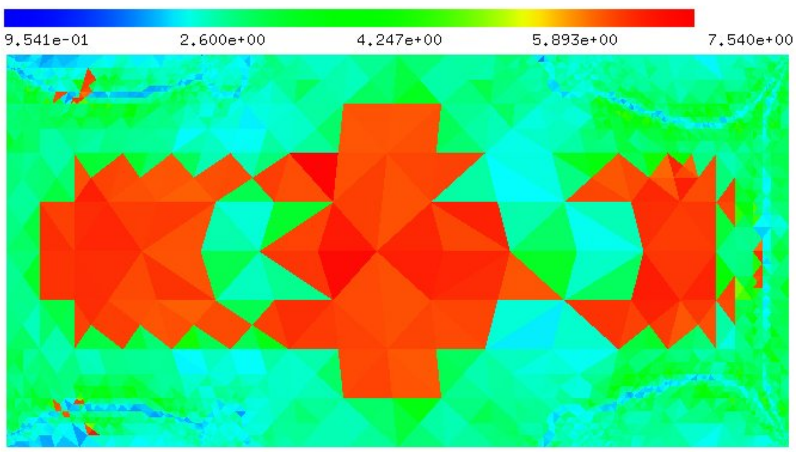

Figure 6.30: The estimated slope of coefficients (Algorithm 2) in Example 6.6.

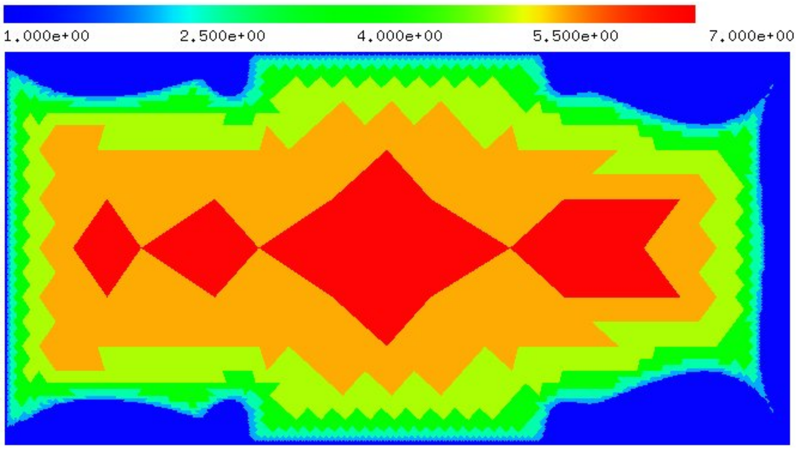

Figure 6.31: Polynomial order with Strategy 1 in Example 6.6.

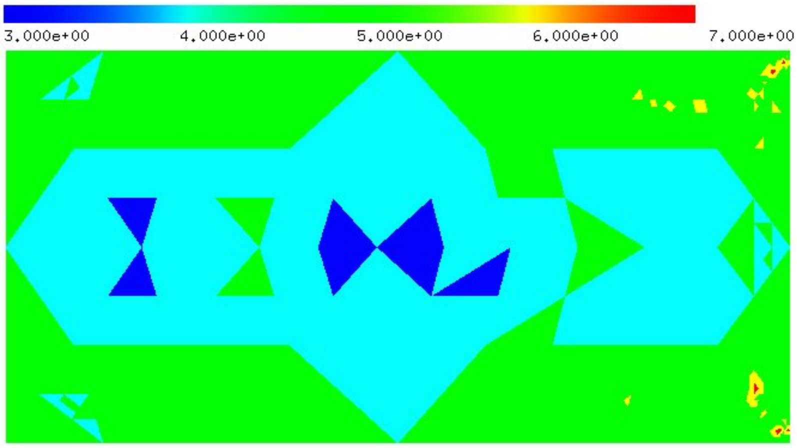

Figure 6.32: Polynomial order with Strategy 2 in Example 6.6.

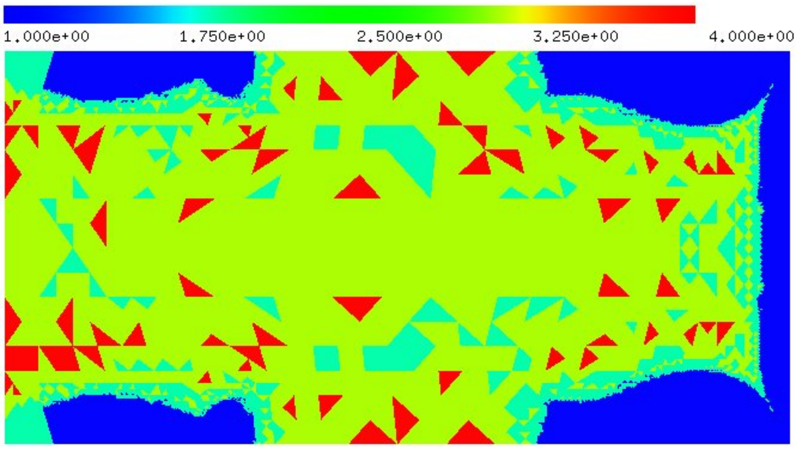

Figure 6.33: Polynomial order with Strategy 3 in Example 6.6.

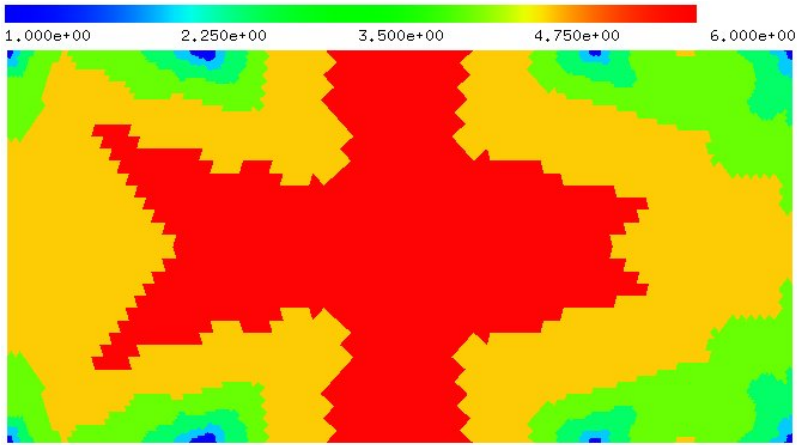

Figure 6.34: Polynomial order with Strategy 4 in Example 6.6.

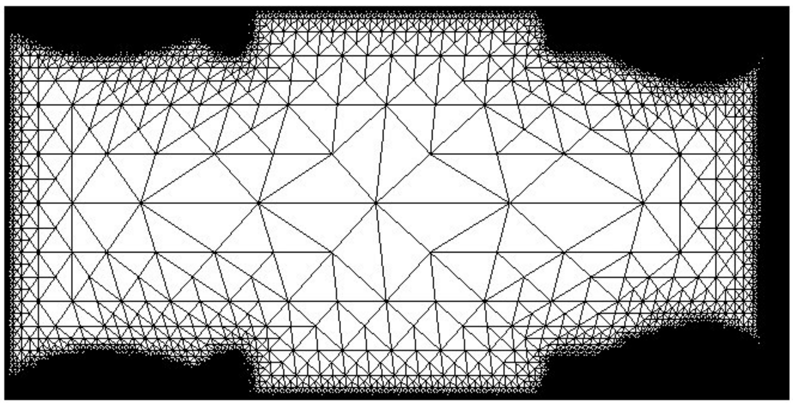

Figure 6.35: Adaptive mesh with Strategy 1 in Example 6.6.

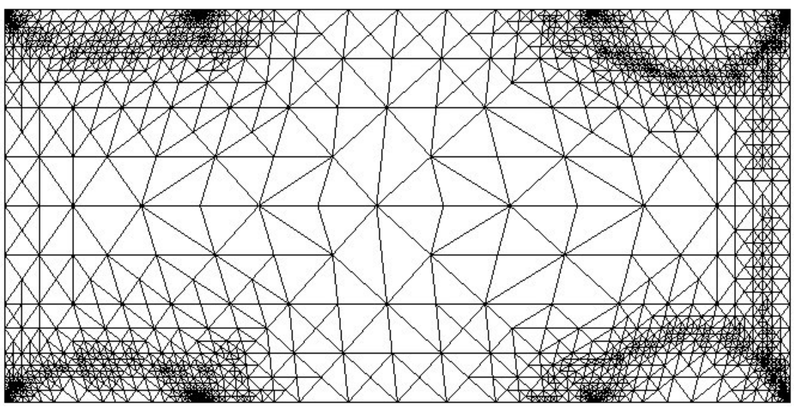

Figure 6.36: Adaptive mesh with Strategy 2 in Example 6.6.

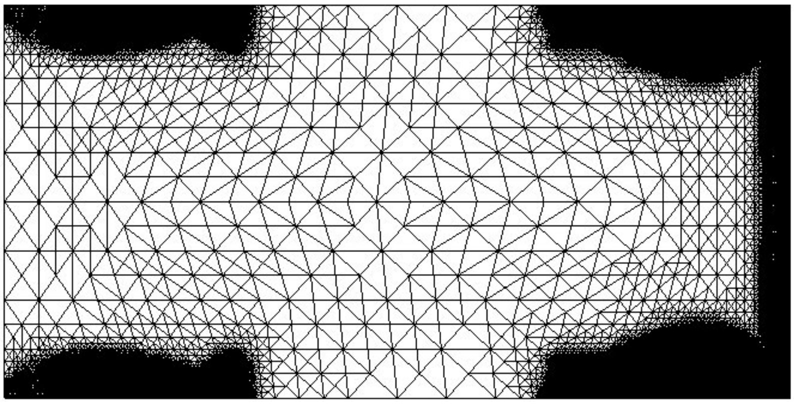

Figure 6.37: Adaptive mesh with Strategy 3 in Example 6.6.

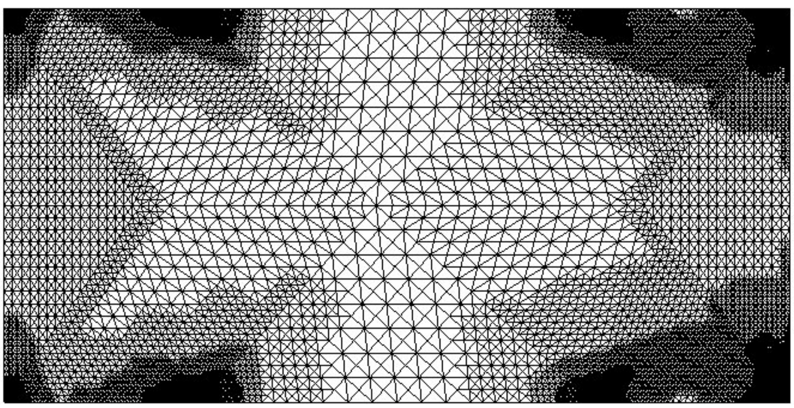

Figure 6.38: Adaptive mesh with Strategy 4 in Example 6.6.

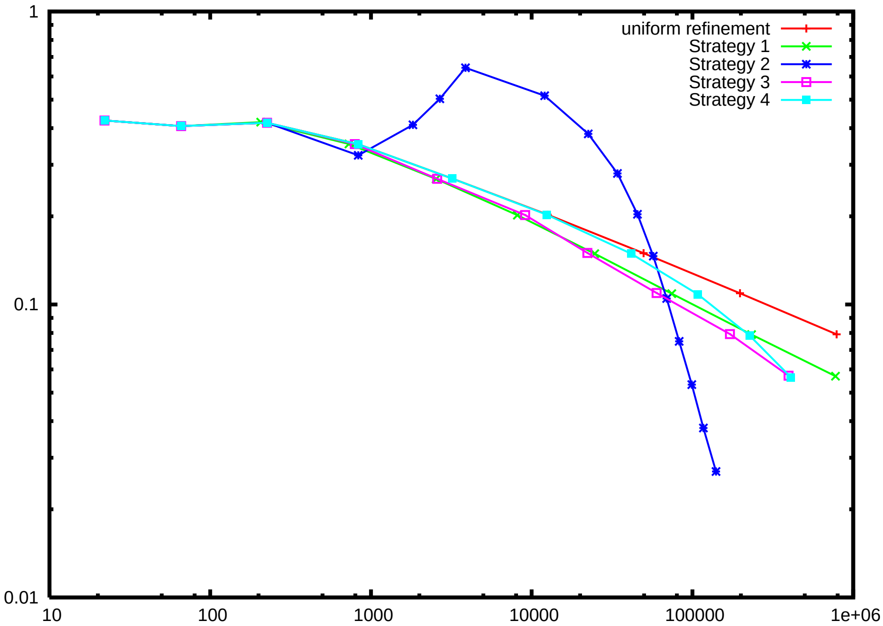

Figure 6.39: The global estimated error (6.2) versus degrees of freedom in Example 6.6.

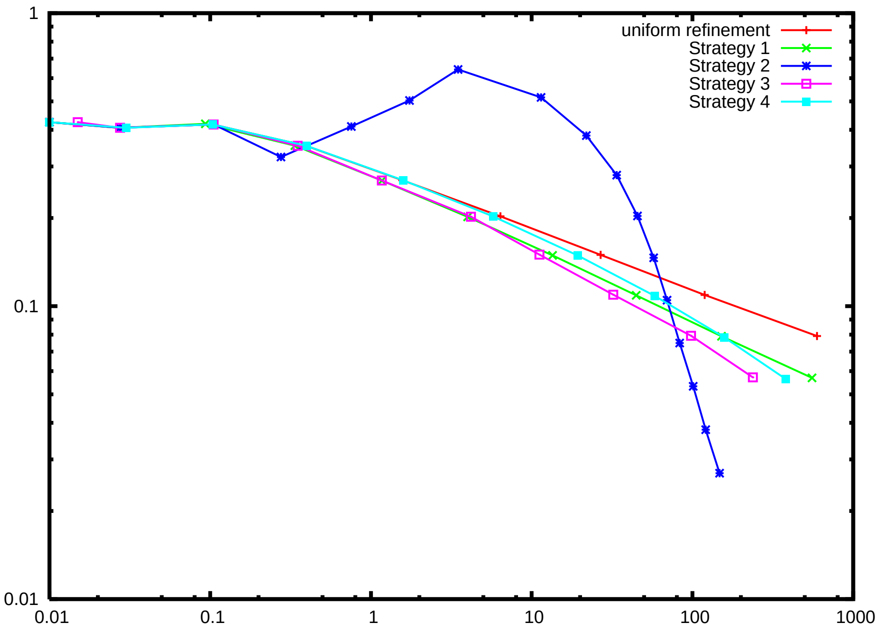

Figure 6.40: Here, the global estimated error (6.2) is plotted versus the time (in seconds) which was spent per Newton step in Example 6.6. One Newton step covers the assembling of the stiffness matrix and a sparse direct solver (PARDISO [90, 91]).

Example 6.7. A plate with a hole $\Omega = \{x \in [-10, 10]^2 \ : \ \|x\| \geq 1\}$ is torn on the top and bottom edges $\Gamma_N = \{(x, y) \in \partial\Omega \ | \ |y| = 10\}$ in normal direction with a traction of intensity $|g| = 450$. Due to the symmetry of the problem, only the top right quarter is considered in the numerical simulation (see Figure 6.41). Note, that gliding conditions are required on the cutting edges. The material parameters are chosen as follows: Young's modulus $E = 206900$ MPa, Poisson ratio $\nu = 0.29$, yield stress $\sigma_y = 450\sqrt{2/3}$ MPa, and modulus of hardening $H = 0.1$. The graphical output after some steps of uniform refinement is as follows: The displacement is plotted in Figure 6.42, which also shows the deformation of the domain magnified by a factor 100. The yield function ϕ (3.23) is plotted in Figure 6.43. In Figure 6.44 the plastic zones (red) versus elastic zones (blue) are shown, whereas Figure 6.45 and 6.46 report on the point-wise Frobenius-norm of the plastic strain. The estimated slope of the FE solution coefficients, as discussed in Algorithm 2, is plotted in Figure 6.47. We numerically tested uniform refinement (h-FEM) versus the hp-FE Strategies 1-4. Let be mentioned, that in all tests the super linear convergence of the Newton like method was observed. Figures 6.48-6.50 illustrate the polynomial order distribution after some steps of adaptive hp-refinement, whereas the resulting meshes are shown in Figures 6.52-6.54. The approximation error $\|u - u_{\mathrm{FE}}\|_{H^1(\Omega)}$ is estimated by the elastic ZZ-error estimator (6.2). Figures 6.56 and 6.57 show the convergence results graphically.

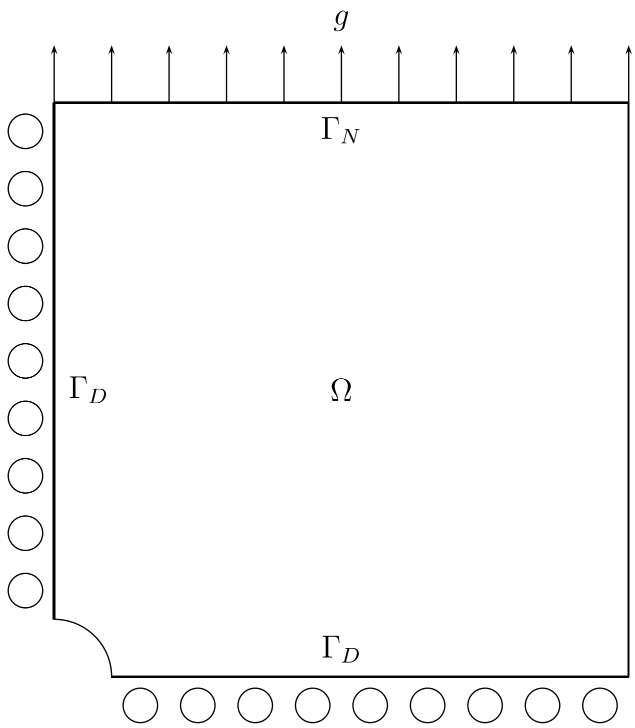

Figure 6.41: Geometry and problem description of Examples 6.3 and 6.7.

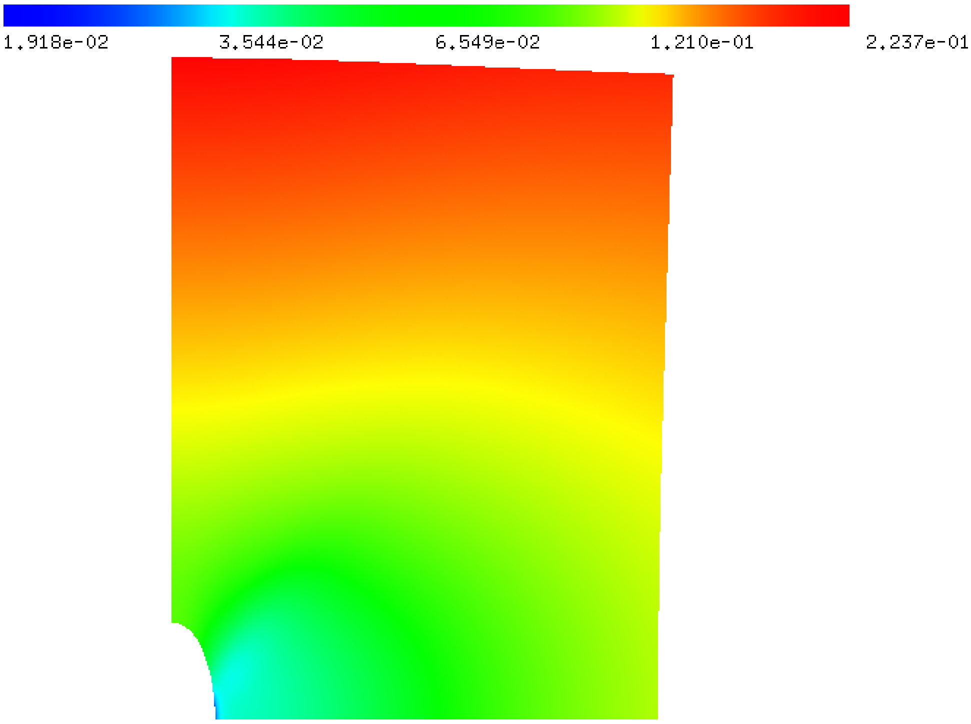

Figure 6.42: Displacement and deformed domain ($\times 100$) in Examples 6.3 and 6.7.

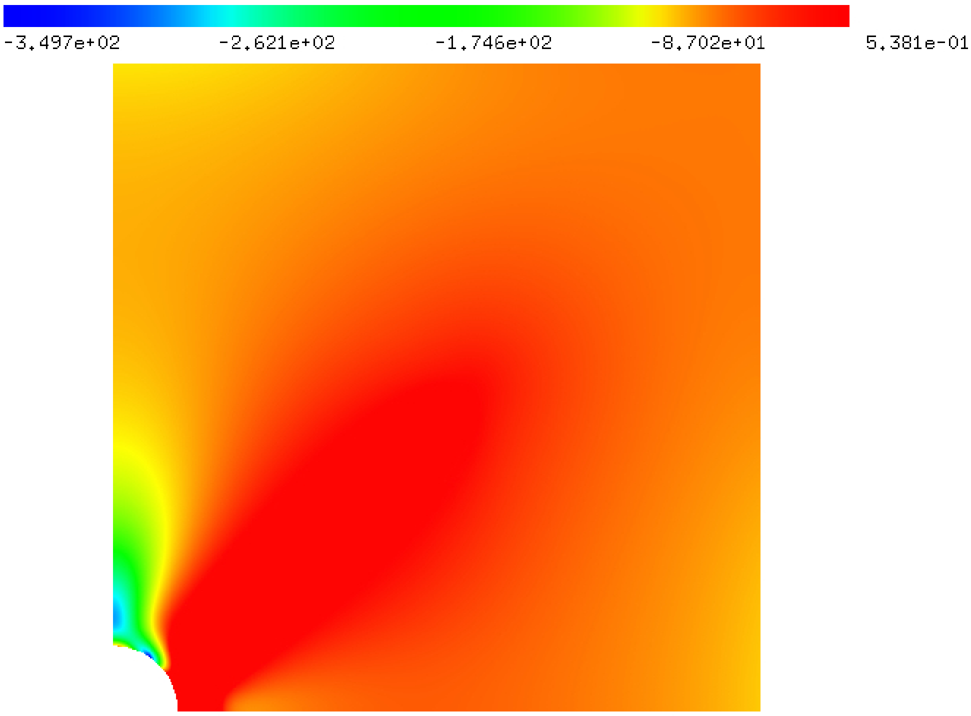

Figure 6.43: Yield function ϕ (3.23) in Examples 6.3 and 6.7.

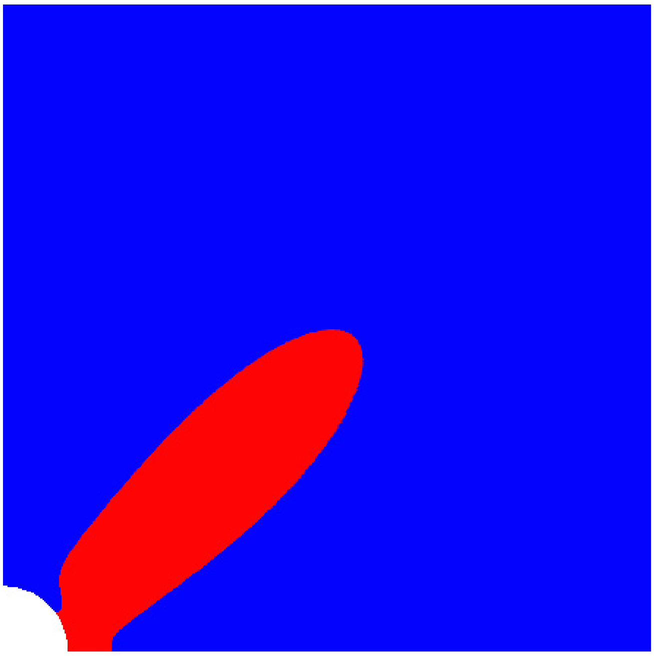

Figure 6.44: Plastic (red) and elastic (blue) zones in Examples 6.3 and 6.7.

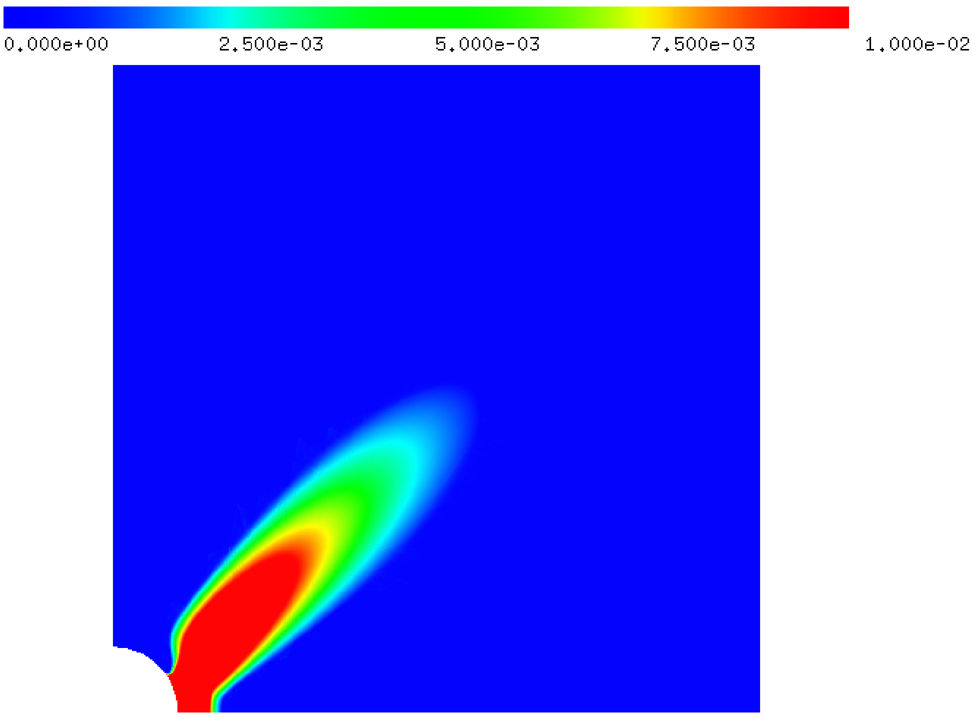

Figure 6.45: Frobenius norm of the plastic strain in Examples 6.3 and 6.7.

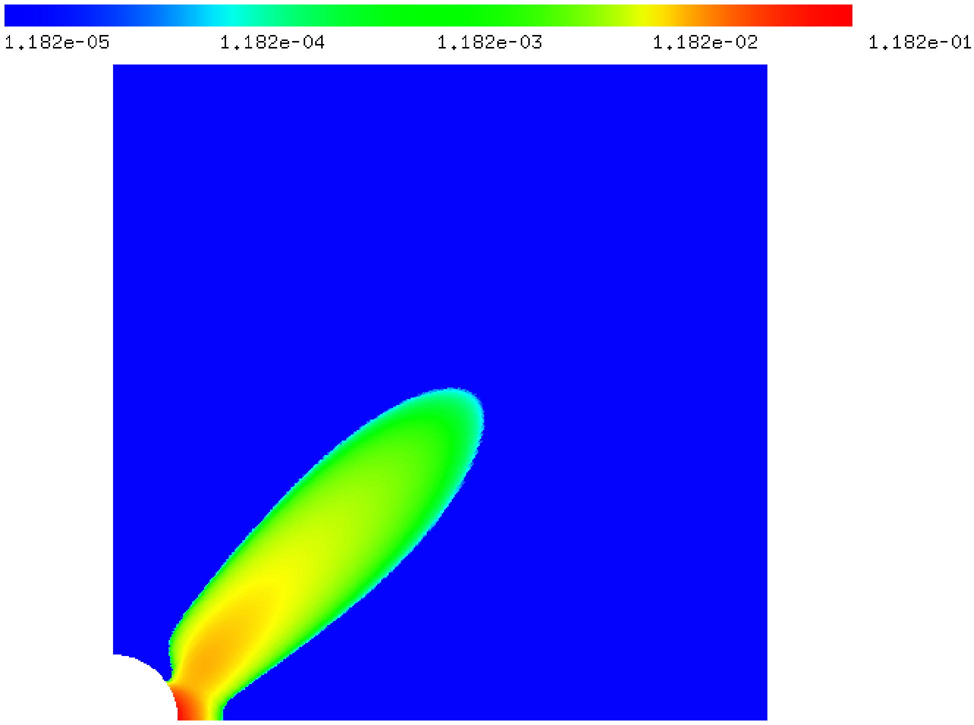

Figure 6.46: Logarithmic Frobenius norm of the plastic strain in Examples 6.3 and 6.7.

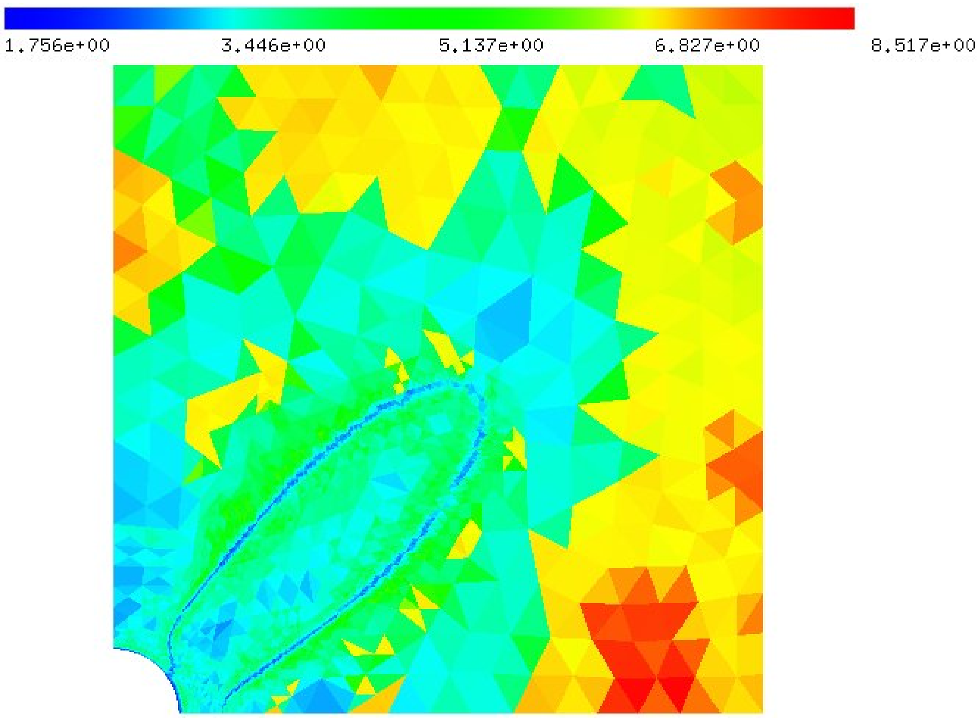

Figure 6.47: The estimated slope of coefficients (Algorithm 2) in Example 6.7.

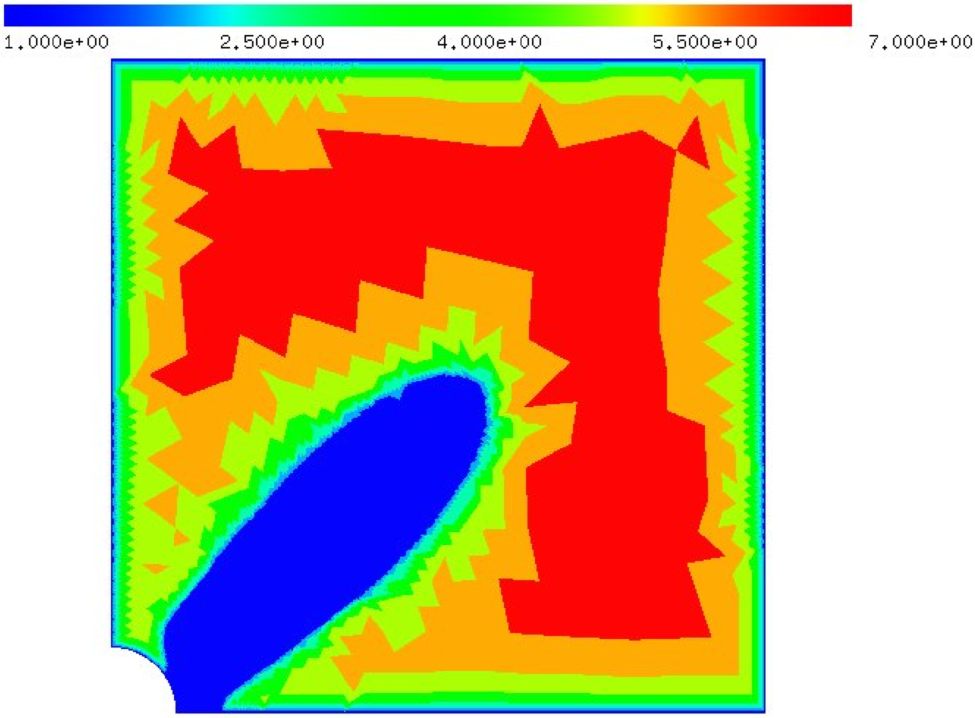

Figure 6.48: Polynomial order with Strategy 1 in Example 6.7.

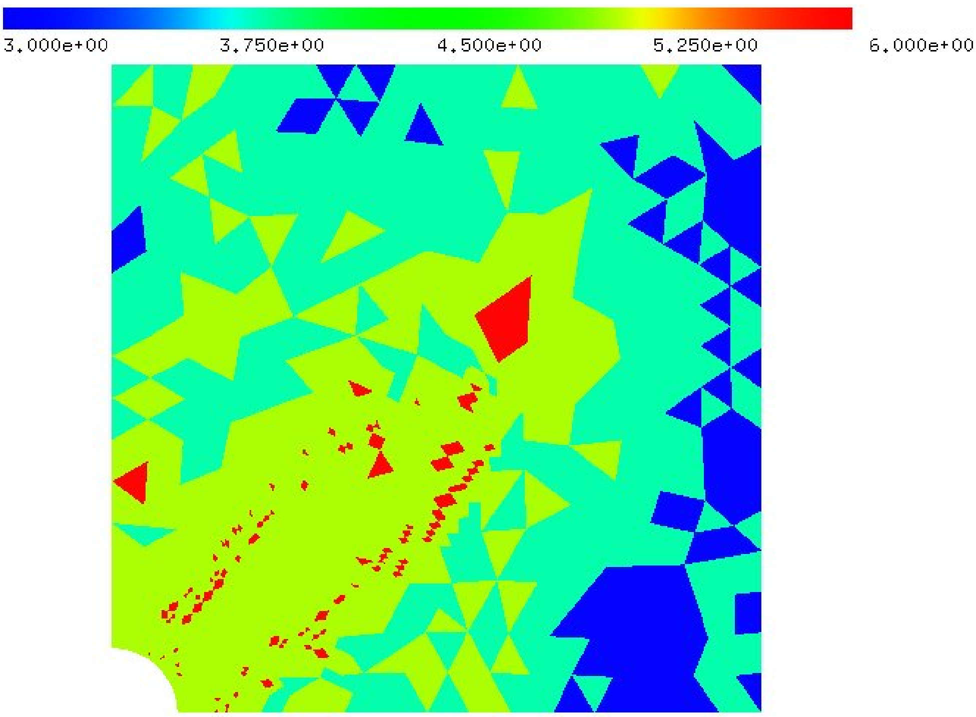

Figure 6.49: Polynomial order with Strategy 2 in Example 6.7.

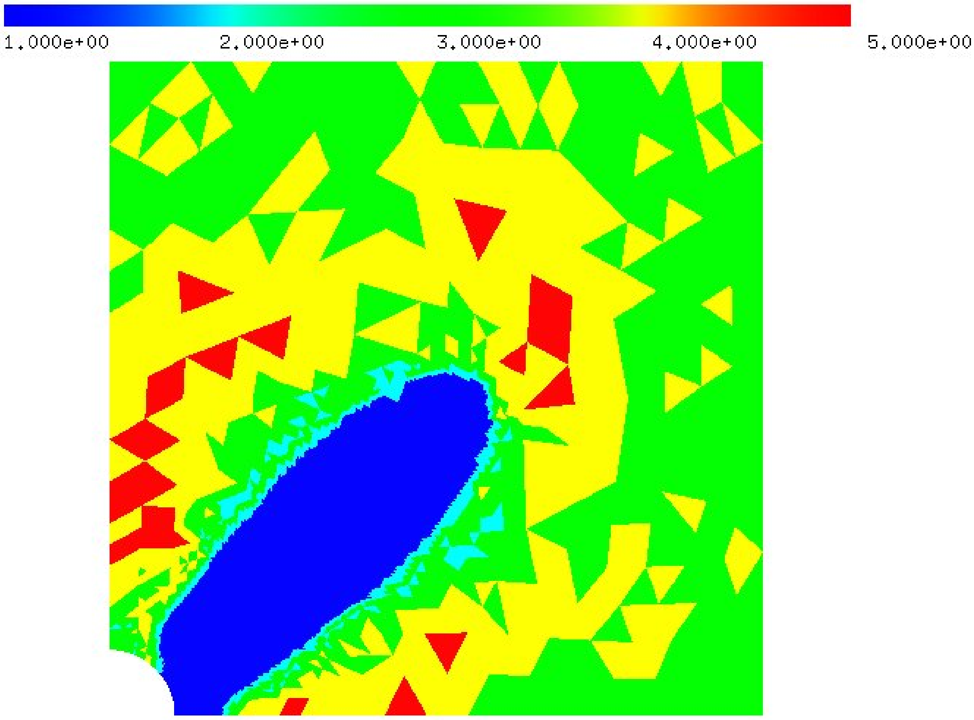

Figure 6.50: Polynomial order with Strategy 3 in Example 6.7.

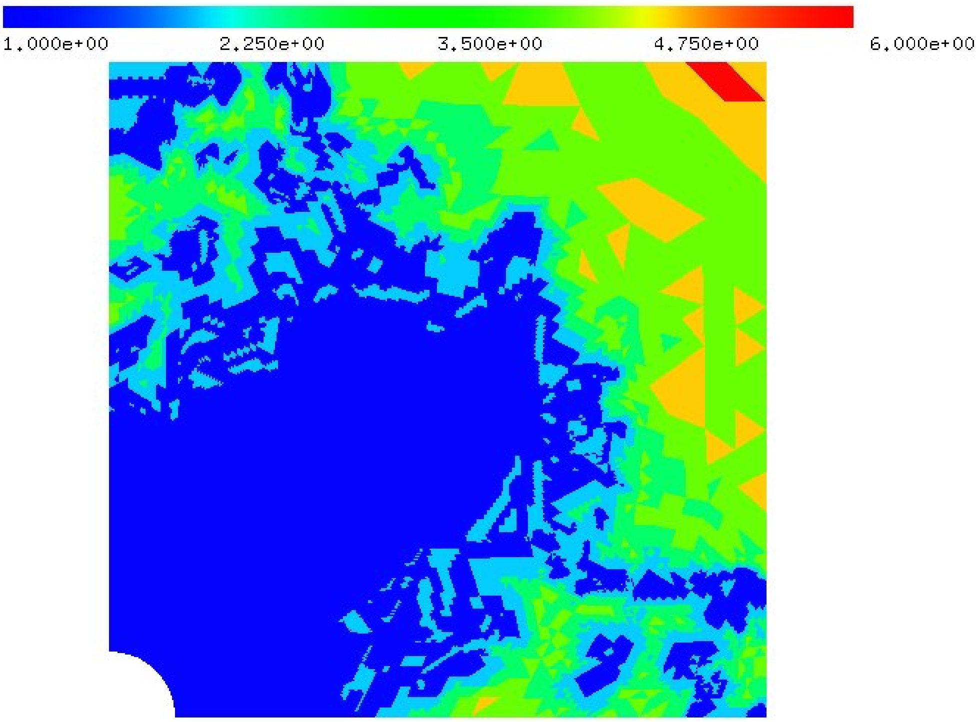

Figure 6.51: Polynomial order with Strategy 4 in Example 6.7.

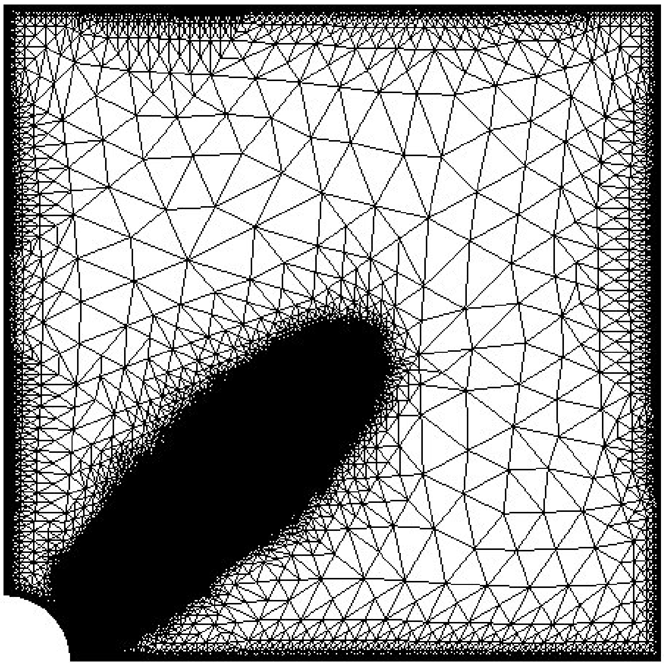

Figure 6.52: Adaptive mesh with Strategy 1 in Example 6.7.

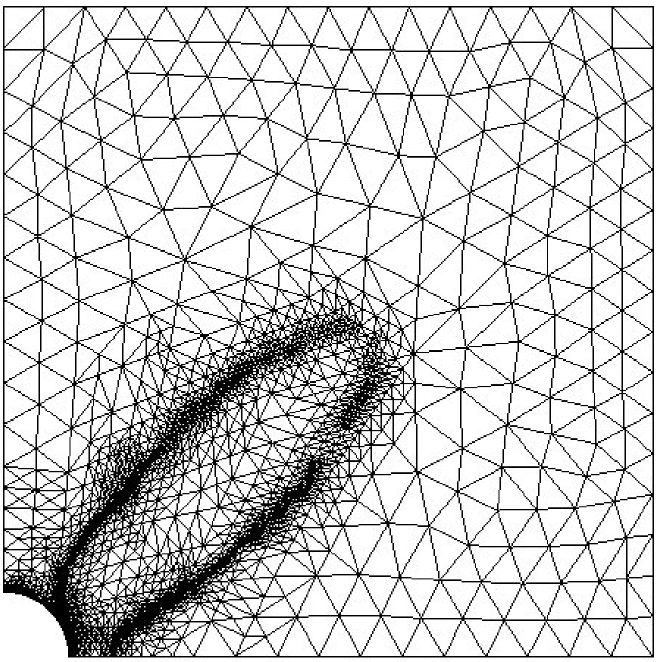

Figure 6.53: Adaptive mesh with Strategy 2 in Example 6.7.

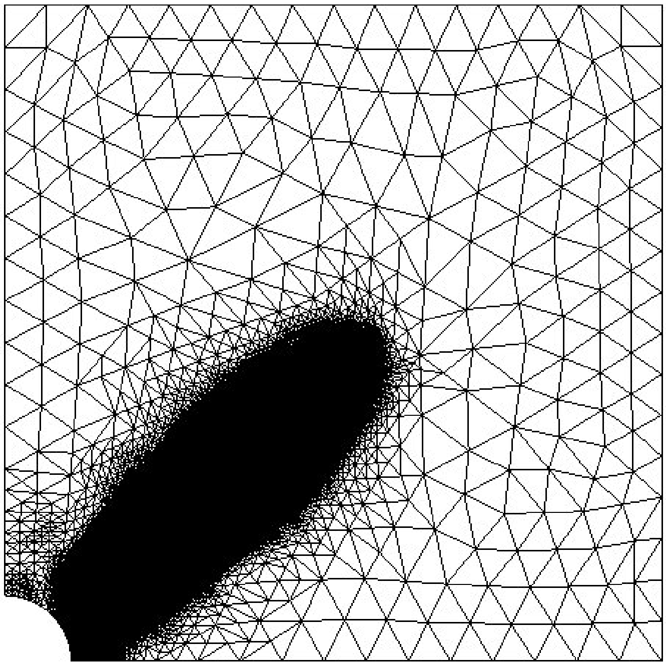

Figure 6.54: Adaptive mesh with Strategy 3 in Example 6.7.

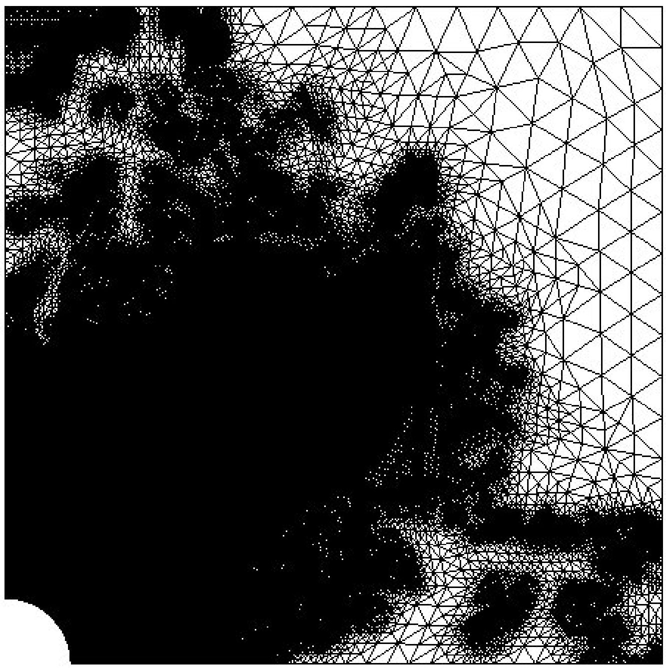

Figure 6.55: Adaptive mesh with Strategy 4 in Example 6.7.

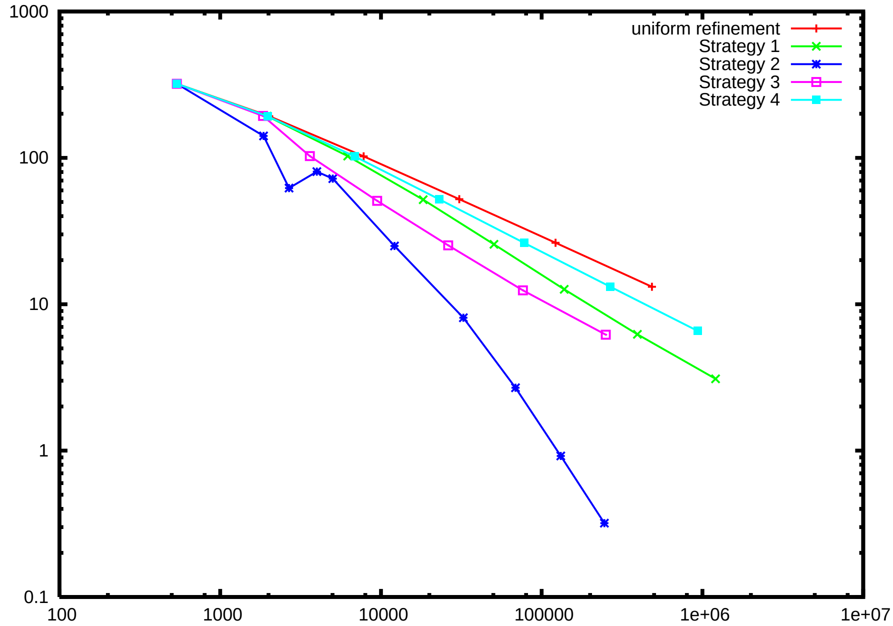

Figure 6.56: The global estimated error (6.2) versus degrees of freedom in Example 6.7.

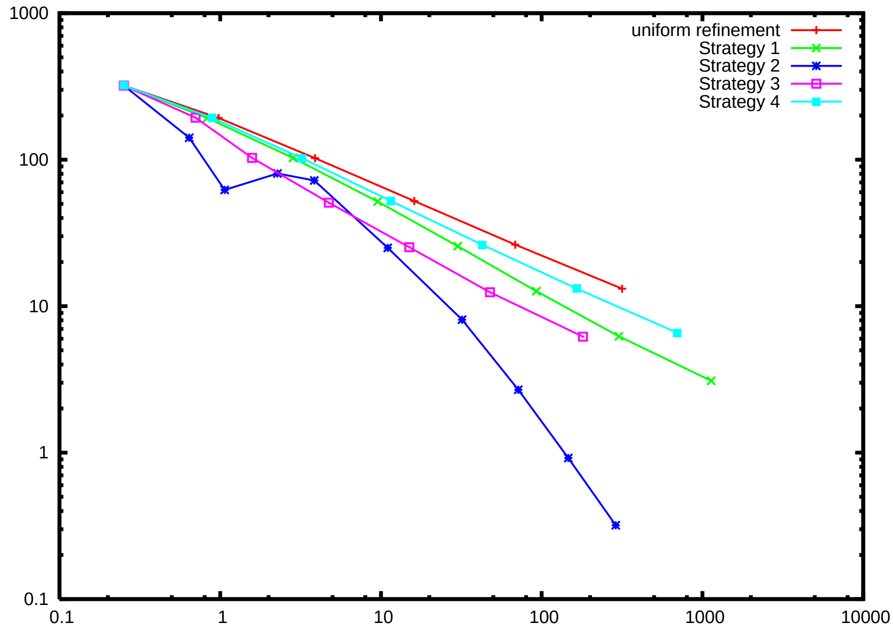

Figure 6.57: Here, the global estimated error (6.2) is plotted versus the time (in seconds) which was spent per Newton step in Example 6.7. One Newton step covers the assembling of the stiffness matrix and a sparse direct solver (PARDISO [90, 91]).

Chapter 7

Conclusion

7.1 Discussion of the Numerical Experiments

The Tables 6.1, 6.2 and 6.3 clearly show the super-linear convergence for each of the Examples 6.1-6.3 at each level of refinement. In order to allow the verification of the convergence tables, the initial value was chosen to be zero for all experiments. Notice, that the last iteration step sometimes shows only a very small improvement compared to the preceding iteration step, which is due to the already reached machine accuracy. Let also be mentioned, that in all examples of Section 6.3, where *hp*-FEM was chosen for the spatial discretization, the super-linear convergence was observed.

Let us finally discuss the convergence plots Figure 6.22, Figure 6.39, and Figure 6.56. Obviously, Strategy 2 works asymptotically best. However, in the first couple of refinements, the strategy seems to fail. This is due to the fact, that the polynomial degree has to be large enough, say greater than 4, for the method to work properly. Remember, the decision of whether to refine in h or in p is left to the least squares fit of a straight line through the point cloud $(\ln |u_{pq}|, p+q)$, where u_{pq} denote the coefficients with respect to the expansion (5.21). So, the convergence of the FE-solution to the solution starts very late but is fast with Strategy 2. The big disadvantage of Strategy 2 is its problem dependency: the adjustment of the parameter b (which indicates, if the slope of the straight line is steep enough) is the key point for the success of the strategy.

With Strategy 3, where we decide for h-refinement if an element was in the plastic zone, the convergence is the second best asymptotically, but it starts off much earlier. Hence, this strategy may be the best choice for use in real-time simulations. The strategy benefits from the fact, that plastic zones cover regions, where the purely elastic solution would have singularities. Thus an extra test on the regularity of the solution is avoided. The difficulty of adjusting the parameters in a proper way, as in Strategy 2, can be avoided in Strategy 3. However, Strategy 3 is pessimistic in the sense, that it can't benefit if the solution has higher regularity within plastic zones, which is especially weird for problems with large plastic zones.

Strategy 4 is not reliable. In many experiments the author encountered a great loss of convergence rate at high levels of refinement (see Figure 6.22). Although the ZZ error estimator [29], which we use in Strategy 4, is known to be efficient and reliable (see [24, 23]), this strategy cannot cope with the success of Strategies 1, 2, and 3. Note, that the equilibration of this error estimator is sensitive with respect to the modulus of hardening H (see (3.23)), which might be an explanation for the bad success of the strategy.

Despite the rather slow convergence rate (only about twice as fast as if we use uniform h-refinement), there is a big advantage of Strategy 1: there are no problem depending parameters to adjust, and it works well for rough boundary data (or geometry). In other words, this strategy is robust and reliable in any case.

7.2 Theoretical Contribution and Outlook

A new framework was presented in Chapter 4, which allows to analyze an elastoplastic problem already in a semi-continuous state, i. e., after time discretization (where we used an implicit Euler scheme), but before spatial discretization. This framework is characterized by the use of

- Moreau's Theorem [77] (see Theorem 4.1 and Corollary 4.1),
- the explicit known minimizer with respect to the plastic strain [5] (see Theorem 4.2 and Equation 4.30), and
- the concept of slanting functions [26](see Subsections 4.2.2 and 4.2.3).

The first item allowed us to find, that the primal formulation (a nonsmooth minimization problem with respect to the displacement and plastic strain), is equivalent to another minimization problem, where the functional depends smooth on the displacement only. By using the second item, the Fréchet derivative of this functional is explicitly given. The following (variational) problem is to find a displacement, such that the Fréchet derivative equals zero. Since the functional is not differentiable a second time, we used the concept of slanting functions in order to iterate the solution of the elastoplastic problem by a slant Newton method. This is a Newton-like method which uses a slanting function of the functionals Fréchet derivative instead of its second derivative.

In the fully discrete case, such a slanting function exists and the resulting slant Newton iterates are converging locally super-linear. This answers an open question of J. Alberty, C. Carstensen, and D. Zarrabi [5, Remark 7.5], who observed the local super-linear convergence numerically. Moreover, if we knew, that Assumption 4.1 was satisfied, a slanting function would exists even in the spatially continuous setting, and the slant Newton method would also converge locally super-linear in this case. Let us conclude this discussion with an open question: Are there elastoplastic problems for which Assumption 4.1 is satisfied?

Appendix A

General Calculus Results

Recall Definition 4.1 and Definition 4.2 in § 4.2.2, and let X, Y and Z be Banach spaces and $\mathcal{H}$ a Hilbert space. Following, the chain rule and the product rule for slanting functions are presented, wherein we use that a slantly differentiable function $F : X \to Y$ is continuous. This is because $\lim_{h\to 0} \|F^o(x+h)\|$ is bounded for all $x \in X$, whence

$$\lim_{h\to 0}\|F(x+h) - F(x)\| = \lim_{h\to 0}\|F^o(x+h)\,h + r(h)\| = 0\,.$$

Theorem A.1. *(chain rule) Let $U \subseteq X$ and $V \subseteq Y$ be open subsets. Let $F \in \mathcal{S}(U, Y)$ such that $F(U) \subseteq V$ and $G \in \mathcal{S}(V, Z)$. Let F^o be a slanting function for F in U and G^o be a slanting function for G in V. Then there holds $G \circ F \in \mathcal{S}(U, Z)$ where*

$$(G \circ F)^o\,(x) := G^o(F(x))\,F^o(x) \qquad \forall x\, \in U$$

serves as a slanting function for $G \circ F$ in U.

Proof. Let $x \in U$ be chosen arbitrary. Since U is open, there exists an open neighborhood $\mathcal{N} \subseteq X$ centered at zero, such that $(x + h) \in U$ if $h \in \mathcal{N}$. One assumption was, that function F is slantly differentiable in U with the slanting function F^o. That is, there exists a mapping $r : X \to Y$ with $\lim_{h\to 0}\|r(h)\|/\|h\| = 0$ such that, for all $h \in \mathcal{N}$, there holds

$$F(x+h) = F(x) + F^o(x+h)\,h + r(h)\,.$$

Also, function G is slantly differentiable in V with the slanting function G^o. That is, there exists a mapping $s : Y \to Z$ with $\lim_{k\to 0}\|s(k)\|/\|k\| = 0$ such that

$$G(y+k) = G(y) + G^o(y+k)\,k + s(k) \tag{A.1}$$

holds for all $y \in V$ and $k \in Y$ which satisfy $(y + k) \in V$. The certain choice

$$y := F(x)\,, \quad k(h) := F(x+h) - F(x) = F^o(x+h)\,h + r(h)$$

for $h \in \mathcal{N}$ satisfies $y \in V$ and $(y + k(h)) \in V$, and yields

$$G(F(x+h)) = G(F(x)) + G^o(F(x+h))\,F^o(x+h)\,h + t(h)\,,$$

with $t(h) := G^o(F(x+h))\, r(h) + s(k(h))$. It remains to show, that

$$\lim_{h\to 0} \frac{\|t(h)\|}{\|h\|} = 0\,.$$

Let $\varepsilon > 0$ be arbitrary. Since $\lim_{h\to 0}\|F^o(x+h)\|$ is bounded, $\lim_{h\to 0} k(h) = 0$, and $\lim_{k\to 0} \frac{\|s(k)\|}{\|k\|} = 0$, there holds

$$\lim_{h\to 0} \left((\|F^o(x+h)\| + \varepsilon)\, \frac{\|s(k(h))\|}{\|k(h)\|} \right) = 0\,. \tag{A.2}$$

There exists $\delta > 0$, such that for all $h \in \mathcal{N}$ with $\|h\| < \delta$ there holds

$$(\|F^o(x+h)\| + \varepsilon)\, \|h\| > \|F^o(x+h)\|\, \|h\| + \|r(h)\| \geq \|F^o(x+h)\, h + r(h)\| = \|k(h)\|\,.$$

Using this together with (A.2), we obtain $\lim_{h\to 0} \frac{\|s(k(h))\|}{\|h\|} = 0$. Hence a slantly differentiable function is continuous, the function F is continuous. Thus, the limit $\lim_{h\to 0}\|G^o(F(x+h))\|$ is bounded, and we conclude

$$\lim_{h\to 0} \frac{\|t(h)\|}{\|h\|} \;\leq\; \lim_{h\to 0} \left(\|G^o(F(x+h))\| \frac{\|r(h)\|}{\|h\|} \right) + \lim_{h\to 0} \left(\frac{\|s(k(h))\|}{\|h\|} \right) = 0\,.$$

□

Theorem A.2. *(product rule) Let $U \subseteq X$ be an open subset. Let F, $G \in \mathcal{S}(U, \mathcal{H})$ for which $F^o : U \to \mathcal{L}(X, \mathcal{H})$ and $G^o : U \to \mathcal{L}(X, \mathcal{H})$ serve as slanting functions in U. Then, the product $P : U \to \mathbb{R}\,,\; x \mapsto \langle F(x)\,,\, G(x)\rangle_{\mathcal{H}}$ is slantly differentiable in U, and the mapping $P^o : U \to \mathcal{L}(X, \mathbb{R})$ with*

$$P^o(x) := \langle F^o(x\,;\,\cdot)\,,\, G(x)\rangle_{\mathcal{H}} + \langle F(x)\,,\, G^o(x\,;\,\cdot)\rangle_{\mathcal{H}} \qquad \forall x \in U \tag{A.3}$$

serves as a slanting function for P in U.

Proof. Let $x \in U$ be arbitrarily and fixed. One has to show

$$\lim_{h\to 0} \frac{|P(x+h) - P(x) - P^o(x+h)\, h|}{\|h\|} = 0\,. \tag{A.4}$$

By the definition of

$$\bar{F}(x,h) := \frac{F(x+h) + F(x)}{2}\,, \quad \bar{G}(x,h) := \frac{G(x+h) + G(x)}{2}$$

for all $h \in X$, there holds

$$P(x+h) - P(x) = \langle \bar{F}(x,h)\,,\, G(x+h) - G(x)\rangle + \langle F(x+h) - F(x)\,,\, \bar{G}(x,h)\rangle\,. \tag{A.5}$$

F and G are slantly differentiable, i. e., there exist mappings $r : X \to \mathcal{H}$ and $s : X \to \mathcal{H}$ with

$$\lim_{h\to 0} \frac{\|r(h)\|}{\|h\|} = \lim_{h\to 0} \frac{\|s(h)\|}{\|h\|} = 0\,,$$

such that

$$F(x+h) - F(x) = F^o(x+h)\,h + r(h)\,, \quad G(x+h) - G(x) = G^o(x+h)\,h + s(h)\,.$$

Substituting this in (A.5) and subtracting $P^o(x+h)\,h$, with P^o defined in (A.3), yields

$$\begin{aligned} P(x+h) - P(x) - P^o(x+h)\,h &= \langle \bar{F}(x,h)\,,\, s(h)\rangle + \langle \bar{G}(x,h)\,,\, r(h)\rangle \\ &+ \frac{1}{2}\,\langle F(x) - F(x+h)\,,\, G^o(x+h)\,h\rangle + \frac{1}{2}\,\langle F^o(x+h)\,h\,,\, G(x) - G(x+h)\rangle\,. \end{aligned}$$

Hence, the limit in (A.4) can be bounded from above by

$$\begin{aligned} \lim_{h\to 0} \Bigg(&\|\bar{F}(x,h)\| \frac{\|s(h)\|}{\|h\|} + \|\bar{G}(x,h)\| \frac{\|r(h)\|}{\|h\|} \\ &+ \|F(x+h) - F(x)\|\,\|G^o(x+h)\| + \|F^o(x+h)\|\,\|G(x+h) - G(x)\| \Bigg)\,. \end{aligned} \tag{A.6}$$

Notice, that due to the continuity of F and G, there holds

$$\lim_{h\to 0} \|\bar{F}(x,h)\| = \|F(x)\|\,, \quad \lim_{h\to 0} \|F(x+h) - F(x)\| = 0$$

and the same for G. Thus, the limit in (A.6) equals zero, which implies that (A.4) is true. $\square$

A few simple properties concerning the deviator are summarized in the following lemma, and often used throughout this work.

Lemma A.1. *Let $n \in \mathbb{N}$, $\lambda \in \mathbb{R}$ with $\lambda > 0$, $\mu \in \mathbb{R}$ with $\mu > 0$, and I denote the identity matrix in $\mathbb{R}^{n\times n}$. Let the mappings $\operatorname{dev} : \mathbb{R}^{n\times n} \to \mathbb{R}^{n\times n}$ and $\mathbb{C} : \mathbb{R}^{n\times n} \to \mathbb{R}^{n\times n}$ be defined*

$$\operatorname{dev} x := x - \frac{\langle x\,,\, I\rangle_F}{\langle I\,,\, I\rangle_F}\, I\,, \quad \mathbb{C}x := \mu(x + x^T) + \lambda \langle x\,,\, I\rangle_F\, I\,.$$

Then, for all matrices x and y in $\mathbb{R}^{n\times n}$, the the following properties hold:

1.	$\langle \operatorname{dev} x\,,\, y\rangle_F = \langle x\,,\, \operatorname{dev} y\rangle_F\,,$	2.	$\operatorname{dev} I = 0\,,$
3.	$\langle \operatorname{dev} x\,,\, I\rangle_F = 0\,,$	4.	$\operatorname{dev}\operatorname{dev} x = \operatorname{dev} x\,,$
5.	$\operatorname{dev} \mathbb{C}x = \mu\left(\operatorname{dev} x + \operatorname{dev} x^T\right)\,,$	6.	$\mathbb{C}\operatorname{dev} x = \mu\left(\operatorname{dev} x + \operatorname{dev} x^T\right)\,,$
7.	$\langle \mathbb{C}x\,,\, I\rangle_F = (2\mu + \langle I\,,\, I\rangle_F \lambda) \langle x\,,\, I\rangle_F\,,$	8.	$\langle \mathbb{C}\operatorname{dev} x\,,\, \operatorname{dev} x\rangle_F \le \langle \mathbb{C}x\,,\, x\rangle_F\,.$

Proof. The first and the second property follow from the definition of the deviator:

$$\langle \operatorname{dev} x\,,\, y\rangle_F = \langle x\,,\, y\rangle_F - \frac{\langle x\,,\, I\rangle_F \langle y\,,\, I\rangle_F}{\langle I\,,\, I\rangle_F} = \langle x\,,\, \operatorname{dev} y\rangle_F\,,$$

$$\operatorname{dev} I = I - \frac{\langle I\,,\, I\rangle_F}{\langle I\,,\, I\rangle_F} I = 0\,.$$

The third property follows from the first two properties:

$$\langle \operatorname{dev} x\,,\, I\rangle_F = \langle x\,,\, \operatorname{dev} I\rangle_F = 0\,.$$

The fourth property holds due to the third property:

$$\operatorname{dev}\operatorname{dev} x = \operatorname{dev} x - \frac{\langle \operatorname{dev} x\,,\, I\rangle_F}{\langle I\,,\, I\rangle_F}\, I = \operatorname{dev} x\,.$$

The fifth property relies on the second property,

$$\operatorname{dev} \mathbb{C}x = \mu(\operatorname{dev} x + \operatorname{dev} x^T) + \lambda\langle x\,,\, I\rangle_F\ \operatorname{dev} I = \mu\left(\operatorname{dev} x + \operatorname{dev} x^T\right)\,,$$

and the sixth property relies on the third property,

$$\mathbb{C}\operatorname{dev} x = \mu\left(\operatorname{dev} x + \operatorname{dev} x^T\right) + \lambda\langle \operatorname{dev} x\,,\, I\rangle_F\, I = \mu\left(\operatorname{dev} x + \operatorname{dev} x^T\right)\,.$$

The seventh property follows from the definition of the mapping $\mathbb{C}$:

$$\langle \mathbb{C}x\,,\, I\rangle_F = \mu(\langle x\,,\, I\rangle_F + \langle x^T\,,\, I\rangle_F) + \langle I\,,\, I\rangle_F \lambda \langle x\,,\, I\rangle_F = (2\mu + \langle I\,,\, I\rangle_F \lambda)\langle x\,,\, I\rangle_F\,.$$

The eighth property can be shown by

$$\begin{aligned}\langle \mathbb{C}\operatorname{dev} x\,,\, \operatorname{dev} x\rangle_F &= \langle \operatorname{dev}\mathbb{C}x\,,\, \operatorname{dev} x\rangle_F = \langle \mathbb{C}x\,,\, \operatorname{dev}\operatorname{dev} x\rangle_F = \langle \mathbb{C}x\,,\, \operatorname{dev} x\rangle_F \\ &= \langle \mathbb{C}x\,,\, x\rangle_F - \frac{\langle \mathbb{C}x\,,\, I\rangle_F \langle x\,,\, I\rangle_F}{\langle I\,,\, I\rangle_F} \le \langle \mathbb{C}x\,,\, x\rangle_F\,.\end{aligned}$$

□

Appendix B

Acknowledgments

I am pleased to acknowledge the support by the Austrian Science Fund 'Fonds zur Förderung der wissenschaftlichen Forschung (FWF)' under the grants SFB F013/F1306 and P19255, the support by the Upper Austrian government under the grant DK W1214. Let me thank: H. Irschik and J. Gerstmayr of the LCM GmbH for giving me the opportunity to practice my knowledge by real life elastoplastic problems; R. Grieße, C. Pechstein, V. Pillwein, J. Schöberl, A. Sinwel, and S. Zaglmayr for so many fruitful discussions and for help with the software package NETGEN/NGSolve; D. Knees for discussions regarding the regularity analysis, and for discovering a crucial failure in one of my proofs. The idea of applying Moreau's Theorem and the concept of slanting functions to the elastoplastic formulation came out during working progresses with H. Gfrerer, J. Kienesberger, U. Langer, J. Valdman, and W. Zulehner. My sincerest thanks go to my supervisor U. Langer, and also to my colleague J. Valdman, who both introduced me into the basics of elastoplasticity and the process of scientific research. Finally, I would like to thank my friends and family for all their patience and love.

Bibliography

[1] M. Ainsworth and B. Senior, *Aspects of an adaptive hp-finite element method: adaptive strategy, conforming approximation and efficient solvers*, Comput. Methods Appl. Mech. Engrg., 150 (1997), pp. 65–87.

[2] H.-D. Alber, *Materials with memory*, vol. 1682 of Lecture Notes in Mathematics, Springer-Verlag, Berlin, 1998. Initial-boundary value problems for constitutive equations with internal variables.

[3] J. Alberty and C. Carstensen, *Numerical analysis of time-depending primal elastoplasticity with hardening*, SIAM Journal on Numerical Analysis, 37 (2000), pp. 1271–1294.

[4] J. Alberty, C. Carstensen, S. A. Funken, and R. Klose, *Matlab implementation of the finite element method in elasticity*, Computing, 69 (2002), pp. 239–263.

[5] J. Alberty, C. Carstensen, and D. Zarrabi, *Adaptive numerical analysis in primal elastoplasticity with hardening*, Comput. Methods Appl. Mech. Engrg., 171 (1999), pp. 175–204.

[6] J. Alberty, C. Carstensen, and D. Zarrabi, *Numerical analysis in primal elastoplasticity with hardening*, Z. Angew. Math. Mech., (2000).

[7] I. Babuska and B. Guo, *The h-p version of the finite element method - Part 1: The basic approximation results*, Comput. Mech., 1 (1986), pp. 21–41.

[8] I. Babuška and M. Suri, *The h-p version of the finite element method with quasi-uniform meshes*, RAIRO Modél. Math. Anal. Numér., 21 (1987), pp. 199–238.

[9] ——, *The optimal convergence rate of the p-version of the finite element method*, SIAM J. Numer. Anal., 24 (1987), pp. 750–776.

[10] I. Babuška, B. A. Szabo, and I. N. Katz, *The p-version of the finite element method*, SIAM J. Numer. Anal., 18 (1981), pp. 515–545.

[11] A. Becirovic, P. Paule, V. Pillwein, A. Riese, C. Schneider, and J. Schöberl, *Hypergeometric Summation Algorithms for High Order Finite Elements*, Computing, 78 (2006), pp. 235–249.

[12] A. Bensoussan and J. Frehse, *Regularity results for nonlinear elliptic systems and applications*, vol. 151 of Applied Mathematical Sciences, Springer-Verlag, Berlin, 2002.

[13] S. Beuchler, T. Eibner, and U. Langer, *Primal and dual interface concentrated iterative substructuring methods*, SIAM Journal on Numerical Analysis, 46 (2008), pp. 2818–2842.

[14] S. Beuchler and V. Pillwein, *Sparse shape functions for tetrahedral p-FEM using integrated Jacobi polynomials*, Computing, 80 (2007), pp. 345–375.

[15] ——, *Completions to sparse shape functions for triangular and tetrahedral p-FEM*, in Domain Decomposition Methods in Science and Engineering XVII, U. Langer, M. Discacciati, D. Keyes, O. Widlund, and W. Zulehner, eds., vol. 60 of Lecture Notes in Computational Science and Engineering, Heidelberg, 2008, Springer, pp. 435–442.

[16] R. Blaheta, *Convergence of Newton-type methods in incremental return mapping analysis of elastoplastic problems*, Comput. Methods Appl. Mech. Engrg., 147 (1997), pp. 167–185.

[17] M. Brokate, C. Carstensen, and J. Valdman, *A quasi-static boundary value problem in multi-surface elastoplasticity. I. Analysis*, Math. Methods Appl. Sci., 27 (2004), pp. 1697–1710.

[18] ——, *A quasi-static boundary value problem in multi-surface elastoplasticity. II. Numerical solution*, Math. Methods Appl. Sci., 28 (2005), pp. 881–901.

[19] C. Carstensen, *Nonlinear interface problems in solid mechanics: Finite element and boundary element couplings*, 1993. Habilitationsschrift, Universität Hannover.

[20] ——, *Coupling of FEM and BEM for interface problems in viscoplasticity and plasticity with hardening*, SIAM J. Numer. Anal., 33 (1996), pp. 171–207.

[21] ——, *Domain decomposition for a non-smooth convex minimization problem and its application to plasticity*, Numer. Linear Algebra Appl., 4 (1997), pp. 177–190.

[22] ——, *Numerical analysis of the primal problem of elastoplasticity with hardening*, Numer. Math., 82 (1999), pp. 577–597.

[23] ——, *Some remarks on the history and future of averaging techniques in a posteriori finite element error analysis*, Z. angew. Math. Mech., 84 (2004), pp. 3–21.

[24] C. Carstensen and J. Alberty, *Averaging techniques for reliable a posteriori FE-error control in elastoplasticity with hardening*, Comput. Methods Appl. Mech. Eng., 192 (2003), pp. 1435–1450.

[25] C. Carstensen, A. Orlando, and J. Valdman, *A convergent adaptive finite element method for the primal problem of elastoplasticity*, Int. J. Numer. Meth. Engng., 67 (2006), pp. 1851–1887.

[26] X. Chen, Z. Nashed, and L. Qi, *Smoothing methods and semismooth methods for nondifferentiable operator equations*, SIAM Journal on Numerical Analysis, 38 (2000), pp. 1200–1216.

[27] P. G. Ciarlet, *The finite element method for elliptic problems*, North-Holland Publishing Co., Amsterdam, 1978. Studies in Mathematics and its Applications, Vol. 4.

[28] R. Courant, *Variational methods for the solution of problems of equilibrium and vibrations*, Bull. Amer. Math. Soc., 49 (1943), pp. 1–23.

[29] A. W. Craig, J. Z. Zhu, and O. C. Zienkiewicz, *A posteriori error estimation, adaptive mesh refinement and multigrid methods using hierarchical finite element bases*, in The mathematics of finite elements and applications, V (Uxbridge, 1984), Academic Press, London, 1985, pp. 587–594.

[30] L. Demkowicz and J. T. Oden, *Application of hp-adaptive BE/FE methods to elastic scattering*, Comput. Methods Appl. Mech. Engrg., 133 (1996), pp. 287–317.

[31] L. Demkowicz, J. T. Oden, W. Rachowicz, and O. Hardy, *Toward a universal h-p adaptive finite element strategy. I. Constrained approximation and data structure*, Comput. Methods Appl. Mech. Engrg., 77 (1989), pp. 79–112.

[32] L. Demkowicz, W. Rachowicz, and P. Devloo, *A fully automatic hp-adaptivity*, in Proceedings of the Fifth International Conference on Spectral and High Order Methods (ICOSAHOM-01) (Uppsala), vol. 17, 2002, pp. 117–142.

[33] L. Demkowicz and P. Šolín, *Goal-oriented hp-adaptivity for elliptic problems*, Comput. Methods Appl. Mech. Engrg., 193 (2004), pp. 449–468.

[34] D. Drucker, *A more fundamental approach to plastic stress–strain relations*, in Proceedings of the 1st US National Congress on Applied Mathematics (New York), 1951, pp. 487–491.

[35] A. Düster, A. Niggl, V. Nübel, and E. Rank, *A numerical investigation of high-order finite elements for problems of elastoplasticity*, in Proceedings of the Fifth International Conference on Spectral and High Order Methods (ICOSAHOM-01) (Uppsala), vol. 17, 2002, pp. 397–404.

[36] A. Düster and E. Rank, *A p-version finite element approach for two- and three-dimensional problems of the J_2 flow theory with non-linear isotropic hardening*, Int. J. Numer. Meth. Engng., 53 (2002), pp. 49 – 63.

[37] G. Duvaut and J. L. Lions, *Inequalities in mechanics and physics*, Springer-Verlag, Berlin, 1976. Translated from the French by C. W. John, Grundlehren der Mathematischen Wissenschaften, 219.

[38] T. Eibner and J. M. Melenk, *An adaptive strategy for hp-FEM based on testing for analyticity*, Comput. Mech., 39 (2007), pp. 575–595.

[39] I. Ekeland and R. Témam, *Convex analysis and variational problems*, vol. 28 of Classics in Applied Mathematics, Society for Industrial and Applied Mathematics (SIAM), Philadelphia, PA, english ed., 1999. Translated from the French.

[40] M. Fuchs and G. Seregin, *Variational methods for problems from plasticity theory and for generalized Newtonian fluids*, vol. 1749 of Lecture Notes in Mathematics, Springer-Verlag, Berlin, 2000.

[41] J. Gerstmayr and M. K. Matikainen, *Analysis of stress and strain in the absolute nodal coordinate formulation with nonlinear material behavior*, in III European Conference on Computational Mechanics, C. A. Motasoares, J. A. C. Martins, H. C. Rodrigues, J. A. C. Ambrsio, C. A. B. Pina, C. M. Motasoares, E. B. R. Pereira, and J. Folgado, eds., Springer Netherlands, 2006, pp. 615–615.

[42] R. Glowinski, J.-L. Lions, and R. Trémolières, *Numerical analysis of variational inequalities*, vol. 8 of Studies in Mathematics and its Applications, North-Holland Publishing Co., Amsterdam, 1981. Translated from the French.

[43] R. Griesse and C. Meyer, *Optimal control of static plasticity with linear kinematic hardening*, tech. report, Weierstrass Institute for Applied Analysis and Stochastics, WIAS Preprint 1370, 2009.

[44] P. Gruber and J. Valdman, *Implementation of an elastoplastic solver based on the Moreau-Yosida theorem*, Math. Comput. Simulation, 76 (2007), pp. 73–81.

[45] P. G. Gruber, J. Kienesberger, U. Langer, J. Schöberl, and J. Valdman, *Fast solvers and a posteriori error estimates in elastoplasticity*, in Numerical and Symbolic Scientific Computing: Progress and Prospects, U. Langer and P. Paule, eds., Springer-Verlag, Wien, (to appear).

[46] P. G. Gruber, D. Knees, S. Nesenenko, and M. Thomas, *Analytical and numerical aspects of time-dependent models with internal variables*, Z. angew. Math. Mech., 40 (2010), pp. 861–902.

[47] P. G. Gruber and J. Valdman, *Newton-like solver for elastoplastic problems with hardening and its local super-linear convergence*, in Numerical Mathematics and Advanced Applications. Proceedings of ENUMATH 2007, K. Kunisch, G. Of, and O. Steinbach, eds., Berlin, 2008, Springer, pp. 795–803.

[48] P. G. Gruber and J. Valdman, *Solution of one-time-step problems in elastoplasticity by a slant Newton method*, SIAM J. Sci. Comput., 31 (2009), pp. 1558–1580.

[49] W. Han and B. D. Reddy, *Computational plasticity: the variational basis and numerical analysis*, Comput. Mech. Adv., 2 (1995), pp. 283–400.

[50] ——, *Plasticity: mathematical theory and numerical analysis*, vol. 9 of Interdisciplinary Applied Mathematics, Springer-Verlag, New York, 1999. Mathematical theory and numerical analysis.

[51] N. Heuer, M. E. Mellado, and E. P. Stephan, *hp-adaptive two-level methods for boundary integral equations on curves*, Computing, 67 (2001), pp. 305–334.

[52] M. Hintermüller, K. Ito, and K. Kunisch, *The primal-dual active set strategy as a semismooth Newton method*, SIAM J. Optim., 13 (2002), pp. 865–888.

[53] I. Hlaváček, *A finite element solution for plasticity with strain-hardening*, RAIRO Anal. Numér., 14 (1980), pp. 347–368.

[54] I. Hlaváček, J. Haslinger, J. Nečas, and J. Lovíšek, *Solution of variational inequalities in mechanics*, (1988).

[55] A. Hofinger and J. Valdman, *Numerical solution of the two-yield elastoplastic minimization problem*, Computing, 81 (2007), pp. 35–52.

[56] P. Houston, B. Senior, and E. Süli, *Sobolev regularity estimation for hp-adaptive finite element methods*, in Numerical mathematics and advanced applications: Proceedings of ENUMATH 2001, Ischia, 2003, Springer Wien, pp. 631–656.

[57] P. Houston and E. Süli, *A note on the design of hp-adaptive finite element methods for elliptic partial differential equations*, Comput. Methods Appl. Mech. Engrg., 194 (2005), pp. 229–243.

[58] C. Johnson, *Existence theorems for plasticity problems*, J. Math. Pures Appl. (9), 55 (1976), pp. 431–444.

[59] ——, *On finite element methods for plasticity problems*, Numer. Math., 26 (1976), pp. 79–84.

[60] ——, *A mixed finite element method for plasticity problems with hardening*, SIAM J. Numer. Anal., 14 (1977), pp. 575–583.

[61] G. E. Karniadakis and S. J. Sherwin, *Spectral/hp element methods for CFD*, Oxford University Press, New York, 1999.

[62] B. N. Khoromskij and J. M. Melenk, *Boundary concentrated finite element methods*, SIAM J. Numer. Anal., 41 (2003), pp. 1–36.

[63] J. Kienesberger, *Efficient Solution Algorithms for Elastoplastic Problems*, PhD thesis, Johannes-Kepler-Universität Linz, 2006.

[64] J. Kienesberger, U. Langer, and J. Valdman, *On a robust multigrid-preconditioned solver for incremental plasticity problems*, in Proceedings of IMET 2004 - Iterative Methods, Preconditioning & Numerical PDEs, 2004, pp. 84–87.

[65] D. Knees and P. Neff, *Regularity up to the boundary for nonlinear elliptic systems arising in time-incremental infinitesimal elasto-plasticity*, SIAM J. Math. Anal., 40 (2008), pp. 21–43.

[66] W. T. Koiter, *Stress-strain relations, uniqueness and variational theorems for elasttic-plastic material with a singular yield surface*, Quart. Appl. Math., 11 (1953), pp. 29–53.

[67] V. G. Korneev and U. Langer, *Approximate solution of plastic flow theory problems*, vol. 69 of Teubner-Texte zur Mathematik [Teubner Texts in Mathematics], BSB B. G. Teubner Verlagsgesellschaft, Leipzig, 1984.

[68] ——, *On the regularity of the solution of plastic flow theory problems (in Russian)*, Diff. Uravnenija, 20 (1984), pp. 667–678.

[69] M. A. Krasnosel′skiĭ, P. P. Zabreĭko, E. I. Pustyl′nik, and P. E. Sobolevskiĭ, *Integral operators in spaces of summable functions*, Noordhoff International Publishing, Leiden, 1976. Translated from the Russian by T. Ando, Monographs and Textbooks on Mechanics of Solids and Fluids, Mechanics: Analysis.

[70] M. Lévy, *Extrait du mémoire sur les équations générales des mouvements intérieurs des corps solides ductiles au delá des limites oú l'élasticité pourrait les ramener á leur premier état*, J. Math. Pures et Appl., 16 (1871), pp. 369–372.

[71] C. Mavriplis, *Adaptive mesh strategies for the spectral element method*, Comput. Methods Appl. Mech. Engrg., 116 (1994), pp. 77–86.

[72] J. M. Melenk, *hp-finite element methods for singular perturbations*, vol. 1796 of Lecture Notes in Mathematics, Springer, Berlin, 2002.

[73] A. Mielke, *Evolution of rate-independent systems*, vol. 2 of Handbook of Differential Equations: Evolutionary Equations, North-Holland, 2006, pp. 461 – 559.

[74] R. v. Mises, *Mechanik der festen Körper im plastisch deformablen Zustand*, Gött. Nach. Math. Phys. Kl., 1 (1913), pp. 582–592.

[75] ——, *Mechanik der plastischen Formänderung von Kristallen*, Z. angew. Math. Mech., 8 (1928), pp. 161–185.

[76] J. Moreau, *Evolution problem associated with a moving convex set in a Hilbert space*, J. Diff. Eqns, 26 (1977), pp. 347–374.

[77] J. J. Moreau, *Proximité et dualité dans un espace hilbertien*, Bull. Soc. Math. France, 93 (1965), pp. 273–299.

[78] Z. Mroz, V. A. Norris, and O. C. Zienkiewicz, *An anisotropic hardening model for soils and its application to cyclic loading*, International Journal for Numerical and Analytical Methods in Geomechanics, 2 (1978), pp. 203–221.

[79] P. Neff, K. Chelminski, W. Mller, and C. Wieners, *A numerical solution method for an inifinitesimal elasto-plastic Cosserat model*, Math. Models Methods Appl. Sci., (2007), pp. 1211–1240.

[80] V. Nübel, *Die adaptive rp-Methode für elastoplastische Probleme*, PhD thesis, TU Munich, Germany, 2007.

[81] V. Nübel, A. Düster, and E. Rank, *An rp-adaptive finite element method for the deformation theory of plasticity*, Computational Mechanics, 39 (2007), pp. 557–574.

[82] J. T. Oden, L. Demkowicz, W. Rachowicz, and T. A. Westermann, *Toward a universal h-p adaptive finite element strategy. II. A posteriori error estimation*, Comput. Methods Appl. Mech. Engrg., 77 (1989), pp. 113–180.

[83] J. T. Oden, W. Wu, and M. Ainsworth, *Three-step h-p adaptive strategy for the incompressible Navier-Stokes equations*, in Modeling, mesh generation, and adaptive numerical methods for partial differential equations (Minneapolis, MN, 1993), vol. 75 of IMA Vol. Math. Appl., Springer, New York, 1995, pp. 347–366.

[84] W. Prager, *Recent developments in the mathematical theory of plasticity*, J. Appl. Phys., 20 (1949), pp. 235–241.

[85] L. T. Prandtl, *Spannungsverteilung in plastischen Körpern*, in Proc. 1st Intern. Congr. Mechanics, Delft, 1924, pp. 43–54.

[86] ——, *Ein Gedankenmodell zur kinetischen Theorie der festen Körper*, Z. angew. Math. Mech., 8 (1928), pp. 85–106.

[87] W. Rachowicz, J. T. Oden, and L. Demkowicz, *Toward a universal h-p adaptive finite element strategy. III. Design of h-p meshes*, Comput. Methods Appl. Mech. Engrg., 77 (1989), pp. 181–212.

[88] A. Reuss, *Berücksichtigung der elastischen Formänderung in der Plastizitätstheorie*, Z. angew. Math. Mech., 10 (1939), pp. 26–274.

[89] J. B. d. Saint Venant, *Mémoire sur l'établissement des équations différentielles des mouvements intérieurs opérés dans les corps solides ductiles*, J. Math. Pures et Appl., 16 (1871), pp. 308–316.

[90] O. Schenk and K. Gärtner, *Solving unsymmetric sparse systems of linear equations with PARDISO*, Journal of Future Generation Computer Systems, 20 (2004), pp. 475–487.

[91] ——, *On fast factorization pivoting methods for symmetric indefinite systems*, Elec. Trans. Numer. Anal., 23 (2006), pp. 158–179.

[92] J. Schöberl, *NETGEN/NGSolve - Finite Element solver software package.* URL: http://www.hpfem.jku.at/netgen/.

[93] C. Schwab, *p- and hp- finite element methods: theory and applications in solid and fluid mechanics*, Oxford University Press, New York, 1998.

[94] J. C. Simo, *Numerical analysis and simulation of plasticity*, in Handbook of numerical analysis, Vol. VI, Handb. Numer. Anal., VI, North-Holland, Amsterdam, 1998, pp. 183–499.

[95] J. C. Simo and S. Govindjee, *Nonlinear B-stability and symmetry preserving return mapping algorithms for plasticity and viscoplasticity*, Internat. J. Numer. Methods Engrg., 31 (1991), pp. 151–176.

[96] J. C. Simo and T. J. R. Hughes, *Computational inelasticity*, vol. 7 of Interdisciplinary Applied Mathematics, Springer-Verlag, New York, 1998.

[97] J. C. Simo, J. G. Kennedy, and S. Govindjee, *Nonsmooth multisurface plasticity and viscoplasticity. Loading/unloading conditions and numerical algorithms*, Internat. J. Numer. Methods Engrg., 26 (1988), pp. 2161–2185.

[98] J. C. Simo, J. G. Kennedy, and R. L. Taylor, *Complementary mixed finite element formulations for elastoplasticity*, Comput. Methods Appl. Mech. Engrg., 74 (1989), pp. 177–206.

[99] J. C. Simo and R. L. Taylor, *A return mapping algorithm for plane stress elastoplasticity*, Internat. J. Numer. Methods Engrg., 22 (1986), pp. 649–670.

[100] E. Stein, *Error-controlled adaptive finite elements in solid mechanics*, John Wiley & Sons, Ltd., 2003.

[101] G. Strang and G. J. Fix, *An analysis of the finite element method*, Prentice-Hall Inc., Englewood Cliffs, N. J., 1973. Prentice-Hall Series in Automatic Computation.

[102] B. Szabó, A. Düster, and E. Rank, *The p-Version of the Finite Element Method*, Encyclopedia of Computational Mechanics, John Wiley & Sons, Ltd, 2004.

[103] R. Temam, *Mathematical Problems in Plasticity*, Gauthier-Villars, Paris, 1985.

[104] R. Temam and G. Strang, *Functions of bounded deformation*, Arch. Rational Mech. Anal., 75 (1980), pp. 7–21.

[105] H. E. Tresca, *Mémoire Présentés par Divers Savants*, Acad. Sci. Paris, 20 (1872), pp. 75–135.

[106] M. Ulbrich, *Semismooth Newton methods for operator equations in function spaces*, SIAM J. Optim., 13 (2002), pp. 805–842.

[107] J. Valdman, *Mathematical and Numerical Analysis of Elastoplastic Material with Multi-Surface Stress-Strain Relation*, PhD thesis, Christian-Albrechts-Universität zu Kiel, 2002.

[108] C. Wieners, *Multigrid methods for finite elements and the application to solid mechanics. Theorie und Numerik der Prandtl-Reuß Plastizität*, 2000. Habilitationsschrift, Universität Heidelberg, Germany.

[109] ——, *Nonlinear solution methods for infinitesimal perfect plasticity*, Z. Angew. Math. Mech., 87 (2007), pp. 643–660.

[110] M. Zyczkowski, *Combined Loadings in the Theory of Plasticity*, P.W.N. Polish Scientific Publishers, Warsaw, 1981.

Curriculum Vitae

Persönliche Daten

Name: Peter Günther Gruber

Geboren am: 01. 10. 1978 in Ried im Innkreis

Staatsbürgerschaft: Österreich

Ausbildung

bis 07/1989: Volksschule

09/1989- 07/1997: Bundesrealgymnasium, Ried im Innkreis

10/1997- 06/1998: Studium der Technischen Mathematik an der JKU (Johannes Kepler Universitt) in Linz

10/1999- 03/2006: Studium der Technischen Mathematik an der JKU in Linz

03/2006: Abschluss des Studiums der Technischen Mathematik

Zivildienst

10/1998- 09/1999: Zivildienst beim Österreichischen Roten Kreuz in Steyr

Beruflicher Werdegang

04/2006- 12/2008: Wissenschaftlicher Projektmitarbeiter am Spezialforschungsbereich F013 (Projekt 06) an der JKU Linz

01/2009- 09/2009: Wissenschaftlicher Mitarbeiter am Institut für Numerische Mathematik

10/2009- 04/2010: Wissenschaftlicher Mitarbeiter am Doktoratskolleg W1214 an der JKU Linz

seit 08/2010: Forschungsingenieur bei LCM GmbH, Altenberger Straße 69, 4040 Linz

Eidsstattliche Erklärung

Ich erkläre an Eides statt, dass ich die vorliegende Dissertation selbständig und ohne fremde Hilfe verfasst, andere als die angegebenen Quellen und Hilfsmittel nicht benutzt, sowie die wörtlich oder sinngemäß entnommenen Stellen als solche kenntlich gemacht habe.

Linz, Dezember 2010